MOLECULAR BASIS FOR ANTIBODY-MEDIATED IMMUNITY AGAINST IRON-BINDING PROTEINS IN *STAPHYLOCOCCUS AUREUS*

By

Monique R. Bennett

Dissertation

Submitted to the Faculty of the

Graduate School of Vanderbilt University

in partial fulfillment of the requirements

for the degree of

DOCTOR OF PHILOSOPHY

in

Microbiology and Immunology

September 30th, 2019

Nashville, Tennessee

Approved:

Peggy L. Kendall, M.D.

James E. Cassat, M.D., Ph.D.

Dana B. Lacy, Ph.D.

Matthew J. Tyska, Ph.D.

Eric P. Skaar, Ph.D.

James E. Crowe, Jr. M.D.

To my husband, who always puts my dreams and needs above his own.

To my mother, who showed me the beauty of science and gave me the strength to stand up for what I believe in.

ACKNOWLEDGEMENTS

I would like to thank my mentors, Dr. James E. Crowe and Dr. Eric P. Skaar. While it has never been easy, I am grateful they took a chance on collaborating with me and thankful for everything I have learned in the process. Dr. Crowe gave me the opportunity to pursue a new project and taught me how to shape that project into a story. Dr. Skaar taught me a great deal scientifically about designing experiments, implementing proper controls and how to design elegant papers.

A sincere thank you as well to my dissertation committee: Dr. Peggy Kendall (chair), Dr. Jim Cassat, Dr. Borden Lacy, and Dr. Matthew Tyska. Thank you for your willingness to meet with me and provide feedback whenever necessary as well as the invaluable guidance and insight you all provided throughout these studies.

I would like to thank both the Crowe and Skaar labs. Both groups of people are at the top of their fields and kept me on my toes for the last four years. It was an honor to work with such talented scientists. Special thanks to Pavlo Gilchuk in the Crowe lab for intellectually contributing to my training and teaching me a tremendous amount. Thank you also to Jacob Choby in the Skaar lab for taking the time to answer countless questions and teach me specialized assays. Starting assays you have never done before was always a little easier with the expert guidance of these two. I would also like to thank all my fellow graduate students for their support and helping make lab life a little more tolerable.

Thank you to my parents who raised me in a scientific environment and taught me to ask questions, think critically, and always encouraged me to pursue my dreams no

matter the cost. Finally and above all, thank you to my husband, Lynch. You did not hesitate to make career sacrifices of your own when I got into Vanderbilt and every day you support me in whatever way you can to make this journey better. I cannot imagine what the last 5 years would have been like without you by my side.

TABLE OF CONTENTS

Page

LIST OF TABLES

LIST OF FIGURES

LIST OF ABBREVIATIONS

mAb	Monoclonal antibody
STAU	*Staphylococcus aureus*
EC_{50}	50% maximum-effective concentration
O.D.	Optical density
BLI	Biolayer interferometry
ELISA	Enzyme-linked immunosorbent assay
IgG	Immunoglobulin G
PBMC	Peripheral blood mononuclear cells
EBV	Epstein-Barr virus
HDX-MS	Hydrogen deuterium exchange mass spectrometry
Hb	Hemoglobin
Isd	Iron-regulated surface determinant system
TSB	Typtic soy broth
TSA	Tryptic soy agar
NW	*S. aureus* strain Newman
NEAT	NEAr iron transporter
ADCC	Antibody-dependent cellular cytotoxicity
CFU	Colony forming units
IGHV	Immunoglobulin heavy chain variable region
EDDHA	Ethylenediamine-*N*,*N*′-bis(2-hydroxyphenylacetic acid)

CHAPTER I

INTRODUCTION

Dissertation overview

My dissertation describes the molecular and structural characterization of human monoclonal antibodies against the *Staphylococcus aureus* (*S. aureus*) iron regulated surface determinant (Isd) system. My work is divided into five chapters. In the first chapter, I review *S. aureus* as a pathogen, previous vaccine candidates and antibody therapeutics, as well as heme acquisition within *S. aureus.*

In the second chapter, I describe the isolation of a panel of human monoclonal antibodies to the Isd system of *S. aureus* using novel hybridoma technology. I further characterize these antibodies for their ability to block heme *in vitro* and reduce *S. aureus* bacterial burden *in vivo*. Two of the identified mAbs work in combination using distinct mechanisms to reduce *S. aureus* burden in a mouse septic model of infection.

Chapter three outlines the important role *IGHV1-69*-encoded mAbs play in binding and inhibiting the NEAT2 domain of IsdB. I crystalized three separate antibodies, one in complex with IsdB-NEAT2 and two *apo* structures. Using a combination of HDX-MS and Rosetta modeling along with X-ray crystallography, we were able to identify three functionally distinct sites on IsdB-NEAT2 and test the biological relevance of these epitopes using *in vitro* growth and *in vivo* mouse studies. We also further expanded our panel of *IGHV1-69*-encoded mAbs to characterize the role

of somatic hypermutation in an immune response to *S. aureus*. Blood from an individual with previous *S. aureus* infection was sequenced and the resulting antibodies were tested for binding and affinity to IsdB.

The fourth chapter takes a closer look at one mAb in particular, STAU-239, and uses it as a case study to investigate cross-reactivity between the NEAT domains of *S. aureus* and *B. anthracis*. The binding sites of STAU-239 to NEAT domains of IsdA and IsdB in *S. aureus* are identified and microscopy is used as a tool to show that STAU-239 binds *B. anthracis* under iron-limiting conditions.

The fifth chapter includes a summary and future directions for my work. I believe the work I have done contributes to the iron field of *S. aureus*, but there are clear avenues that link this work to the field of nutritional immunity on a wider scale. The tools I describe here may also be useful in informing vaccine design or serving as tools for drug-conjugates.

Introduction to *Staphylococcus aureus*

S. aureus is a Gram-positive, commensal bacterium and a member of phylum Firmicutes. *S. aureus* asymptomatically colonizes the anterior nares and skin of ~30% of the human population (Wertheim et al. 2005). Though it may start as a commensal, *S. aureus* often becomes an invasive pathogen once it has breached normal host innate immune defenses and is capable of infecting nearly every organ in the body. *S. aureus* is a leading cause of skin and soft issue infections, bacteremia, endocarditis, and osteomyelitis (Tong et al. 2015). These infections can be varied in both their origin and severity with healthy individuals more likely to have community-acquired skin or soft

tissue infections such as impetigo while nosocomial infections may occur after surgery of an implanted device like a catheter (Hogan et al. 2015). The increased incidence and severity of these infections has led to overtreatment with antibiotics, resulting in the current paucity of effective treatment options for *S. aureus*. Methicillin-resistant *Staphylococcus aureus* (MRSA) has reached high prevalence leading to the World Health Organizations adding it to a list of high priority pathogens in 2017 (WHO 2017). Currently, the standard treatment for MRSA is vancomycin but resistance has begun to emerge to this antibiotic (Davis et al. 2015). Because of these issues, there is a need for novel alternative therapeutic treatments for *S. aureus* infections.

The importance of iron acquisition and heme metabolism

Heme is an important cofactor for hemoglobin and the acquisition of iron from heme is fundamental to Staphylococcal growth and pathogenesis. Biochemically, heme consists of an iron ion complexed to a porphyrin ring. This structure fundamentally contributes to heme's function by allowing heme-iron to play a role in the transfer of electrons. Further, heme itself is an important cofactor, contributing to enzymes that function in the electron transport chain, produce catalase, and process microRNA (Choby and Skaar 2016). Heme-iron specifically, has been targeted as a relevant area of interest as the most abundant and preferred form of iron in the human host, with heme iron representing greater than 80% of the body's total iron. While iron can be sequestered by heme-iron, transferrin-iron, or hemoglobin-iron, both hemoglobin- and heme-derived iron have been shown to be the preferred source of iron by *S. aureus* (Skaar et al. 2004; Torres et al. 2006). In order to access this rich iron source, staphylococcal factors lyse red blood

cells, releasing hemoglobin. *S. aureus* has evolved an iron regulated surface determinant system (Isd), which contains surface receptors specific for binding this freed hemoglobin. Once hemoglobin is bound, the Isd protein removes the heme cofactor and transports free heme into the cytoplasm. Finally, free heme is released from the tetrapyrrole by heme-degrading monooxygenases. This allows *S. aureus* to scavenge heme iron from the human host, utilizing the iron for its own metabolism (Pishchany et al. 2014). Because of this, targeting heme metabolism is a promising area of research for potential therapeutics.

The iron-regulated surface determinant system and NEAr Iron Transport domains

Previous work with *S. aureus* indicates that cell wall-anchored proteins play a large role in virulence, evasion of the immune system, and adhesion to host cells (Foster et al. 2014). These cell wall proteins are enzymatically anchored by the actions of sortase enzymes, which cleave proteins at a conserved LPXTG motif. Sortase mutants have been shown in a variety of studies to reduce the virulence of *S. aureus* in animal models of infection (Jonsson et al. 2002; Mazmanian et al. 2000; Mazmanian et al. 2002; Mazmanian et al. 2003). Many of these proteins also partner with ABC transporters to import metals or nutrients in and out of the cell as needed. Most transporters are composed of three main proteins: an ATP-binding protein, an integral membrane transporter, and a surface binding lipoprotein. The heme-iron binding system of interest here, the Isd system, contains cell wall anchored proteins that bind hemoglobin and haptoglobin to extract heme (Figure 1). The three surface-exposed proteins, IsdA, IsdB, and IsdH, are responsible for binding extracellular heme and transferring it to IsdC, which is also anchored in the peptidoglycan. Heme is next transferred from IsdC to the

first member of the ABC transporter, IsdE. IsdE is a substrate-binding lipoprotein that works in association with IsdF, the membrane permease. IsdD is another membrane protein that is thought to function in association with IsdEF for ATP hydrolysis (Hammer and Skaar 2011). The ATPase that powers the ABC transporter is undefined, but it is speculated that it is FhuC, the same ATPase that powers the HtsABC and SirABC transporters, which are involved in siderophore transport (Beasley et al. 2009).

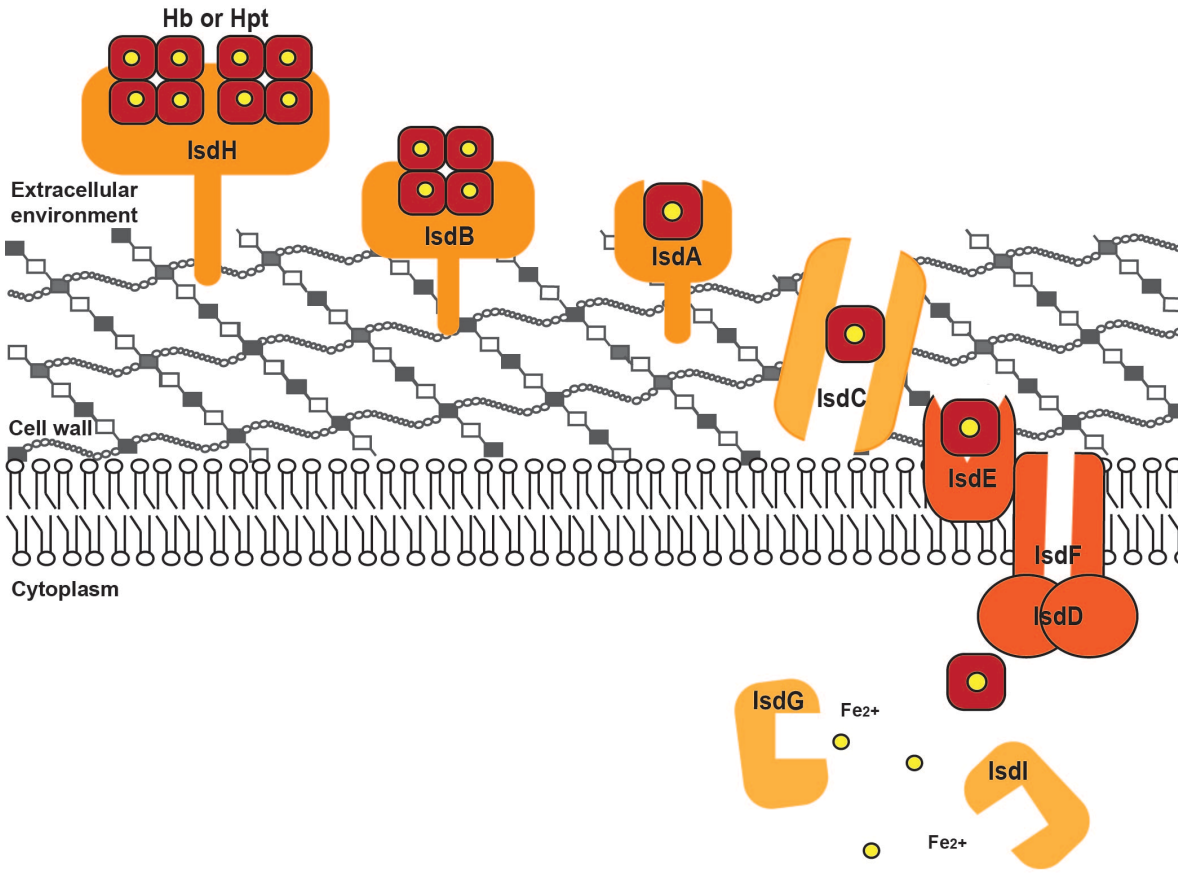

Figure 1-1. Isd system of *S. aureus*.

The iron regulated surface determinant system (Isd) contains cell wall anchored proteins that bind hemoglobin and haptoglobin to extract heme. The three surface-exposed proteins, IsdA, IsdB, and IsdH, help with the binding and transferring of heme to IsdC, which transfers heme to the ABC transporter IsdDEF.

The Isd system is the predominant source of iron acquisition in *S. aureus*. Although iron can be acquired through transferrin mediated mechanisms or siderophore transport systems such as SirABC or HtsABC, a number of studies have shown that the three surface anchor proteins, IsdA, IsdB and IsdH, are important in staphylococcal virulence due to their critical role in the uptake of heme-iron. Inactivation of the hemoglobin receptors *isdB* and *isdH* leads to a decrease in staphylococcal growth when hemoglobin is the sole iron source. Furthermore, inactivation of both *isdB* and a double mutant *isdBH*, leads to a 1-log reduction in bacterial burden in both the kidney and spleen of mice when used in a murine sepsis model of infection (Torres et al. 2006). Mutation of *isdA* or *isdB* decreases organ abscess formation and bacterial burden in a murine systemic infection model (Pishchany et al. 2009). Experiments have shown that IsdA and IsdB are important for adhesion and colonization of staphylococcal infection. Specifically, IsdA is important for the colonization of nares and is involved in the adhesion of *S. aureus* to the squamous epithelium (Zapotoczna et al. 2013). IsdB directly binds to B-3 integrins, which promotes bacterial adhesion and invasion of mammalian cells (Zapotoczna et al. 2013). All of this evidence underscores that these proteins are necessary for the growth and virulence of *S. aureus* (Grigg et al. 2007a; Pishchany et al. 2010; Reniere and Skaar 2008; Torres et al. 2006).

The surface proteins of the Isd system are classified by a conserved NEAr iron transporter (NEAT) domain that is important for the capture of heme and hemoglobin (Grigg et al. 2010). The NEAT domain is a stretch of approximately 120 amino acids that structurally resembles an immunoglobulin β-sandwich fold (Pilpa et al. 2006) (Figure 1-2). NEAT domains are widely conserved throughout Gram-positives, and there are

NEAT containing proteins in *B anthracis*, *C. perfringens*, and *C. diphtheria* (Choo et al. 2016; Ekworomadu et al. 2012; Lyman et al. 2018). In the model proposed here for *S. aureus*, the three surface Isd proteins contain different numbers of NEAT domains. IsdH contains three NEAT domains with IsdH-N1 and IsdH-N2 binding hemoglobin and haptoglobin but IsdH-N3 binding heme (Dryla et al. 2003; Pilpa et al. 2009). IsdB has two NEAT domains with IsdB-N1 binding hemoglobin and IsdB-N2 binding heme (Bowden et al. 2018; Fonner et al. 2014). Finally, IsdA has one NEAT domain (Figure 1-2), IsdA-N1 that binds heme when it is transferred from IsdB and IsdH (Grigg et al. 2007b; Mazmanian et al. 2003). Current structural data support a model where heme is extracted from hemoglobin or haptoglobin and unidirectionally transferred from either IsdB or IsdH to IsdA or IsdC (Muryoi et al. 2008). Heme transfer data suggest that IsdC serves as a critical and central conduit for heme transfer and that IsdE receives heme from IsdC (Moriwaki et al. 2013). IsdE does not, however, contain a NEAT domain but rather belongs to a group of periplasmic heme-binding proteins that coordinate heme using histidine and methionine instead of tyrosine (Grigg et al. 2007a).

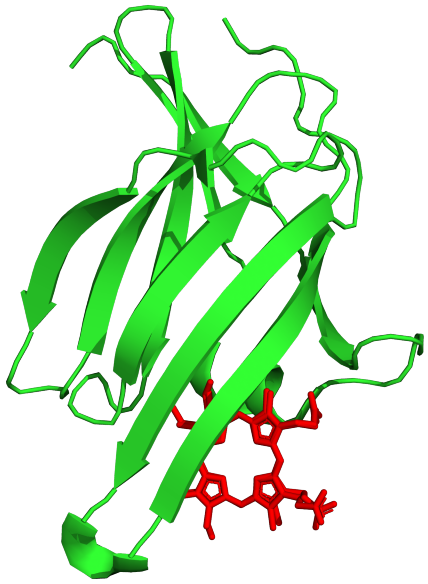

Figure 1-2. Crystal structure of IsdA-NEAT1 bound to heme.

The solved crystal structure of IsdA-NEAT1 is shown in green, highlighting the distinct β-sandwich folds that are characteristic of the NEAT domains. Heme is shown in red (PDB ID: 2ITF) (Grigg et al. 2007).

The Isd system as a therapeutic target

While IsdB, IsdA, and IsdH are all important components of the Isd system, IsdB is the main mechanism by which *S. aureus* binds hemoglobin. As mentioned, the NEAT domain of IsdB is responsible for its hemoglobin binding ability (Grigg et al. 2007b; Pishchany et al. 2014). Blocking of this NEAT domain by antibodies may serve as an effective inhibitor of hemoglobin binding and iron uptake for the bacterium. IsdB is also particularly immunogenic, which increases the chances of isolating mAbs, and the likelihood that these isolated mAbs will successfully elicit an immune response within the host (Kuklin et al. 2006). Because of these studies, IsdB has been recognized as a promising candidate for vaccine trials. In a study conducted at Merck in 2006, mice

immunized with recombinant IsdB were protected against lethal *S. aureus* infection. A single dose of IsdB was also shown to increase the antibody titer to IsdB five-fold in rhesus macaques after one immunization (Kuklin et al. 2006). A panel of murine monoclonal antibodies specific to IsdB was subsequently isolated at Merck in 2009. Characterization of these antibodies revealed that there are several unique epitopes recognized by anti-IsdB mAbs, which increases the potential range of targets for future antibody therapeutics. Furthermore, several of these monoclonal antibodies were shown to be protective in a murine model, although the exact mechanism of action was not elucidated (Brown et al. 2009; Ebert et al. 2010). These preliminary studies indicate that the Isd system is a valid preclinical model. These studies and others led to the development of a novel vaccine by Merck, Merck V710, containing only IsdB as an antigen (Harro et al. 2010). Although the IsdB vaccine ultimately failed in Phase III trials, there are a number of reasons related to the design of the vaccine that may have undermined the study, including lack of an adjuvant, dosage (one), and use of only a single antigen (Bagnoli et al. 2012; Fowler and Proctor 2014; Joshi et al. 2012; Proctor 2012).

While IsdB has been of extreme interest in the field, much less has been studied about the related surface protein, IsdA and its role in protective immunity. However, one group identified increased IsdA antibody levels in patients with MRSA, comparative to the serum antibody response to IsdB (Diep et al. 2014; Verkaik et al. 2010; Vu et al. 2016). Anti-IsdA antibodies were also detected in the sera of nearly every bacteremic patient tested in another study (Verkaik et al. 2010). The colonization levels of ~60 young children with *S. aureus* were also tested and the levels of IsdA and IsdH were

higher in colonized children than non-colonized children, indicating these proteins are important for establishing *S. aureus* carriage from a young age (Verkaik et al. 2010). IsdA has been identified as playing a role in biofilm formation both in Leiden human epidermal models and on polysterene surfaces (den Reijer et al. 2016). IsdA antisera is also able to bind and opsonize both *S. aureus* and *S. agalactiae*, establishing the cross-reactive potential of IsdA as a vaccine target (Stapleton et al. 2012). Altogether, this body of work suggests that multiple proteins within the Isd system might be effective targets for antibody therapy.

Human immune response to *S. aureus*

How to develop a productive immune response to *S. aureus* continues to be a problem in the staphylococcal field. Studies have shown that healthy adults maintain a pool of *S. aureus* specific T-cells as well as serum IgG (Colque-Navarro et al. 2010; Kolata et al. 2015). Despite this, there is a high frequency of recurrent infections to *S. aureus* that is not prevented through an initial robust immune response. Therefore, an immune response to *S. aureus* is not protective and it is unclear why. Before vaccine design can be effective, a better understanding of the immune correlates of protection to *S. aureus* will be crucial.

The initial innate immune response to *S. aureus* is overcome by the large array of toxins and virulence factors that can be produced. One of the first barriers to *S. aureus* infection presented by the innate immune system is the complement cascade. This cascade can be activated through three separate pathways: classical, alternative, or lectin; but they all converge at one central protein called the C3 convertase (Pietrocola et al.

2017). *S. aureus* produces a number of virulence factors that specifically target complement including aureolysin (Laarman et al. 2011), fibrinogen-binding protein (Efb) (H. Chen et al. 2010), and staphylococcal binder of immunoglobulin (Sbi) (Zhang et al. 1998; Zhang et al. 1999). Another important component of the innate immune response to *S. aureus* infection is the recruitment of professional cells like phagocytes, dendritic cells and neutrophils to the site of infection by cytokines and chemokines. Once *S. aureus* is recognized at the site of infection, neutrophils leave the blood and migrate to the site of infection to engulf the foreign cells (Pietrocola et al. 2017). *S. aureus* also excretes multiple proteins to inhibit this process including chemotaxis inhibitory protein of *S. aureus* (CHIPS) that interferes with neutrophil activation and Staphopain A (de Haas et al. 2004), a protease which cleaves a portion of the CXCR2 chemokine receptor (Laarman et al. 2012). *S. aureus* also produces a protein called formyl peptide receptor-like 1 inhibitory protein (FLIPr) that can bind and inhibit the FPRL1 receptor on the surface of neutrophils. FLIPr along with FLIPr-like have both been shown to act as FcγR antagonists as well, reducing successful opsonophagocytosis of *S. aureus* (Guerra et al. 2017; Stemerding et al. 2013).

With the innate immune response being subject to a spectrum of staphylococcal virulence factors, the need for the adaptive immune response to be effective is clear. Evidence for the importance of humoral immunity in fighting staphylococcal infections is reinforced by the observation that individuals who have B cell disorders from Bruton's tyrosine kinase or common variable immunodeficiency, suffer from a greater risk of *S. aureus* infection (Buckley 2004). The hero of the humoral branch of the adaptive immune system is the B cell that recognizes circulating foreign pathogens, like *S. aureus*,

triggering its activation and differentiation into antibody-secreting plasma cells. Once antibodies are secreted, they can neutralize *S. aureus* in four main ways (Figure 1-3) (Broker et al. 2014). Antibodies can block by directly binding to either a toxin and neutralizing its effect or to a target receptor, thereby preventing the bacteria from activating it. They also coat the foreign bacteria and the Fc portion of the antibody is recognized by phagocytes, which then engulf and kill *S. aureus*. Antibodies bound to *S. aureus* can also be recognized by the complement system, which can either lead to destruction by the membrane attack system or indirectly trigger the chemotactic activity of C3b and C5b which help recruit other immune cells (Thammavongsa et al. 2015). Finally, effector cells such as natural killer cells can release granzymes to kill *S. aureus* by binding the Fc portion of antibodies (Broker et al. 2014).

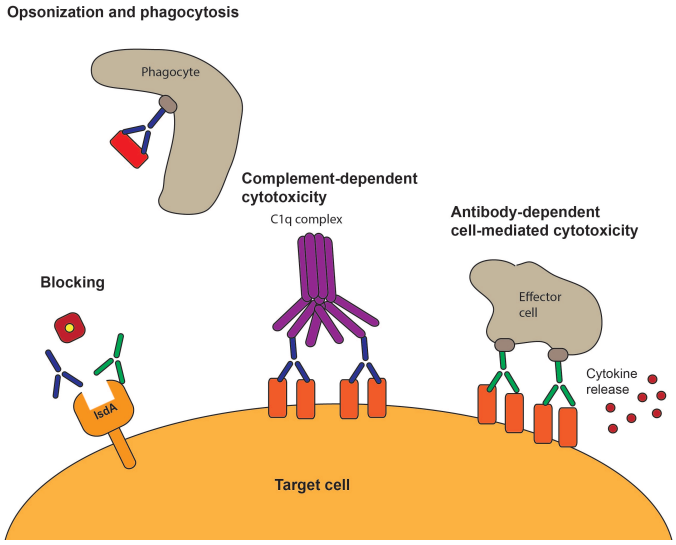

Figure 1-3. Four effector functions of antibodies

Antibodies can fight an invading target cell using a number of different mechanisms including 1. Direct blocking of a receptor or surface protein, 2. Opsonization and phagocytosis, where the antibody marks foreign objects for destruction by target cells 3. Complement-dependent cytotoxicity, where the MAC is engaged and 4. Antibody-dependent cell-mediated cytotoxicity, when an effector cell lyses the invading target cells.

Similarly to its battle against the innate immune system, *S. aureus* manipulates the humoral response through the production of staphylococcal protein A (SpA). SpA is powerful because it can bind to both sides of the antibody molecule, the Fc domain as well as the Fab portion (Thammavongsa et al. 2015). By binding and blocking the Fc portion of the antibody, SpA prevents opsonophagocytosis and binding to the Fab region results in the superantigenic clonal expansion of B cells (Goldmann and Medina 2018). A second protein of similar function was appropriately named second binding protein of immunoglobulin or Sbi. Sbi binds both the Fc portion and the C3 convertase fragment of the complement system, helping *S. aureus* evade neutrophil killing and opsonophagocytosis (E. J. Smith et al. 2011).

Current *S. aureus* vaccines and therapeutics

Although there are a number of antibiotics approved for the treatment of *S. aureus* infection, there are currently no licensed vaccines available. This is due in large part to the numerous immune evasion and virulence factors that may be potential candidates for vaccine development. Unfortunately, previous efforts have failed primarily because of the functional redundancies of these evasion factors, which is further aggravated when only one antigen is targeted in development, which has often been the case. Some previous antigen targets of both vaccines and antibodies include lipoteichoic acid (Pagibaximab) (Weisman et al. 2009), panton-valentine leukocidin (Adhikari et al. 2012), clumping factor A (Veronate) (DeJonge et al. 2007), capsular polysaccharide (Altastaph) (Rupp et al. 2007), IsdB (V710) (Harro et al. 2010), and α-hemolysin (Salvecin, MEDI4893) (Yu et al. 2017). The plethora of failed vaccines has been informative and moving forward

current designs have targeted multiple immune evasion factors. Unfortunately, the most recent vaccine failure to note came in December of 2018 from Pfizer, SA4Ag. This vaccine was terminated "due to futility" during a Phase III expansion study. The name describes its design as it targets four distinct antigens: clumping factor A, MntC, and capsular polysaccharides 5 and 8 (Begier et al. 2017; Creech et al. 2017; Frenck et al. 2017). It is worth noting that several of these antigens have been involved in failed vaccine attempts previously but they were deemed worthy of exploring an additional time in combination with other important virulence factors. The first-generation vaccine did not include MntC and it was added later because of the recognition of how important targeting nutrient acquisition in *S. aureus* is as well as its strong protective phenotype *in vivo* when used to actively immunize mice (Anderson et al. 2012).

It is currently unclear why SA4Ag ultimately failed, but the vaccine was partially effective during the study with >50% efficacy in the study population of individuals undergoing spinal fusion surgery. This was lower than the 80% goal, which is why the vaccine was terminated. This indicates that the scientific principles underlying the vaccine design may still be effective. Something worth considering moving forward is taking into account the genetic regulation of the proteins in the vaccine. For example, expression of MntC in *S. aureus* is tightly regulated and its expression is upregulated in Mn-deplete conditions (Sheldon and Heinrichs 2012). A vaccine may be more effective if a chelator is administered, thereby increasing MntC expression in *S. aureus* and ensuring anti-MntC antibodies are effective. Further, four antigens may simply not be enough. Perhaps a fifth antigen should be added to account for further redundancies in staphylococcal immune evasion mechanisms. Notably, there was no toxin included in

SA4Ag, perhaps because many *S. aureus* toxins are strain specific. However, α-hemolysin is widely conserved and antibodies to this target have previously been shown to be effective in pneumonia, skin and bacteremia murine models of infection (Foletti et al. 2013; Hua et al. 2014).

Drug	Company	Target	Status
StaphVAX	Nabi	CP5/CP8	Stopped Phase III
Pentastaph	Nabi/GSK	CP5/CP8	Stopped Phase III
GSK2392103A	GSK	CP5, CP8, Hla, Clfa	Completed and stopped Phase I
SA75	VRI	Whole cell vaccine	Completed and stopped Phase I
STEBvax	IBT	Seb	Completed Phase I
V710	Merck	IsdB	Stopped Phase III
NVD3	NovaDigm	Als3	Stopped Phase II
SA4Ag	Pfizer	CP5, CP8, ClfA, MntC	Stopped Phase IIb

Figure 1-4. Failed vaccines to *S. aureus*.

There have been a number of vaccines in recent clinical development against *S. aureus*. Many of these vaccines like STEBvax and V710 only targeted one antigen whereas other vaccines focused on multiple antigens but still ultimately failed. The most recent failure, SA4Ag, was ended in late 2018 after recommendations that it would not ultimately be successful in a Phase III trial.

Treatment of *S. aureus* with antibiotics has been made difficult by the emergence of methicillin-resistance. By definition, MRSA is resistant to multiple beta-lactam antibiotics of which methicillin is a part. When this infection occurs, treatment with

vancomycin is one of the first choices for treatment. If vancomycin is not effective, there are a number of alternative antibiotics available depending on the type of infections, such as linezolid or daptomycin. Vancomycin resistance *S. aureus* (VRSA) first occurred in 2002 but is still rare with a total of 14 isolates in the United States (McGuinness et al. 2017; Walters et al. 2015). VRSA infections are characterized by the presence of the *vanA* gene on a plasmid and are associated with persistent *S. aureus* infections and reduced susceptibility to vancomycin (McGuinness et al. 2017). A much more common problem is vancomycin intermediate-resistant *S. aureus* (VISA). Combination therapy may be a successful option when there are problems with vancomycin effectiveness or slow drug efficacy. A number of antibiotic combinations have been tested and found to have additive effects when either vancomycin or daptomycin is used (Davis et al. 2015; Tsuji and Rybak 2006). In severe recurrent cases, triple therapies have been shown to be effective such as a cocktail of vancomycin, daptomycin and rifampicin which was successfully used to treat orthopedic infections (Antony 2006; Tsuji and Rybak 2006). Unfortunately, there is limited clinical trial data to support antibiotic combinations to treat serious MRSA infections. Moving forward, identifying and validating a plan of action using double and triple antibiotic therapies may go a long way in the fight against resistant *S. aureus*.

CHAPTER II

HUMAN MONOCLONAL ANTIBODIES TO *STAPHYLOCOCCUS AUREUS* ISD PROTEINS PROVIDE PROTECTION THROUGH HEME-BLOCKING AND FC-MEDIATED MECHANISMS

Introduction

The public health need for effective *S. aureus* treatments is substantial. With 30-50% of the population asymptomatically colonized (Wertheim et al. 2005), resistance to vancomycin emerging, and no licensed vaccine, there is a demand for a reevaluation of the current treatments. One way to address this problem is pursuing alternative treatments, like antibodies. The importance of the humoral immune response to *S. aureus*, as well as what are the correlates of protection, have been hotly debated due to all the previous failed vaccine attempts. One way to contribute to this discussion is to define the human immune response to relevant staphylococcal proteins, such as those involved in metal transport. I did this by isolating human monoclonal antibodies from subjects with previous natural infection and determining their epitopes. Heme is an important cofactor for hemoglobin and the acquisition of iron from heme is fundamental to staphylococcal growth and pathogenesis. Because of their specialized ability to capture and transport heme-iron, these proteins are necessary for the growth and virulence of *S. aureus*. The iron-regulated surface determinant (Isd) system contains cell wall anchored proteins that can bind these hemoproteins and extract heme. Because of their specialized ability to

capture and transport heme-iron, the proteins of the Isd system represent viable targets not only for antibody discovery, but also for exploring the protective role of antibodies in *S. aureus* infection.

In this chapter, I identified cross-specific human monoclonal antibodies that bind to the three surface proteins of the Isd system: IsdA, IsdB, and IsdH. I identified antibodies that were both specific for each Isd protein and cross-reactive for all Isd proteins, underscoring the conservation of heme- and hemoglobin-binding within these proteins. Using a murine septic model of infection, we discovered two antibodies that work cooperatively to decrease bacterial burden by an Fc-mediated mechanism, whereby the Fc portion of an antibody binds and cross-links the FcγR receptor of an effector cell. These data expand upon current understanding of the importance of IsdA-antibodies and highlight the value of Fc-mediated antibody functions in protective immunity to *S. aureus* infection.

I would like to acknowledge Dr. Marcus B. Nagel and Kevin L. Schey for performing HDX-MS of STAU-239 in complex with IsdA. I would finally like to thank Dr. Isaac P. Thomsen for securing MRSA donors for this study.

Isolation and characterization of anti-Isd *S. aureus* human mAbs

Donor blood samples used in this study were obtained at Vanderbilt University Medical center after confirmation that subjects were positive for invasive MRSA or MSSA (methicillin-sensitive *S. aureus*) infection. Samples were collected during the convalescent period, approximately 4-6 weeks following *S. aureu*s infection. We obtained peripheral blood mononuclear cells (PBMCs) by Ficoll density centrifugation

from the de-identified blood samples and cryopreserved them. Six human subjects of varying age, sex, and degree of infection severity were used (Table 2-1).

Table 2-1. Summary of human subject information.

Subject Number	Age	Sex	Race	Invasive Disease	Clinical diagnosis
1	20	F	White	MSSA[1]	Cellulitis and osteomyelitis
2	9	M	African American	MSSA	Septic arthritis and osteomyelitis
3	41	M	White	Healthy donor[2]	N/A
4	46	M	African American	MRSA[3]	Endocarditis
5	11	F	White	MSSA	Sepsis and pyomyositis
6	15	M	White	MSSA	Sepsis and multifocal osteomyelitis

[1] MSSA indicates methicillin sensitive *Staphylococcus aureus*

[2] Otherwise healthy subject with an unrelated history of recent viral infection. There was no specific medical history of *S. aureus* infection in this subject. We used the sample from a healthy subject as a matter of convenience. Since many subjects in the healthy adult population have been colonized on infected with *S. aureus* in the past, it is expected that many healthy subjects have circulating memory B cells reacting with *S. aureus* antigens.

[3] MRSA indicates methicillin resistant *Staphylococcus aureus*

The human hybridoma process began by transforming these PBMCs with Epstein-Barr virus along with Chk2 inhibitor, cyclosporin A, and CpG. I then plated the transformed cells in 384 well plates for approximately one week before expanding them to 96 well plates using irradiated feeder layers. After another five days, I screened supernatants for binding to recombinant *S. aureus* surface antigens using an enzyme-linked immunosorbent assay (ELISA). Recombinant proteins were checked by SDS-PAGE gel to ensure correct size. Transformed B cells that were reactive against Isd proteins were fused with HMMA2.5 myeloma cells via electrofusion to generate human hybridoma cell lines. This process was used to isolate 29 antibodies that bound IsdA, IsdB, IsdH or some combination of these three proteins. The majority of the isolated mAbs bound to more than one Isd protein. 3 antibodies: STAU-37, -307, and -399 bound to all three surface Isd proteins as determined by ELISA. I determined the half-maximal binding concentration (EC_{50}) of the mAbs to their antigen using an ELISA (Table 2-2). Most cross-specific mAbs bound best to one particular antigen with secondary binding activity to another antigen. A combination of ELISA and RACE sequencing was also done to determine both the immunoglobulin subclass and light chain type of each mAb (Table 2-2).

Table 2-2. Isd mAb binding characterization

Isd binding pattern of antibody[a]	STAU antibody	Subject #	IgG subclass	Light chain	EC_{50}[d] (μg/mL) of indicated mAb		
					IsdA	IsdB	IsdH
A/B/H	307	1	1	λ	0.01	0.00028	0.00001
	399	1	2	λ	8.7	0.53	0.95
	37	2	1	κ	3.8	16.1	17.5
A/H	147	1	2	λ	0.01	>	0.8
	407	1	1	λ	1.6		3.1
B/H	281	3	1	κ	>[c]	0.002	0.0027
	328	1	1	λ		0.08	0.06
	389	1	n.d.[b]	λ		0.13	0.34
A/B	239	1	1	λ	0.07	0.001	>
	229	1	3	λ	0.7	0.01	
	221	1	1	λ	0.03	1.9	
	218	1	1	κ	0.08	4.1	
	201	1	1	λ	0.26	9.5	
	299	1	n.d.	λ	0.22	12.7	
	402	1	1	λ	8.2	3.4	
	138	4	1	n.d.	5.9	9.5	
	401	1	1	λ	25.1	3.7	
	280	1	1	κ	52.1	7.6	
H	139	4	1	λ	>	>	2.7
B	75	5	1	κ	>	0.02	>
	64	5	1	κ		0.14	
	141	4	1	κ		10.2	
A	158	1	1	κ	0.01	>	
	231	1	1	λ	0.9		
	181	1	n.d.	κ	0.7		
	245	1	1	κ	0.2		
	22	6	1	κ	0.3		
	228	1	1	κ	3.2		
	149	1	1	κ	0.2		

[a]Indicates the binding pattern of each antibody based on IsdA, IsdB, or IsdH protein binding.
[b]n.d. indicates the experiment was repeated but the subclass or light chain could not be determined.
[c]> symbol indicates binding was not detected at the maximal concentration tested of 20 μg/mL.
[d]EC_{50} denotes the half-maximal binding concentration of antibody to the antigen

Competition binding of anti-Isd human mAbs

To group the identified mAbs and determine the major epitopes targeted, I performed biolayer interferometry or BLI. Recombinant IsdA or IsdB was biotinylated and used to coat streptavidin biosensor tips, which were then associated with a first and then second mAb. Competition was determined by calculating the percent binding of the second mAb in the presence of the first mAb (Figure 2-1). Antibodies did not strongly bind on BLI were not used in this analysis. Ten antibodies to IsdA were grouped into 3 competition groups based on binding and another 13 antibodies to IsdB were grouped into 3 distinct competition groups as well (Figure 2-1). CS-D7 was included in the experiment with IsdB as it is a previously isolated human mAb to IsdB that was the basis of the V710 vaccine (Ebert et al. 2010). It did not compete with any of the tested anti-IsdB mAbs.

STAU-149 is the only mAb that binds sufficiently to both IsdA and IsdB that it competed with both antigens. Although multiple other cross-reactive mAbs bound to both IsdA and IsdB by ELISA, they did not bind to both antigens by BLI. This prevented these antibodies from being assigned to a proper competition group by this analysis but points to the possibility of a fourth overlapping antigenic site for these mAbs. Two additional antibodies, STAU-239 and -245, were members of an overlapping competition group to IsdA (shown in blue and orange in Figure 2-1), which suggests they may bind to a major antigenic site of importance.

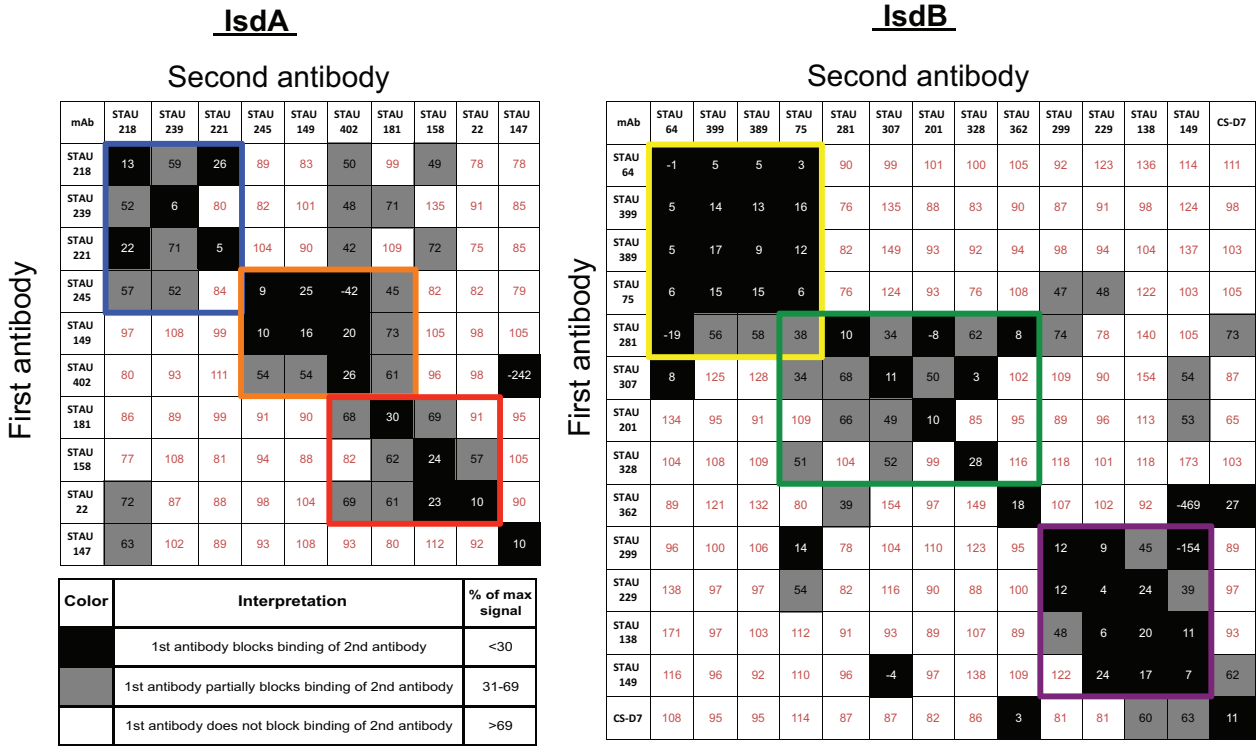

Fig 2-1. Competition-binding of IsdA- or IsdB-specific antibodies.

Biolayer interferometry was used on anti-IsdA (left panel) and anti–IsdB (right panel) human mAbs. IsdA and IsdB were biotinylated before loading onto streptavidin tips and binding to a first and then second antibody. Data above indicate the percent binding of the second antibody to the biosensor tip in the presence of a bound first antibody. Black boxes show the first antibody blocked binding of the second antibody by more than 70%, grey boxes show partial blocking and white boxes indicate the first antibody did not block binding of the second antibody to the biosensor tip. Assigned competition-binding groups are outlined in colored boxes.

Human mAb prophylaxis against *S. aureus* in a murine septic model of infection.

I tested antibodies from each competition group in a septic model of murine infection either alone or in combination (Figure 2-2). In this mouse model, antibodies are given via the intraperitoneal route approximately 2 hours before retroorbital infection with *S. aureus*. Strain Newman was used unless specified at an inoculum of ~10^7 CFU. Purified antibodies were given at a total dose of 10 mg/kg (if 2 antibodies were given in combination then each individual mAb would be at a 5 mg/kg concentration). After 96 hours, mice were euthanized by CO_2 inhalation and the heart, kidneys, and liver were harvested and processed in sterile PBS to determine colony forming units/organ. As Figure 2-2 shows, the majority of tested antibodies did not show a significant reduction in bacterial burden when tested, indicating that these antibodies did not bind to a biologically relevant epitope. However, two antibodies, STAU-239 and -245, reduced bacterial burden nearly 100-fold in the heart, kidneys and liver compared to the isotype control (Figure 2-3). As mentioned previously, these antibodies are in overlapping competition groups, so it was unclear which mAb was responsible for the *in vivo* phenotype or if both mAbs played a role. In order to determine which mAb was sufficient for the observed prophylactic effect, I tested each one alone. STAU-239 did not significantly reduce bacterial burden in any organ when administered alone whereas STAU-245 reduced burdens in the heart, kidneys, and liver. Interestingly, STAU-245 reduced bacterial burden by only 10-fold, less than the 100-fold reduction when used in combination with STAU-239. These results indicate that the combination of STAU-239 with STAU-245 results in a cooperative effect with a greater reduction to *in vivo* burdens

than when either mAb is used alone. The 10-fold reduction obtained with STAU-245 is also consistent with what would be expected by blocking the function of *isdA*, as previously published data had shown that when infecting mice with an Δ*isdA* mutant *S. aureus* strain there is a 10-fold reduction in burden (Pishchany et al. 2009). The cooperative effect of STAU-239 and -245 is further supported by the weight loss data which show that the animals injected with both antibodies lost the least amount of weight as calculated as percent starting weight (Figure 2-3).

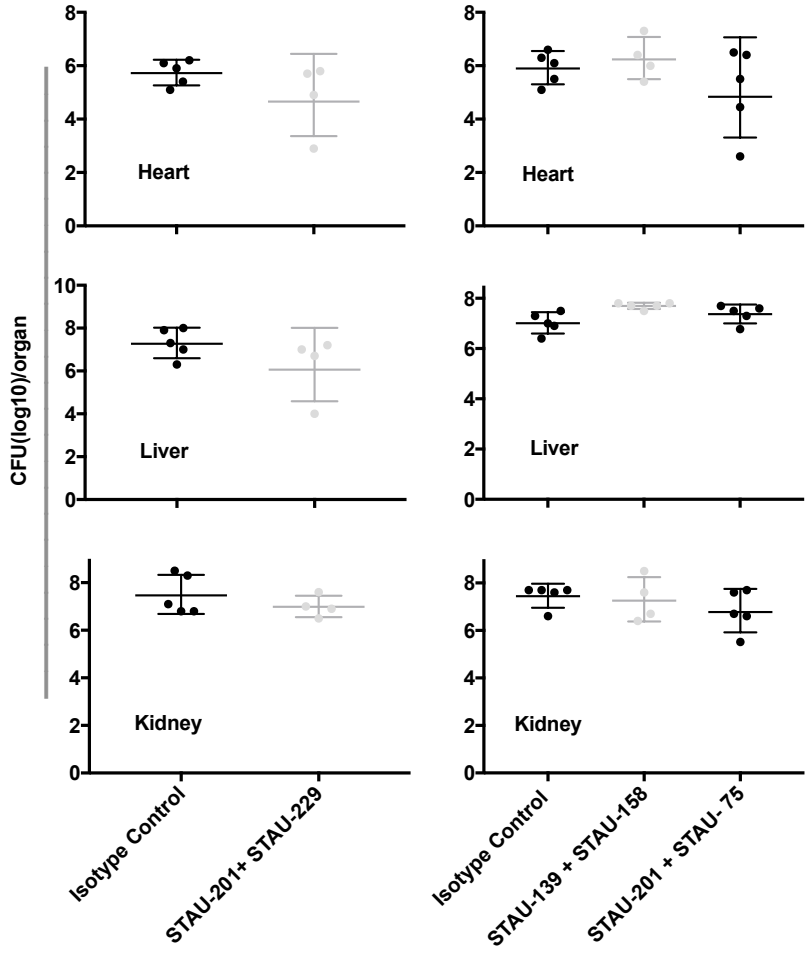

Figure 2-2. mAbs from competition binding groups do not reduce bacterial burden.

Antibodies from each competition group were tested by IP administration two hours before infection with *S. aureus*. The two competition groups represented by STAU-239 and STAU-245 are shown in Figure 2-3. Each panel represents an independent experiment and was not combined. mAbs were given at a concentration of 5 mg/kg for a total mAb dose of 10 mg/kg. After 96 hours, organs were harvested for CFU enumeration. Statistical significance was determined by ANOVA but there was no significant reduction in burden in any group tested.

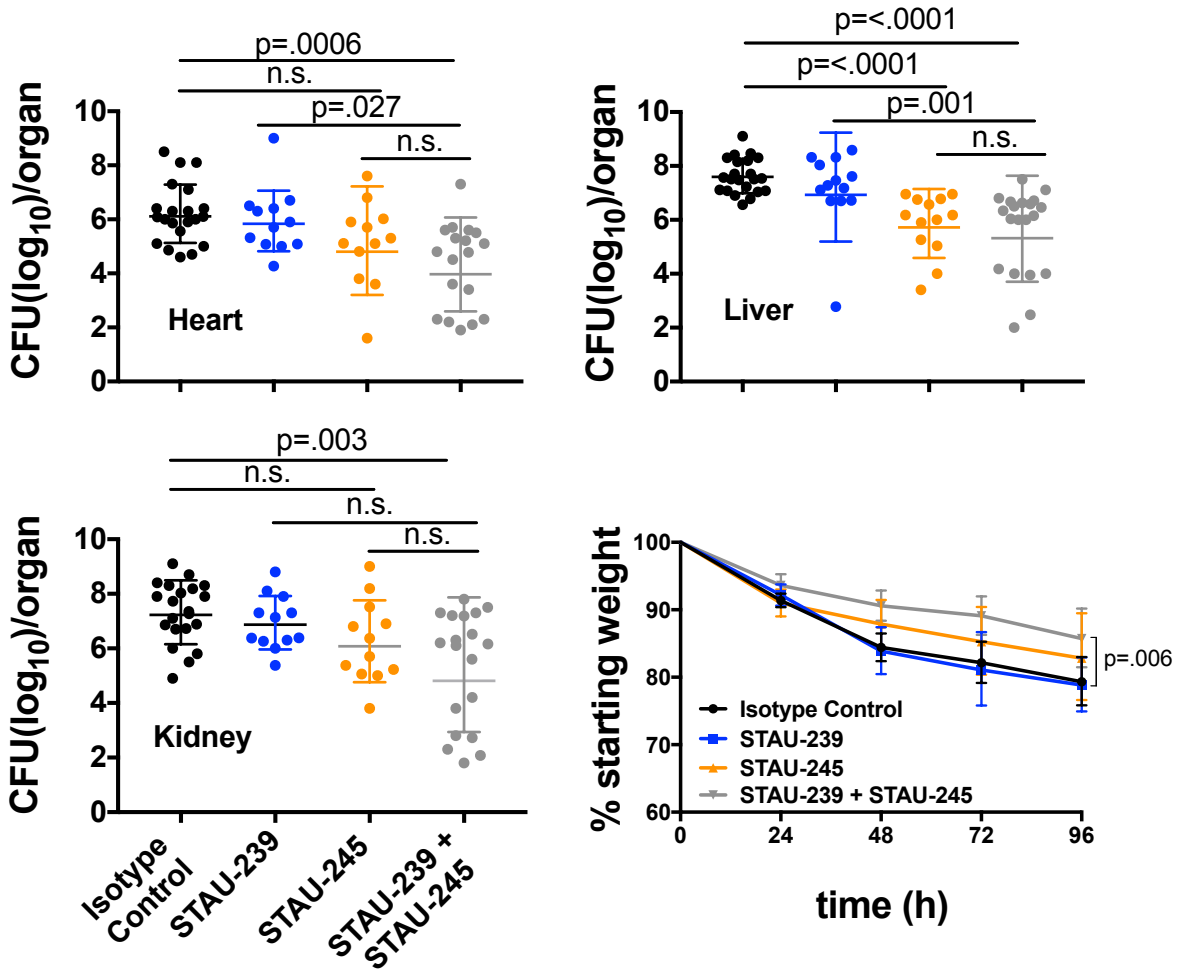

Figure 2-3. STAU-239 and STAU-245 work cooperatively to reduce bacterial burden *in vivo*.

Seven-week old female BALB/c mice were inoculated retro-orbitally with *S. aureus* strain Newman. After ninety-six hours, the heart, livers, and kidneys of the infected mice were harvested and CFU counts were determined by serial dilution plating. P values as determined by ANOVA are shown. Weight loss over the course of 96 hours was calculated as a percentage of the starting weight.

Partial inhibition of *S. aureus* by mAbs with hemoglobin as a sole iron source

I hypothesized that STAU-239, STAU-245 or both mAbs were inhibiting the pathogenesis of *S. aureus* by preventing binding to hemoglobin and subsequent uptake of

heme-iron. This was tested *in vitro* using *S. aureus* growth curves in iron-depleted conditions. I incubated *S. aureus* overnight in the presence of an iron chelator, EDDHA. The overnight was then normalized to 1.0 according to OD_{600} and subcultured into fresh tubes along with media containing 1) no hemoglobin (untreated), 2) hemoglobin, 3) hemoglobin + STAU-239, 4) hemoglobin + STAU-245, or 5) hemoglobin + the STAU-239 + STAU-245 combination. A Biotek reader was used to measure OD_{600} at time points 0, 9, 24, and 34 hours (Figure 2-4). As expected, untreated samples that did not contain hemoglobin did not grow well due to a lack of hemoglobin as an iron source. Samples that were treated with hemoglobin grew to an OD_{600} of >1.0 by the end of the experiment. Treatment with each combination of mAbs lead to a partial inhibition of growth in comparison to hemoglobin alone treated groups. I did not detect a significant decrease in the amount of growth between the three antibody treated groups, underscoring the hypothesis that the combination of mAbs was most effective at hemoglobin blocking (Figure 2-4). Finally, the ability of *S. aureus* to still partially grow in the presence of hemoglobin + mAbs indicates that hemoglobin blocking may not be the principal or sole mechanism by which these mAbs inhibit *S. aureus* growth.

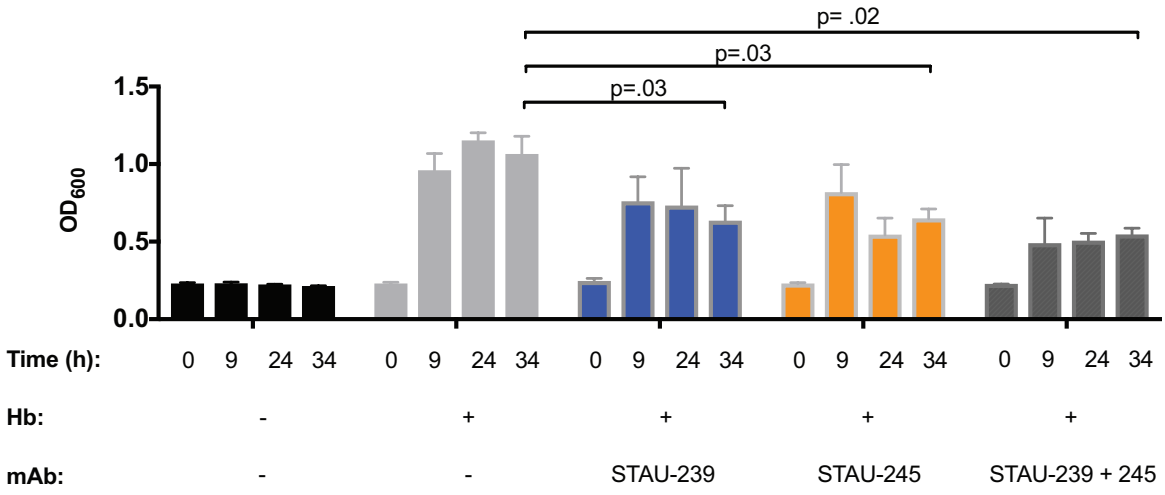

Figure 2-4. Partial inhibition of *S. aureus* hemoglobin-dependent growth.

S. aureus strain Newman was cultured overnight in RPMI with 1 μM EDDHA to iron-starve and normalized before being subcultured and grown for 34 hours. Untreated indicates there was no addition of hemoglobin (Hb) or mAb. Statistically significant differences were determined by an unpaired t-test where the Hb treated group was set as the comparator.

Comparison of the binding sites of STAU-239 and -245 on IsdA

In collaboration with the mass-spec research center, a technique called hydrogen-deuterium exchange mass spectrometry (HDX-MS) was used to determine binding sites at peptide level resolution of STAU-239 and STAU-245. HDX-MS compares the relative deuterium uptake in two different states in order to identify amino acids involved in protein-protein interactions. This is helpful for identifying antigen-antibody binding sites because HDX-MS digests the antigen into overlapping peptides and those peptides with decreased deuterium uptake are the sites where the antigen is bound. Purified Fab fragments of STAU-239 and STAU-245 were tested for binding to IsdA and both mAbs were found to bind within the NEAT domain of IsdA (Figure 2-5). The binding site is shown modeled onto a previously crystallized structure of the NEAT domain with the NEAT domain in green and heme shown in red. STAU-239 bound to peptide residues H158-V161 and P162-Y166 (blue), which is near the heme-binding pocket of IsdA-NEAT1. In contrast, STAU-245 bound away from the heme-binding pocket, to peptides N120-L126 and A127-T128 (orange).

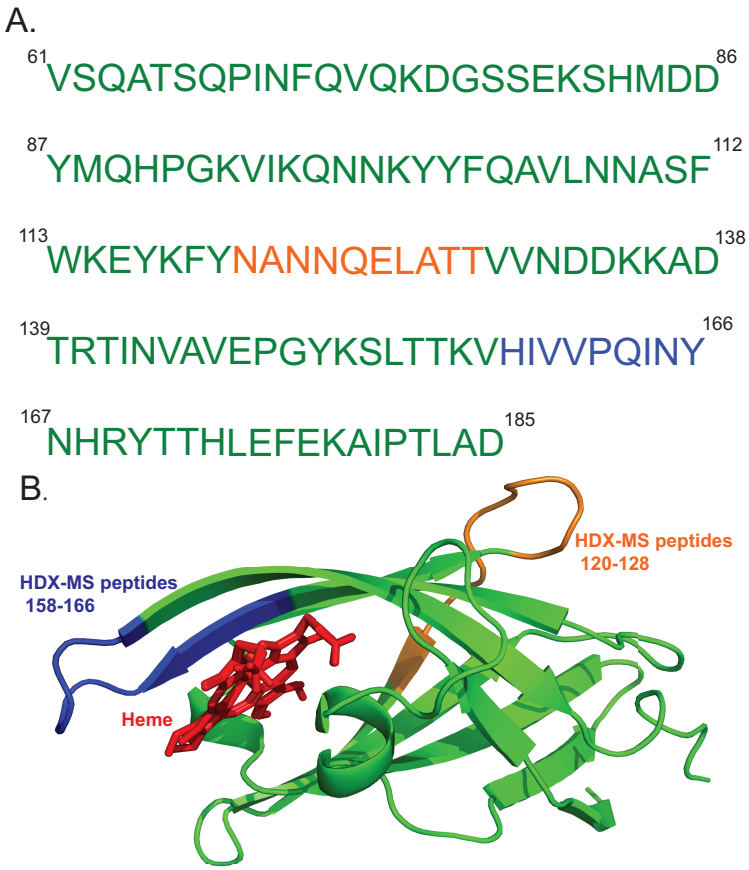

Figure 2-5. Binding sites of STAU-239 and STAU-245 on IsdA-N1 are identified using HDX-MS.

A, The sequence of IsdA-N1 is shown and residues with the strongest decrease in deuterium uptake when IsdA is tested in the presence of either STAU-239 (blue) or STAU-245 (orange) are colored *B,* The crystallized structure of the IsdA-N1 [PDB ID]: 2ITF is shown binding heme (red) with the predicted binding sites of STAU-239 (blue) and STAU-245 (orange).

Fc-mediated functions important for anti-Isd mAbs

An antibody is divided into two regions, the top half, called the Fab which is variable and binds antigen and the bottom, called the Fc which binds to Fc receptors and mediates secondary functions. These secondary functions include antibody-dependent cellular phagocytosis (ADCP), complement activation (CDC), and antibody-dependent cellular cytotoxicity (ADCC). The Fc region of the antibody is divided into two sections, CH2 and CH3 and their interface is important for binding Fcγ receptors. Substitutions in this region functionally prevent antibody binding to FcγRI, FcγRII, or FcγRIIIa. In order to test the contribution of the Fc region of mAbs STAU-239 and STAU-245 to the observed *in vivo* phenotype, variant antibodies were made where leucine residues at positions 234 and 235 of the CH2 domain were mutated to alanine (L234A/L235A or LALA). These substitutions prevent binding of the antibodies to Fcγ receptors, thereby functionally preventing downstream Fc effector functions. The LALA mAbs were expressed recombinantly in Expi293 cells and tested using BLI to ensure they still bound to IsdA despite the mutation. I then tested both types of mAbs: full length IgG and LALA variants in the *in vivo* septic model of infection. There was not a detectable difference in bacterial burden between the two LALA variants and the isotype control in any of the organs (Figure 2-6). This finding indicates STAU-239 and STAU-245 employ Fc-mediated function to reduce bacterial burden *in vivo*.

To narrow down which secondary Fc-function these mAbs might use, I tested them *in vitro* in an antibody-dependent cellular phagocytosis (ADCP) flow based assay. ADCP is when antibodies coat the surface of foreign particles, targeting them for elimination in a process called phagocytosis by macrophages. This assay used fluorescent

beads coupled to the antigen, IsdA. Antibody titrations were incubated with the antigen and a human leukemia monocytic cell line, THP-1. Phagocytic activity was measured as "phagocytic score" and determined by calculating (%FITC + cells) * (MFI of FITC + cells). This assay showed that STAU-245 had a 2-fold increase in phagocytic score compared to the negative control sera, indicating STAU-245 facilitates phagocytosis (Figure 2-7). Although STAU-239 may function by blocking heme, it appears STAU-245 mediates phagocytosis. These data help explain the observed cooperativity phenotype as these mAbs mediate two separate and distinct functions.

.

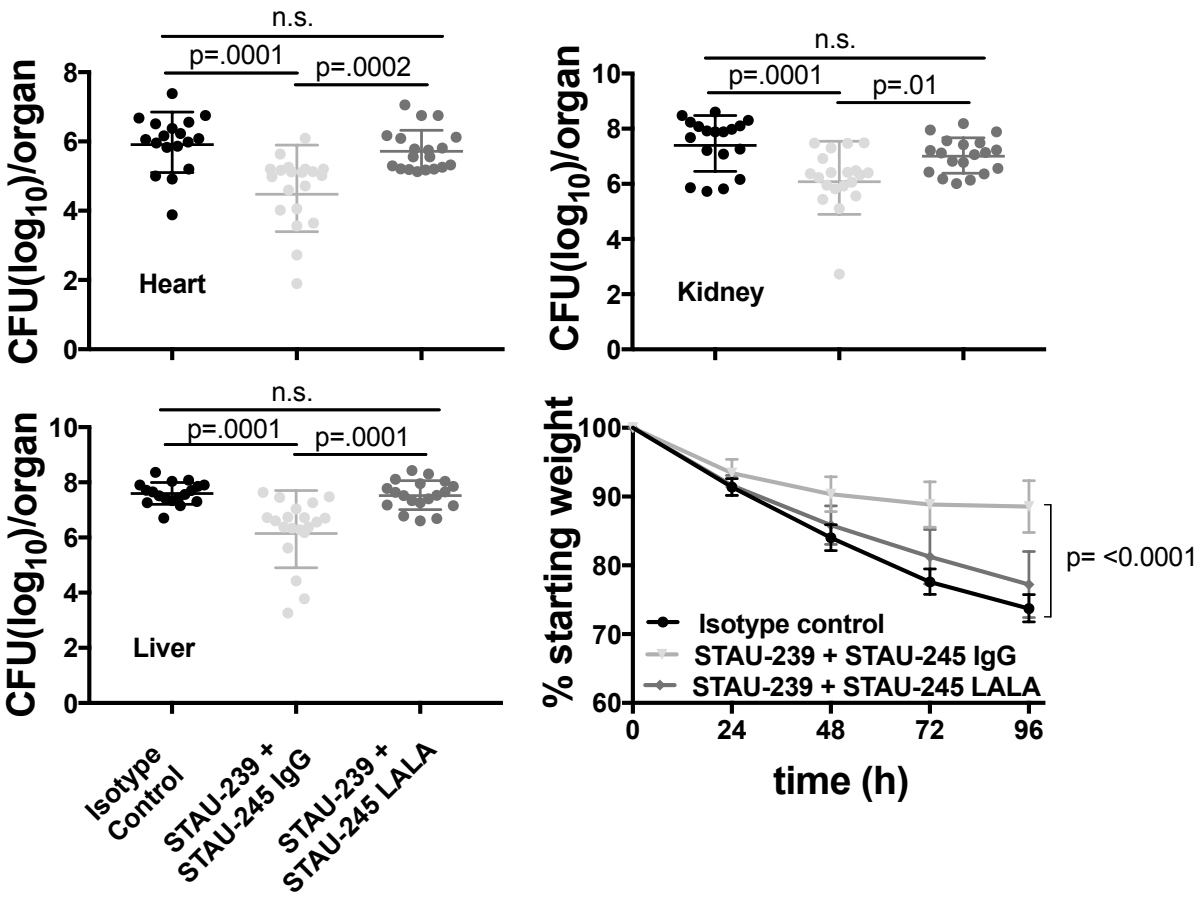

Figure 2-6. STAU-239 + STAU-245 Fc variants do not reduce bacterial burden in a septic model of murine infection.

Seven-week old female BALB/c mice were inoculated retro-orbitally with *S. aureus* strain Newman. Mice were given one of two mixes: STAU-239 + 245 IgG or STAU-239 + 245 LALA (L234A, L235A) by the IP route two hours before infection. After ninety-six hours, the heart, livers, and kidneys of the infected mice were harvested and CFU counts were determined by serial dilution plating. P values as determined by ANOVA are shown. Weight loss over the course of 96 hours was calculated as a percentage of the starting weight.

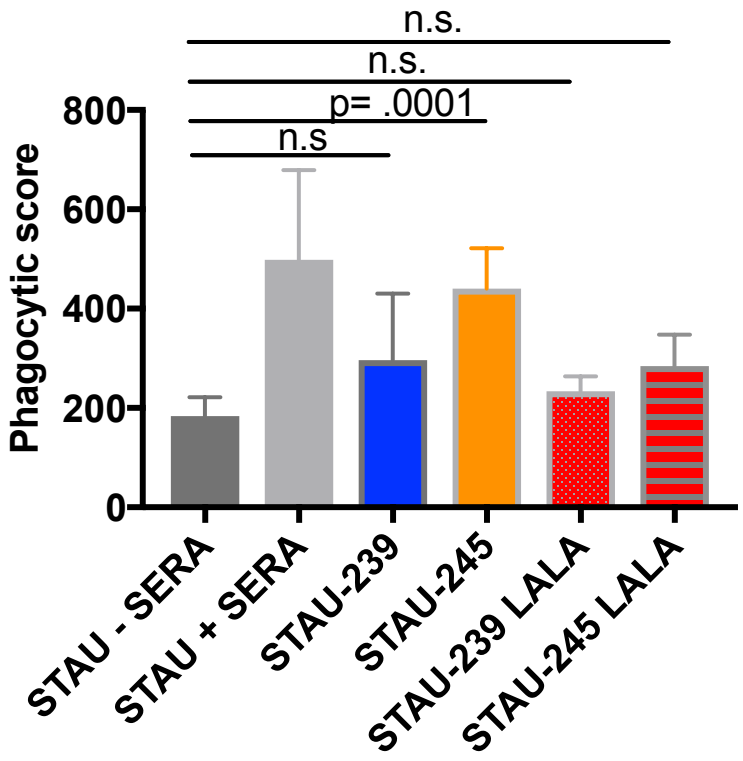

Figure 2-7. STAU-245 induces ADCP.

Recombinant IsdA was biotinyated and coupled to Alexa Flour 488 NeurAvidin beads before incubating with STAU-239 and STAU-245. THP-1 cells were added at 2.0 x 10^4 cells/well and incubated overnight at 37°C. Cell were fixed and read by a flow cytometer to determine phagocytic score using (%FITC + cells) * (MFI of FITC + cells).

Discussion

Despite the continuing public health threat that *S. aureus* poses, the search for a licensed vaccine continues. Diverse bacterial targets have been studied previously including toxins, adherence factors and lipoproteins without success (Diep et al. 2014; Foster et al. 2014; O'Riordan and Lee 2004; Rouha et al. 2015). Targeting staphylococcal iron acquisition is a decisive way to interrupt *S. aureus* pathogenesis and a number of previous studies have shown the importance of these proteins in multiple infection models in mice, rats, and macaques' (Clarke et al. 2006; Ebert et al. 2010; Joshi et al. 2012; Stranger-Jones et al. 2006). A previously isolated panel of murine mAbs specific to IsdB showed protection in an *in vivo* murine model of infection but the mechanism of action for the mAbs was not clearly defined (Brown et al. 2009), leaving room for further studies to define and highlight the relevance of the Isd system to staphylococcal pathogenesis (Ebert et al. 2010; Joshi et al. 2012).

Here I describe multiple proteins within the Isd system that might be effective targets for antibody therapy. I identified naturally occurring human Isd antibodies after infection and isolated the first ever panel of IsdA- and IsdH-specific human mAbs, including mAbs that bound to all three Isd surface proteins. Two of the isolated IsdA mAbs showed a cooperative protective effect *in vivo*, which appears to be due to their ability to function by heme-blocking and Fc-mediated phagocytosis. It has been unclear in previous studies whether Isd-antibodies mediate bacterial inhibition solely through the blocking of iron acquisition or whether they also use other antibody functions. My work shows that IsdA, a largely overlooked surface component of the IsdA system, could be an effective component of a preventative vaccine due to its ability to not only interfere with

the acquisition of heme-iron but also by stimulating Fc-binding and its downstream protective effects. One previous study showed that an Isd-specific mAb could inhibit *S. aureus* without blocking heme-iron uptake (Pancari et al. 2012). The anti-IsdB mAb CS-D7 did not possess heme-blocking activity, but rather functioned via a complement-dependent mechanism (Pancari et al. 2012). In the work presented here, the mAbs STAU-239 + STAU-245 only partially inhibited the *in vitro* hemoglobin-dependent growth of *S. aureus*, and this finding indicates this occurs by an indirect mechanism of inhibition based on the mAbs binding locations. Neither mAb binds to the NEAT domain of IsdA; therefore, any reduction in hemoglobin-dependent growth likely is due to allosteric changes occurring when the mAbs bind to IsdA, rather than to direct blockade of heme binding. Instead, the protective effect of these mAbs appears to be related to an Fc-dependent function requiring FcγR binding. IgG mutant variants of STAU-239 + STAU-245 (L234A, L235A) that functionally abrogate binding to Fc receptors lacked the ability to protect mice from *S. aureus* infection, suggesting that antibody effector functions play a critical role in the action of antibodies reducing *S. aureus* infection. Upon further experimentation, I was able to determine that the Fc effector function that was important for these antibodies to function was antibody dependent cellular phagocytosis or ADCP.

Moving forward, it will also be of interest to combine Isd antibodies, with or without iron-blocking activity, that use antibody effector functions in combination with antibodies to other vaccine targets in an effort to inhibit *S. aureus* through multiple mechanisms. Blocking *S. aureus* pathogenesis via different pathways may be the best chance to inhibit disease caused by such a multifaceted pathogen. Antibodies such as the

ones described here hold promise as potential therapeutic molecules for treatment or prevention of *S. aureus* infection, especially if used in an antibody cocktail.

Experimental Methods

Human subjects. Heparizined peripheral blood was collected from human subjects at Vanderbilt University Medical Center (VUMC) who had previously documented history of invasive MRSA or MSSA infection. The studies were approved by the Institutional Review Board of VUMC and samples were collected only after informed parent consent and subject assent.

Generation of human monoclonal antibodies. Peripheral blood mononuclear cells (PBMCs) were isolated by Ficoll density centrifugation from de-identified blood samples. Human hybridomas were generated by transforming PBMCs with media containing Epstein-Barr virus, agonist CpG (phosphorothioate-modified oligodeoxynucleotide OEZOEZZZZZOEEZOEZZZT, Life Technologies), Chk2 inhibitor [Chk2i] (Sigma), and cyclosporine A (Sigma). Cells were plated in 384 cell culture plates and grown for seven days before expanding to 96 well plates with irradiated heterologous human PBMCs (obtained from sterile discarded de-identified leukofiltration filters, Red Cross, Nashville, TN). After an additional four to five days, cells were screened via enzyme-linked immunosorbent assay (ELISA) using *S. aureus* surface antigens to identify cell culture wells that contained B-cells secreting antigen specific antibodies. Cell culture wells that contained reactant wells were fused with HMMA2.5 myeloma cells via electrofusion. After fusion, hybridoma cell lines were

sorted using single-cell fluorescence-activated cell sorting to achieve monoclonal hybridoma lines. Cell lines were screened and expanded before purifying filtered hybridoma supernatants using HiTrap Protein G columns.

Bacterial strains. The *S. aureus* strain Newman was grown at 37°C for 12-18 hours on TSA and in TSB. Isogenic mutants were made by allelic recombination in a Newman background and include *isdB*, *isdA*, and *isdH*.

Antigen generation. Soluble forms of the antigens of interest (excluding the sorting signal and signal peptide) were cloned into the pET15b plasmid vector and expressed recombinantly using the BL21 (DE3) *E. coli* expression system. Cultures were grown in Luria-Bertani (LB) broth and induced after 6 hours at 30℃ with 1 mM Isopropyl β-D-1-thiogalactopyranoside (IPTG). After 36 hours, cells were centrifuged and resuspended in 50mM Na_2HPO_4 + 500 mM NaCl before sonication. The soluble fraction was purified by affinity chromatography using a cobalt HiTrap TALON column. Purified antigen (including IsdA, IsdB, and IsdH) was used at a concentration of 2 μg/mL when screening PBMCs and supernatants for reactivity.

Hemoglobin growth curves. *S. aureus* strain Newman was grown overnight in tubes in RPMI + 1 μM EDDHA. The culture was normalized to 1.0 based on $O.D._{600}$ and subcultured into RPMI + EDDHA + 20 nM of human hemoglobin + 2 μg/mL mAb. Tubes were grown at 37°C and aliquots were removed at 12, 24, and 36 hours and put

into a 96-well plate to record $O.D._{600}$ values using the pathlength correction in the Gen5 microtiter plate software (Bio-Tek).

Biolayer interferometry competition-binding assay. Competition-binding studies were performed using biotinylated IsdA, IsdB, or IsdH (5 μg/mL) on an Octet RED biosensor (Pall FortéBio). After a brief washing step, biosensor tips were immersed into the wells containing a first antibody at a concentration of 100 μg/mL and then into the wells containing a second mAb, also at a concentration of 100 μg/mL. The percent binding of the second mAb in the presence of the first mAb was determined by comparing the maximal signal of second mAb applied after the first mAb complex to the maximal signal of second mAb when it was applied alone.

Mouse experiments. Mouse work used the murine model of septic *S. aureus* infection. Wild-type *S. aureus* strain Newman was streaked from frozen stocks onto TSA plates two days before infection. Overnight cultures then were grown in TSB broth. On the day of infection, overnight cultures were subcultured 1:100 and grown for two hours to mid-exponential phase. During this time, mice were weighed and injected with 10 mg/kg mAb via the intraperitoneal route. *S. aureus* cells were harvested by centrifugation and washed with cold PBS to a final concentration of 10^7 CFU/100 μl injection. Mice were anesthetized prior to retro-orbital injection with *S. aureus*. The infection continued for 96 hours before euthanization of the mice using CO_2 inhalation. The heart, liver, and kidneys were homogenized in PBS and serially diluted before plating on TSA for colony enumeration. Mouse experiments were approved and performed according to the

guidelines of the Vanderbilt University School of Medicine Institutional Animal Care and Use Committee (IACUC).

Hydrogen-deuterium exchange mass spectrometry. IsdA and Fabs of STAU-239 and -245 were prepared individually and in complex at a protein-concentration of 10 pmol/µl in 1x PBS pH 7.4 and incubated for 2 h at 0 °C. Labeling with Deuterium was performed by a 20-fold dilution of 3 µl protein-sample in 1x PBS pH 7.4 in D_2O and incubation at 20 °C for 30 s or 4 h respectively, or in 1x PBS pH 7.4 in H_2O for zero-time points. Subsequently the reaction was quenched by a 2-fold dilution in 1x PBS, 4 M guanidinium/HCl, 100 mM tris(2-carboxyethyl)phosphine to a final pH of 2.3 at 0 °C. Samples were immediately injected into a nano-ACQUITY UPLC system with HDX technology (Waters Corporation, Milford, MA, USA). Online digestion was performed at 15 °C, 10.000 psi at a flow of 134 µl/min of 0.1 % formic acid in H_2O using an immobilised-pepsin column. Peptides were simultaneously trapped at 0 °C on a Waters VanGuard™ BEH C18 1.7 µm guard column for 6 min. Accordingly, peptides were eluted over 6 min with a gradient of 5-35 % acetonitrile, 0.1 % formic acid in H_2O and separated on a Waters ACQUITY UPLC BEH C18 1.7 µm, 1 mm × 100 mm column at a flow of 40 µl/min at 0 °C. Eluted peptides were analyzed online on a Waters Xevo G2-XS with electrospray ionization and lock-mass acquisition (human Glu-1-Fibrinopeptide B peptide, m/z=785.8427) of 3 scans every 60 s in MS^E-mode. The capillary was set to 2.8 kV, source-temperature to 80 °C, desolvation temperature to 175 °C, desolvation gas to 400 L/h and the instrument was scanned over a m/z-range of 50-2000. A blank injection was performed between samples to avoid carry-over and all experiments were

carried out in triplicate. Peptide-identification was performed using Waters ProteinLynx Global Server 3.0.3 software with non-specific protease, min fragment ion matches per peptide of three, FDR 4 % and oxidation of methionine as a variable modification. Deuterium-uptake was calculated using DynamX 3.0 software, with filters set to minimum intensity of 500, minimum products 3, minimum products per amino acid 0.3 and a mass error < 15 ppm. The deuterium incorporation result is reported as the difference of the centroid values across the backbone amide population compared to the 0 s time point. Results were averaged across replicate analyses, at a given time point and the standard deviation determined. For this series of experiments, the average error for a single data point was ±0.5 Da or less within a replicate.

Statistical analysis. All data were analysed in Prism v 7.0 (GraphPad Software Inc.) and expressed as mean values and their standard error of the mean (SEM). P-values for animal experiments were calculated using an ANOVA with multiple comparisons for pair-wise comparisons as indicated. Hemoglobin-dependent growth p-values were calculated using an unpaired t-test.

CHAPTER III

IGHV1-69-ENCODED ANTIBODIES TO *STAPHYLOCOCCUS AUREUS* INHIBIT BACTERIAL GROWTH AND PATHOGENESIS

Introduction

S. aureus persistently colonizes up to 50% of the human population either on the skin or in the nares (Tong et al. 2015), but it unclear what factors play a role in these colonized individuals going on to develop invasive *S. aureus* infections. Because *S. aureus* is one of the leading causes of morbidity and mortality as well as a significant financial burden to the healthcare system (Tong et al. 2015), there is considerable effort invested into developing a vaccine or alternative immunotherapy drug. In order for these to be successful, the immune factors that protect individuals from initial or reoccurring *S. aureus* infection (Dillen et al. 2018) need to be reliably identified and defined. Not understanding the correlates of protection that protect against *S. aureus* infection contributes to the lack of successful vaccine. To address this, we investigated the molecular and structural basis for antibody-mediated correlates against a member of the Isd system, IsdB. Of the three surface proteins of the Isd system, IsdB has been studied the most due to its ability to bind hemoglobin and heme as well as the notable *in vivo* phenotype displayed when knocking it out (Fonner et al. 2014; Pishchany et al. 2014; Torres et al. 2006). While the importance of IsdB to *S. aureus* is well understood, I was interested in determining the host response to IsdB. Antibody repertoire studies to

pathogens have previously shown that certain human antibody variable genes may associate with specific antigens, and that may be the case here (F. Chen et al. 2019; Lang et al. 2017).

In this chapter, I describe the association of immunoglobulin heavy variable (*IGHV*) *1-69*-gene encoded human monoclonal antibodies against *S. aureus* IsdB. It has been observed previously that *IGHV1-69*-gene encoded antibodies to human pathogens often use a hydrophobic HCDR2 to bind antigenic sites. Many studies have shown key examples of this with viruses including influenza (Bangaru et al. 2018), HIV (Wu et al. 2011), and HCV (Tzarum et al. 2019) but less so with bacteria. I show that although these antibodies share germline variable genes, they bind to three distinct locations on IsdB-NEAT2 using both an HCDR2 and HCDR3 mode of binding. I also characterized the biological function of this class of antibodies, testing their ability to inhibit *S. aureus* growth *in vitro* and pathogenesis *in vivo*. Further analysis of *IGHV1-69*-encoded mAbs against *S. aureus* IsdB revealed diversification of antibody lineages by somatic hypermutation. These findings identify epitopes on IsdB that can be targeted for rational vaccine design and emphasize the importance of both heme-blocking and Fc-mediated functions for a successful *S. aureus* vaccine with a critical IsdB component.

I would like to acknowledge Dr. Jinhui Dong for resolving the crystal structure of STAU-399 Fab and STAU-281-IsdB-NEAT2. I would like to acknowledge Dr. Marcus B. Nagel and Kevin L. Schey for performing HDX-MS of STAU-229 and STAU-399 in complex with IsdB. I would also like to thank Dr. Clara T. Schoeder and Dr. Jens Meiler for Rosetta Modeling the HDX-MS data.

Isolation of *IGHV1-69*-encoded anti-IsdB human mAbs

I have previously discussed the isolation of IsdB specific human monoclonal antibodies using donors with a history of previous *S. aureus* infection. When analyzing the variable heavy chain gene usage of my panel, I discovered that 37% of the IsdB panel (seven antibodies) was encoded by *IGHV1-69* and that these antibodies were isolated from two independent donors. For this study, the definition of *IGHV1-69* includes two genes: *IGHV1-69*01* and *IGHV1-69-2*01*. These two genes are 84% conserved according to IMGT (Alamyar et al. 2012; Yousfi Monod et al. 2004), which is why they were defined as one class. *01 is used to denote alleles within genes according to IMGT nomenclature. One mAb, STAU-229, is encoded by *IGHV1-69-2*01* with the other six antibodies being encoded by *IGHV1-69*01*.

The HCDR2 of an *IGHV1-69* antibody often encodes three hydrophobic residues at positions 52-54- "*PIF*". These contribute to the overall hydrophobicity of this loop. *VH1-69* is a highly polymorphic locus, however, and variation at residue 54 has been described in particular because differences can affect the binding affinity and function of antibodies. In the general population, ~33% of people are homozygous for the F allele, around 56% are heterozygous for F/L, and 11% of individuals are homozygous L/L (Pappas et al. 2014). This level of variation is thought to play a role in antibody function, with individuals who carry the F allele producing a more broadly neutralizing antibody response (Avnir et al. 2016). Interestingly, the antibody panel isolated here originates from the conserved F allele (Figure 3-1). To further investigate whether this high percentage of germline-encoded antibodies and their particular HCDR2 sequence was biologically significant, I hypothesized that functional *IGHV1-69*-encoded antibodies

preserve hydrophobic residues in their HCDR2 loop to block hemoglobin. This hypothesis was based on previous studies showing the importance of hydrophobicity within the HCDR2 of *IGHV1-69*-encoded antibodies for interacting with antigenic sites.

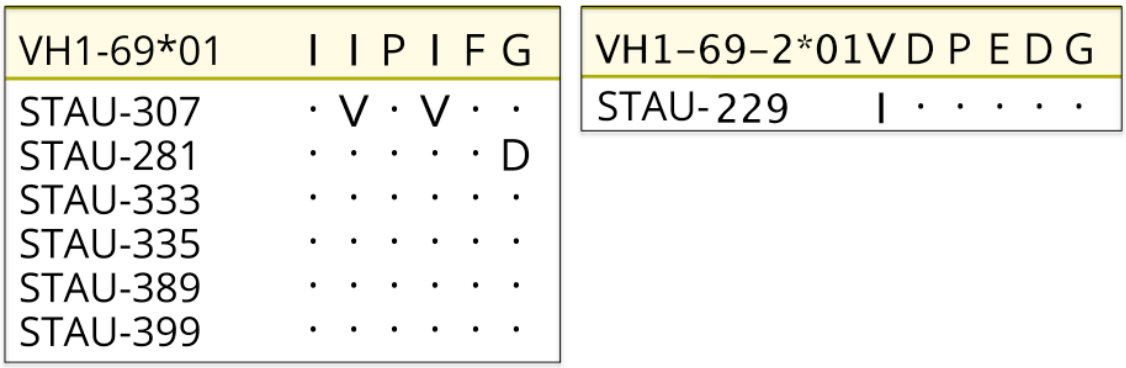

Figure 3-1. *IGHV1-69*-encoded anti-IsdB human mAbs panel.

The isolated *IGHV1-69*-encoded antibody HCDR2 sequences are shown with the consensus germline HCDR2 sequence indicated on top for reference. Differences to the germline are shown specifically.

Structural characterization of three *IGHV1-69*-encoded antibodies reveals three modes of binding to NEAT2

To determine if the isolated mAbs used these residues to interact directly with the heme-binding pocket on NEAT2, the antigen-antibody complex structure for three representative mAbs was identified and their modes of interaction with IsdB-NEAT2 compared. I obtained crystals of mAb STAU-281 in complex with IsdB-NEAT2 as well as two *apo* Fab structures, STAU-229 and STAU-399. These crystals were solved with the help of Dr. Jinhui Dong (Figure 3-2). In order to identify the epitope of the *apo* Fab structures, a hybrid structural method was implemented with the help of Dr. Kevin Schey's group who performed HDX-MS and Dr. Jens Meiler's team who used Rosetta

modeling to dock the complex. Using a combination of crystallography, proteomics-based epitope mapping, and Rosetta modeling we were able to obtain equivalent antigen-antibody complex structures (Bender et al. 2016; Chaudhury et al. 2011).

The solved crystal structure of mAb STAU-281 in complex with IsdB-NEAT2 was obtained at 3.0-Å resolution. STAU-281 binds to the heme-binding pocket of IsdB-NEAT2, and is predicted to inhibit *S. aureus* growth by preventing heme from binding to IsdB. This interaction relies on the *IGHV1-69*-gene encoded hydrophobic *PIF* residues at the tip of the HCDR2 loop. Residue F55 on the STAU-281 HCDR2 loop inserts into the IsdB heme-binding pocket, making polar contacts with both Y444 on β-8 and M362 on α-helix 1. The antibody HCDR2 residue K57 interacts with IsdB residue Y440 on β-8 and I52 interacts with Y391. Less side chain interactions were observed between the heme-binding pocket and the antibody HCDR1 loop, but pi-pi stacking occurs between Y32 of the HCDR1 and N388 on NEAT2. This structure revealed a major epitope, designated here as IsdB antigen site 1, where the hydrophobic HCDR2 protrudes into the similarly hydrophobic heme-binding site, precluding subsequent heme binding.

Fab fragments were crystalized in *apo* form for the mAbs STAU-399 (2.4 Å resolution) and STAU-229 (2.1 Å resolution), and peptides in the antigenic site recognized by these antibodies were identified using HDX-MS. The interaction of Fab and antigen for each mAb was modeled using the *apo* Fab and *apo* IsdB crystal structures (PDB ID: 5VMM) (Bowden et al. 2018) with the Rosetta modeling software suite (Bender et al. 2016), with restrictions to the HDX-MS data to determine predicted Fab-IsdB-NEAT2 complexes. These data were used to identify key differences between the structure of STAU-281-IsdB-NEAT2 at antigenic site 1 with the modeled structures of

STAU-399 and -229 to IsdB-NEAT2, at a new epitope designated antigenic site 2. The long HCDR3 of STAU-399 played a key role in altering the angle of binding compared to STAU-281 by interacting near the α-helix 3 of NEAT2, forming non-covalent interactions between I103 with T330 and V105 with K326. The canonical F55 on the HCDR2 of STAU-399 still interacts with IsdB, but binds Q400, away from the heme-binding site. STAU-229 bound Isd-NEAT2 similarly at antigenic site 2 near the α-helix 3 of NEAT2 using the HCDR3 as the predominantly interacting loop. A number of aromatic amino acids stabilize this interaction including Y113-E340 and F114- N339.

Despite their common *IGHV-1-69* germline usage, mAbs STAU-399 and STAU-229 bind to IsdB-NEAT2 at epitopes distal from the heme-binding site and rely mostly on the HCDR3 as the principal interacting antibody loop. Interestingly, this HCDR3-NEAT2 binding does not occur near the heme-binding pocket. Therefore, it is not expected that the presence of these antibodies would block heme binding. STAU-399 and STAU-229 both contain longer HCDR3 loops, which fill the cavity of the heme-binding pocket of the NEAT2 domain. The LCDR3 loop of STAU-281 opposite the binding cavity is shorter in STAU-281 than STAU-399 or STAU-229, leaving more space for the engagement of the NEAT2 domain. Taken together, the structures show that the hydrophobic patch in *IGHV1-69*-encoded HCDR2s must be combined with a short HCDR3 loop and a light chain that can accommodate the tip of the domain to bind the NEAT2 domain at the heme-binding pocket. These antigen-antibody structures reveal three separate modes of binding by *IGHV1-69*-encoded mAbs onto IsdB-NEAT2, but only one mAb, STAU-281, targets the heme-binding pocket using its HCDR2.

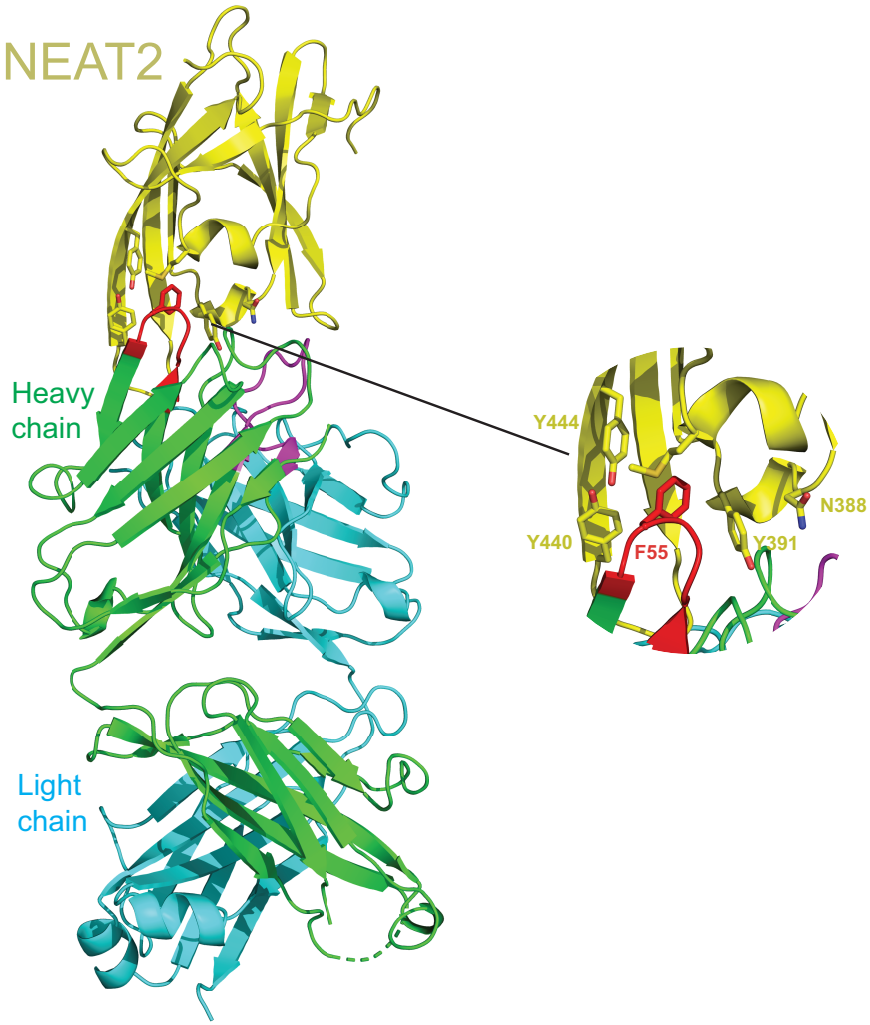

Figure 3-2. *IGHV1-69*-encoded antibody binding to IsdB-NEAT2.

A crystal structure of the mAb STAU-281 is shown in complex with IsdB-NEAT2 (PDB ID: 6P9H). The structure was solved to 3.0-Å resolution and identifies key residues involved in binding at the heme pocket of NEAT2. The HCDR2 is shown in red with the F55 side chain shown in stick form. The HCDR3 is shown in magenta for reference. Other interacting residues such are also shown as side chains.

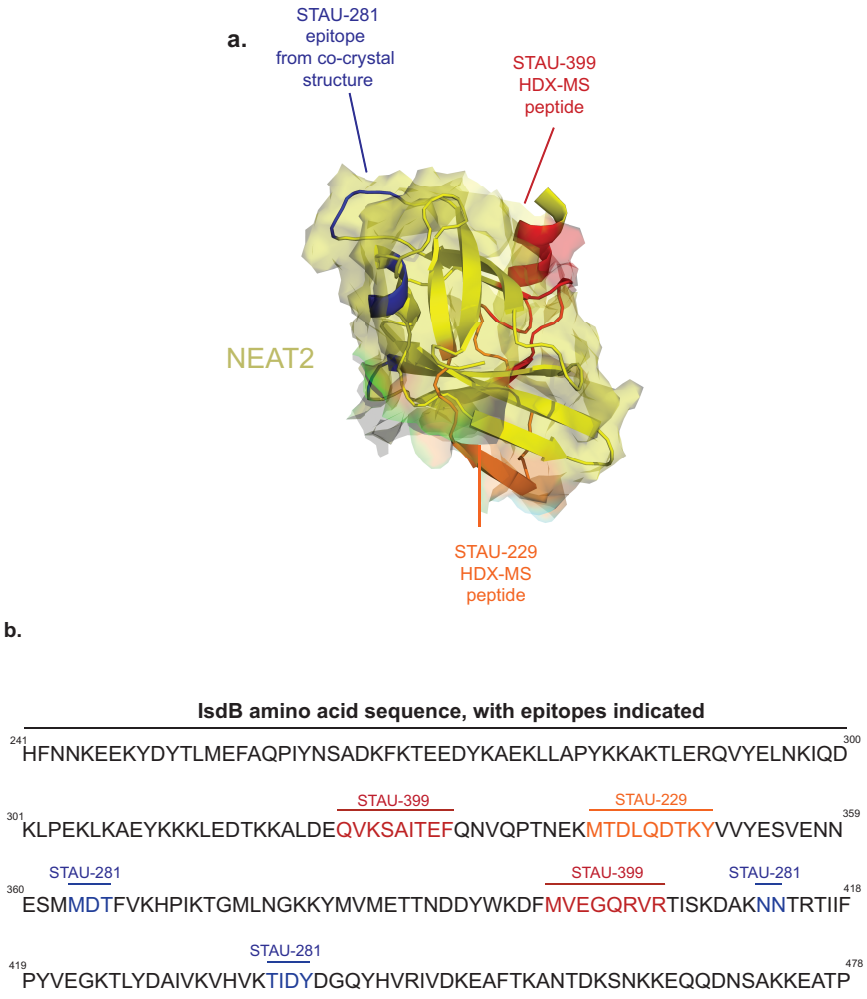

Figure 3-3. Epitopes for two *IGHV1-69*-encoded antibodies on NEAT2.

Hydrogen-deuterium exchange mass spectrometry (HDX-MS) was used to map the binding sites of STAU-229 (orange)(PDB ID: 6P9J) or STAU-399 (red) (PDB ID: 6P9I). **(a)** Peptides participating in the two epitopes were determined by reduced labeling in the presence of antibody and visualized on the surface of the IsdB NEAT2 domain (PDB 5DIQ), shown in yellow ribbon and surface projection. The binding site of STAU-281 as determined by X-ray crystallography of a complex of STAU-281 Fab and recombinant NEAT2 is indicated in blue for reference. **(b)** Peptides in epitopes for STAU-229 (orange) or STAU-399 (red) are indicated in the amino acid sequence of IsdB, and the contact residues in the co-crystal structure for STAU-281/NEAT 2 are indicated in blue.

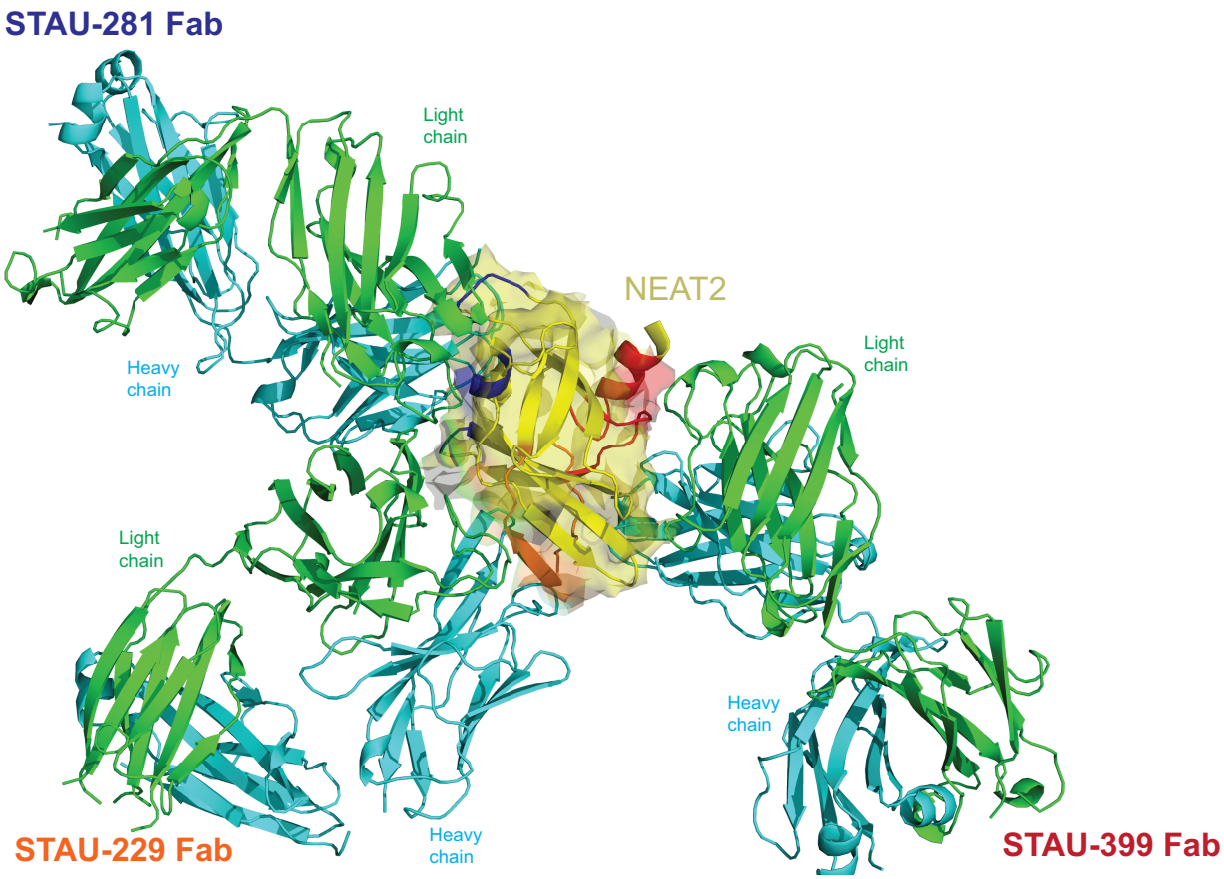

Figure 3-4. Overlay model of the structure of three *IGHV1-69*-encoded antibodies reveals three modes of binding to NEAT2.

The structures of the *apo* forms of Fabs STAU-229 (2.1 Å) and STAU-399 (2.4 Å) were determined by crystallography. Those two Fabs were docked to the STAU-281/NEAT 2 complex structure using the Rosetta modeling suite, restricting docking to their binding sites (orange or red, respectively) predicted by HDX-MS studies of NEAT 2 and the Fabs (see Figure 2). Heavy chains are shown in cyan ribbon, and light chains are shown in green.

Table 3-1. Data collection and refinement statistics for *IGHV1-69* crystal structures

Data collection			
Crystal	STAU-281/Neat2	STAU-399	STAU-229
PDB ID	6P9H	6P9I	6P9J
Wave Length (Å)	0.97872	0.97856	0.97872
Space group	$P2_1$	$P2_1$	$P2_1$
Unit cell dimensions			
a, b, c (Å)	72.6, 115.3, 88.3	49.6, 99.9, 93.9	57.8, 66.0, 112.3
α, β, γ	90.0, 100.1, 90.0	90.0, 96.3, 90.0	90.0, 96.4, 90.0
Resolution (Å)	48.04 – 3.00	49.29 – 2.40	48.92 – 2.20
Unique reflections	28660 (4141)	35657 (5197)	43034 (6144)
Redundancy	3.9 (3.8)	3.8 (3.9)	3.8 (3.8)
Completeness (%)	99.8 (98.9)	100.0 (100.0)	99.7 (98.0)
R_{merge} (%)	6.9 (31.6)	8.7 (58.1)	8.1 (78.8)
I/σ(I)	15.2 (3.8)	12.8 (2.4)	10.9 (1.8)
Refinement statitics			
R_{factor}	20.64	18.50	21.81
R_{free}	22.50	24.34	26.70
R.m.s.d. (bond) (Å)	0.0020	0.0016	0.0048
R.m.s.d. (angle) (deg)	0.519	0.482	0.722
Ramachandran plot			
Favored (%)	96.99	96.86	97.43
Allowed (%)	2.82	3.14	2.57
Outliers (%)	0.19	0.00	0.00

$R_{merge} = \Sigma\ \Sigma\ |I_{hkl} - I_{hkl(j)}|/\Sigma\ I_{hkl}$, where $I_{hkl(j)}$ is the observed intensity and I_{hkl} is the final average intensity.

$R_{work} = \Sigma\ ||Fobs| - |Fcalc|/\Sigma\ |Fobs|$ and $R_{free} = \Sigma\ ||Fobs| - |Fcalc||/\Sigma\ |Fobs|$, where R_{free} and R_{work} are calculated using a randomly selected test set of 5% of the data and all reflections excluding the 5% test set, respectively. Numbers in parentheses are for the highest resolution shell.

In vitro blocking of heme binding and inhibition of growth mediated by *IGHV1-69*-encoded mAbs

The biological significance of these antibodies and their binding sites was not clear based on the structural data alone. In order to answer investigate this, I used two separate *in vitro* assays to determine if there were any differences in their ability to inhibit *S. aureus*. First, each *IGHV1-69*-encoded mAb was tested for its ability to block heme or hemoglobin binding to IsdB using a biolayer interferometry biosensor. Biotinylated hemoglobin was loaded onto streptavidin sensors and then each well was associated with either IsdB alone, mAb alone, IsdB + mAb together, or buffer. The only mAb that significantly blocked the IsdB-hemoglobin binding interaction was STAU-281. Conversely, when STAU-229 and -399 were incubated with IsdB and then associated with hemoglobin, there was no detected difference in binding signal compared to IsdB and hemoglobin binding alone (Figure 3-5a-c). STAU-281 not only directly binds to the heme-binding pocket but also prevents binding of hemoglobin to IsdB. This mode of action is similar to that of the previously described mAbs D2-06-N2 and D4-30-N2 (Yeung et al. 2016).

Next, the mAbs were tested for their ability to inhibit *in vitro* replication of *S. aureus* when grown in the presence of heme as a sole iron source. *S. aureus* strain Newman (or a protein A and *isdB* deficient strain, *ΔspaisdB,* were grown overnight and then subcultured 1:200 into 96-well plates containing RPMI + ethylenediamine-*N*,*N*′-bis(2-hydroxyphenylacetic acid) to reduce the available iron. When heme was added to wells containing the *ΔspaisdB* strain, there was no increase in growth due to a lack of functional *isdB* (Pishchany et al. 2014). In contrast, addition of heme led to an increase of

growth of wild type *S. aureus* to an OD_{600} of ~1.5 (Figure 3-5d-e). STAU-281 reduced growth when added to the medium, while an inhibitory effect was not detected for the STAU-399- or STAU-229-treated groups, in which the OD values did not differ from those of the group treated with heme alone. These data show that representative mAbs that bind to antigenic site 2 or 3 on NEAT2 do not prevent heme or hemoglobin binding and do not inhibit strain wild type growth using heme as a sole iron source *in vitro,* in contrast to STAU-281 which does inhibit *S. aureus* growth.

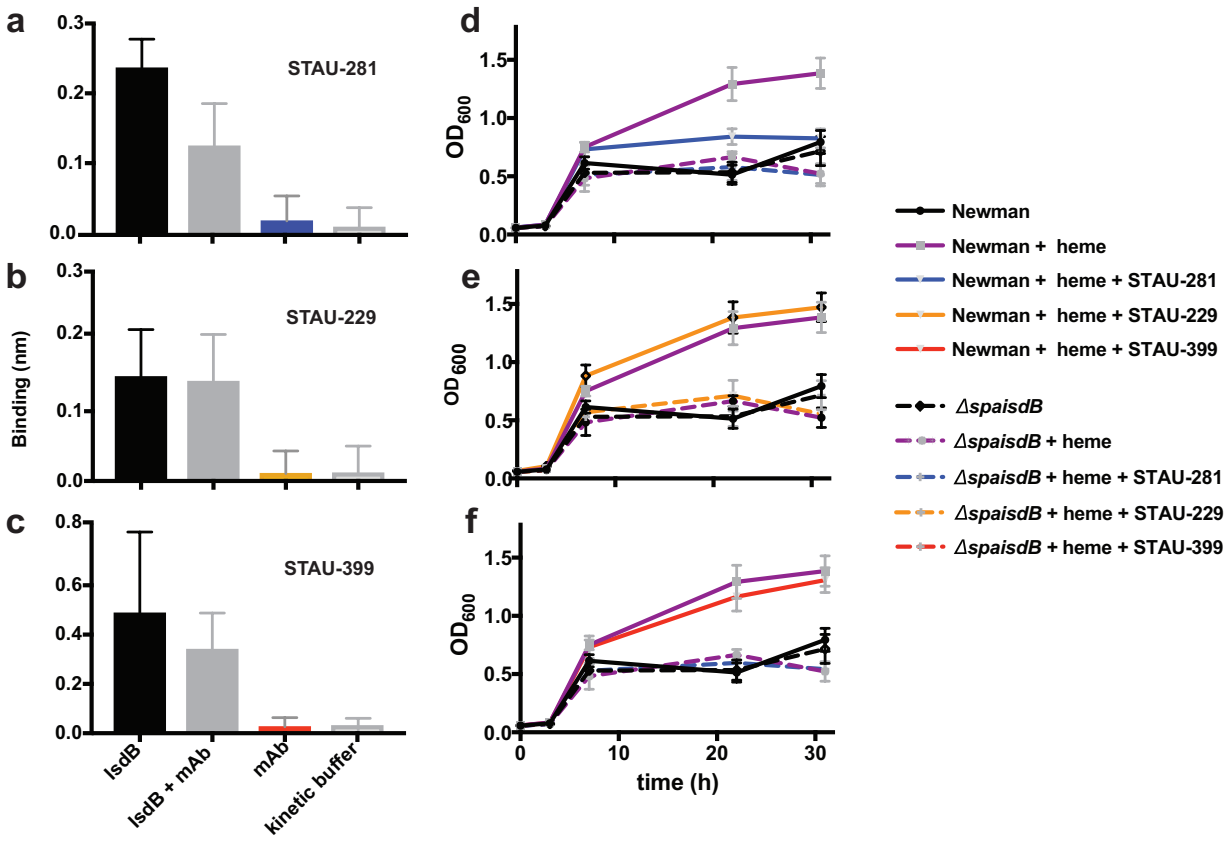

Figure 3-5. *In vitro* blocking of binding in (a-c) or inhibition of growth of *S. aureus* (d-e) mediated by *IGHV1-69*-encoded mAbs. (a-c)

Biolayer interferometry was used to detect whether the mAbs blocked binding of hemoglobin to NEAT2. Biotinylated hemoglobin was loaded onto streptavidin-coated biosensor tips before association with IsdB alone, IsdB mixed with mAb, mAb alone or kinetic buffer. Error bars represent standard error of the mean. **(d-e.)** *S. aureus* heme-dependent *in vitro* growth curves were performed in 96-well plates over 32 hours. *S. aureus* strain Newman was subcultured at a 1:200 dilution into RPMI with EDDHA and normalized to an OD_{600} 1.0. Error bars represent standard deviation.

All three classes of IGHV1-69-encoded mAbs reduce bacterial burden in vivo

These mAbs next were tested in a murine septic model of *S. aureus* infection to determine whether mAb binding to any of the three major antigenic sites on NEAT2 mediates a protective effect *in vivo*. Two variant forms of *IGHV1-69*-encoded mAbs were tested in this infection model: full-length IgG1 with a wild-type Fc region or IgG1 Fc-variant antibodies with L234A/L235A (LALA) mutations in the CH2 domain, which reduces antibody binding to FcγR receptors (Hezareh et al. 2001; Wines et al. 2000). The interaction between FcγR receptors and the Fc portion of an antibody mediates secondary functions such as phagocytosis and antibody-dependent cytotoxicity. Therefore, mutating these critical residues can reveal whether Fc effector functions are an important part of the inhibitory effect of antibodies *in vivo* (Alter et al. 2018). Testing both forms of mAbs enables identification of Fc effector function in *IGHV1-69*-encoded mAbs as well as a determination of antigenic site 1 and 2 in mediating *in vivo* protection against *S. aureus*.

Seven-week old BALB/c mice were given one of three *IGHV1-69*-encoded mAb by intraperitoneal injection and then inoculated retro-orbitally with 10^7 CFU of wild type *S. aureus*. The kidneys, livers, and hearts of the mice were harvested after 96 hours, and the bacterial burden was enumerated from colony forming units by serial dilution plating (Figure 3-6). Treatment with the IgG1 form of mAb STAU-281 caused a significant reduction in bacterial burden compared to isotype control treated animals in all three organs tested, including a greater than 100-fold reduction in bacterial burden in the heart and kidneys and 60-fold reduction in the liver. While STAU-399 did not block binding of hemoglobin or heme *in vitro*, it did significantly reduce burden in the kidneys, liver, and heart. STAU-229 significantly reduced burden in the kidneys. In contrast, we did not

detect a significant reduction in bacterial burden in any tissue for the LALA mutant IgGs when compared to mice treated with the isotype control IgG. Therefore, binding of the full-length *IGHV1-69*-encoded IgG mAbs to FcγR contributes to the protective mechanism of these mAbs. These findings indicate antibodies that recognize antigen site 2 do not mediate direct blocking of the NEAT2-heme interaction and may show a protective effect *in vivo* through alternate mechanisms involving FcγR-mediated interaction with immune cells.

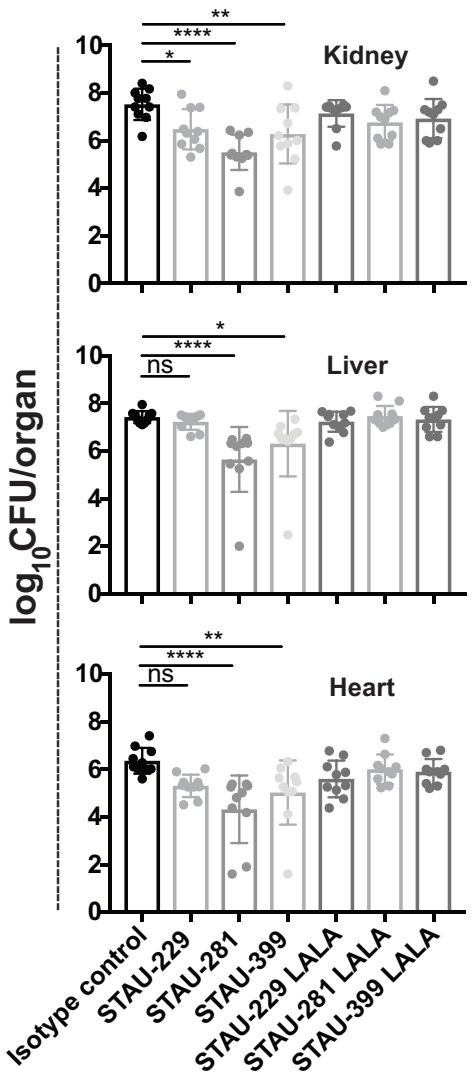

Figure 3-6. *IGHV1-69*-encoded mAbs reduce bacterial burden *in vivo*.

Seven-week-old female BALB/c mice were inoculated retro-orbitally with an OD_{600} 0.4 suspension of *S. aureus* strain Newman. Mice were given *IGHV1-69*-encoded full-length wild-type IgG LALA Fc variant (L234A/L235A) IgG antibodies by the intraperitoneal route. The hearts, livers, and kidneys of the infected mice were harvested after 96 hours. Statistical significance was evaluated by ANOVA. All other comparisons, including LALA mAbs compared to the isotype control, were not significant. Experiments were performed two independent times and the pooled data are shown.

Repertoire analysis of IGHV1-69-encoded mAb siblings

We next sought to identify somatic variants of the mAbs to determine if clonal lineages developed and if affinity maturation of the clonotypes affected function of the protective *IGHV1-69*-encoded antibodies. We used an additional aliquot of cryopreserved peripheral blood mononuclear cells (PBMCSs) collected in the convalescent period from subject 1 and performed antibody heavy chain repertoire sequencing. We obtained 3,395,084 unique and productive heavy chain variable gene sequences from approximately 1.1 million PBMCs (estimated by taking 7% of the total number of PBMCs). To minimize the influence of potential sequencing error, we employed the concept of a V3J clonotype, which uses the variable (V) and joining (J) germline genes (ignoring allelic distinction) along with the CDR3 amino acid sequence (Soto et al. 2019). Reducing the total pool of unique and productive heavy chain reads according to the clonotype definition resulted in identification of a total of 1,047,493 unique V3J clonotypes.

Because STAU-399 and -229 were isolated from the same donor for which we performed deep sequence analysis, we were able to search for somatic variants that were also *IGHV1-69*-encoded antibody sequences in that donor. Our sequence search process involved searching for V3J clonotypes from the repertoire sequencing that possessed the same V and J germline gene and shared 70% or greater amino acid sequence identity in their CDR3. The phylogenies of the somatic variants associated with the V3J clonotypes from the repertoire sequencing were then analyzed to infer a possible maturation pathway. Point mutations were identified in the V_H region, and we synthesized and tested these variant antibodies for differences in binding to IsdB. cDNA was synthesized

encoding the variant heavy chains and paired with the light chain gene of the original hybridoma for recombinant expression by transient co-transfection of heavy and light chain encoding DNA plasmid vectors in ExpiCHO or 293F cells. We then determined binding and affinity differences for the variants by ELISA and biolayer interferometry (Figures 3-7, -8, -9).

The V_H gene *IGHV1-69*01* was used as an out-group for neighbor joining tree analysis (Figure 3-7b). Ten sequences of the STAU-399 clonotype (encoded by *V_H1-69/J_H6*) were identified with 3 of them (variant 2, 8, 9) being identical. Somatic variants within a lineage ('siblings') clustered into 3 groups (Figure 3-7b). STAU-399 IgG and variants 3 and 4 grouped together in cluster 1, based on their conservation of the germline gene sequence encoding the HCDR2 loop, which has a threonine at position 57 (Figure 3-7a). This finding is in contrast to all other variants that shared a T57A mutation in the HCDR2 loop. The presence of threonine in the germline encoded HCDR2 likely participates in important hydrogen bonds with surrounding side chains and water, and the T57A mutation may alter the HCDR2 loop interactions, as alanine is non-polar and less hydrophobic than threonine. The largest cluster of this clonotype is cluster 3, which encodes 6 total variants. Most of the mutations in this cluster did not lead to noticeable changes in the binding affinity of these variants, with the exception of variant 6. Variant 6 has three mutations to glycine (V24G in FR1, S31G in CDR1, and V37G in FR2), making this clone the most distant genetically from the inferred germline gene sequence. Correspondingly, this mAb exhibited the lowest affinity for binding (27-fold less than the hybridoma IgG) and highest EC_{50} value for binding in ELISA (18-fold worse than the hybridoma IgG) (**Figure 3-7c**). Typically, it is expected that somatic variants in a clonal

lineage with increased numbers of mutations may exhibit increased affinity for binding and function. Here, we observe the unexpected finding that acquisition of increased numbers of somatic mutations in clonal lineage variants does not always confer biological benefits. In fact, all of the somatic variants obtained for this lineage exhibited a similar reduction in binding and function.

An additional *IGHV1-69*01*-encoded mAb, STAU-307, was found to have clonal variants within the donor sample and behaved similarly to STAU-399. Ten sequences of the STAU-307 clonotype (encoded by V_H*1-69*01/*J_H*4*02*) were identified with two of these sequences being identical. Siblings were divided into two main clusters based on the phylogenetic analysis (Figure 3-8b). Cluster 1 contains the original IgG and variants 5, 8-10 whereas cluster 2 contains variants 1-4, 6-7. Interestingly, the main differences between these two clusters occurs in the DE loop (Figure 3-8a) where three different runs of mutations occurs. All variants included in clusters 1 and 2 have mutations in their HCDR2 that differ from the germline *IGHV1-69*01* sequence. This is striking as a conserved HCDR2 can have important implications for blocking the heme pocket of NEAT2, however, none of the STAU-307 variants maintain 100% identity with the germline sequence and instead all 10 variants as well as the hybridoma IgG have the mutations I52V and I54V. Although both isoleucine and valine are branched hydrophobic amino acids, mutating between these residues has been shown to alter function in a number of studies previously and perhaps a similar event happens here (Yuan 2010, Brosnan 2006). Despite these point mutations, these variants had largely the same ability to bind IsdB when tested by ELISA. One variant, however, variant 1, did have a

noticeably worse K_D than all other variants tested (Figure 3-8c). This difference may be attributed to the Y108D mutation found in the HCDR3 that is unique to this sequence.

We identified nine sequences within the STAU-229 clonotype and three clusters of variants (encoded by *V_H1-69-2*01/J_H6*02*) (Figure 3-9b). Some common mutations were noted, with variants 1-2, 4, and 10 being the same as well as variants 3 and 6. Because STAU-229 is encoded by the *IGHV1-69-2*01* allele, this antibody has a different inferred germline gene sequence than that of STAU-399. Notably, the residues in positions 53 to 55, encoding the key amino acid motif *PIF* that was conserved in all of the *IGHV1-69*01*-encoded antibodies, are changed to *PED* in *IGHV1-69-2*01*-encoded antibodies. These alleles represent two distinct gene sequences. In the STAU-229 mAb heavy chain variable gene sequence and all 1,047,493 clonotype variants identified in the repertoire sequencing, the *PED* motif was maintained (Figure 3-9a). The I54E and F55D alternate residues encoded by the *IGHV1-69-2*01* gene make this germline-encoded HCDR2 loop more polar and hydrophilic than that encoded by *IGHV1-69*01*. Interestingly, STAU-229 IgG is the only antibody isolated with a mutation in the HCDR2 (V51I), which is the same residue in place in the germline *IGHV1-69*01,* suggesting these canonical hydrophobic isoleucine residues facilitate optimal binding to NEAT2. A number of STAU-229 variant sequences were shared within cluster 3, so we tested the representative sequences for variant 1 and 3 after recombinant expression. Variant 3 only differs from variant 1 by a S21P substitution in FR1, however, this difference was sufficient to alter the K_D of this antibody to 1.44 nM, nearly 7 times less avid than that of the hybridoma IgG, making it the antibody with the worst K_D in this clonotype (Figure 3-9c).

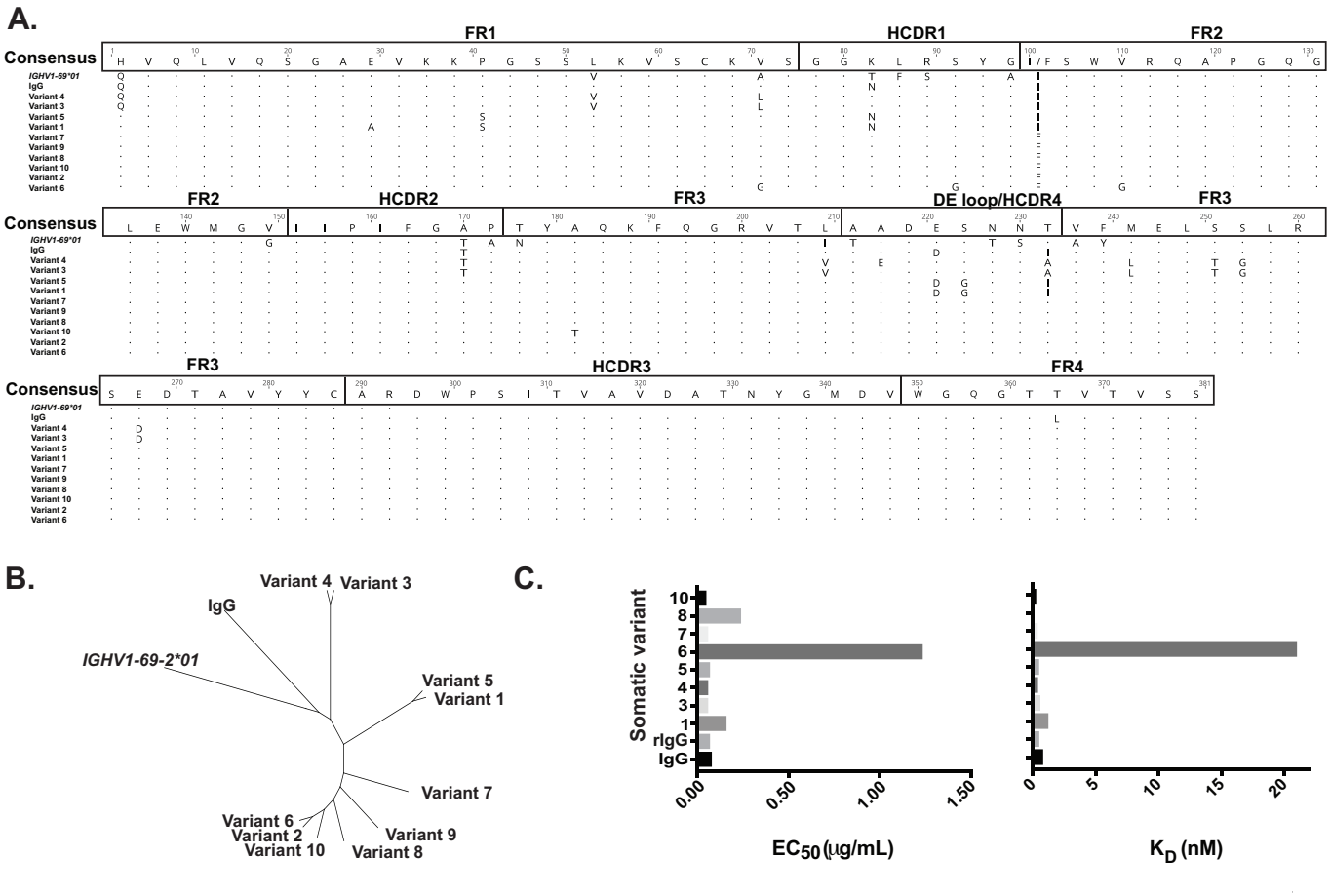

Figure 3-7. ***Sequence alignment of STAU-399 and clonal variants.***

(A) A global alignment using Geneious was performed with the germline *IGHV1-69*01* sequence, hybridoma IgG, and all 399 clonal variants. Each HCDR and FR region is denoted with a consensus sequence shown. Point mutants that differ from the consensus are shown as individual amino acids whereas conserved residues are represented as dots. (B) Neighbor joining tree analysis of mAb clonal variants was performed and is rooted with the *IGHV1-69*01* germline gene sequence. (C) Each variant mAb was tested for binding to IsdB, and the half-maximal effective concentration (EC_{50}) for binding is shown. Biolayer interferometry was used to determine the on and off rate of each mAb for binding to NEAT2, and the calculated K_D is graphed.

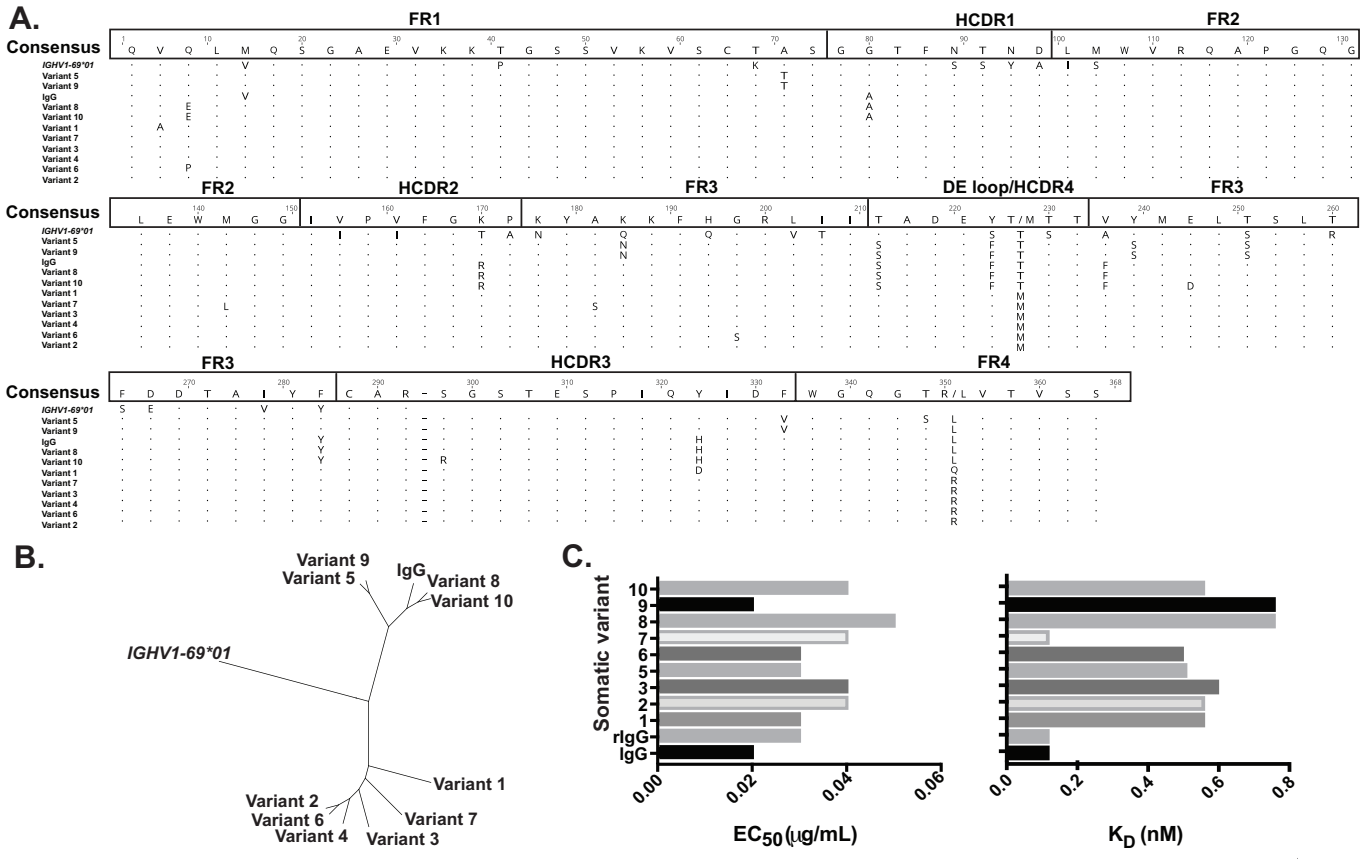

Figure 3-8. ***Sequence alignment of STAU-307 and clonal variants.***

(A) A global alignment using Geneious was performed with the germline *IGHV1-69*01* sequence, hybridoma IgG, and all 307 clonal variants. Each HCDR and FR region is denoted with a consensus sequence shown. Point mutants that differ from the consensus are shown as individual amino acids whereas conserved residues are represented as dots. (B) Neighbor joining tree analysis of mAb clonal variants was performed and is rooted with the *IGHV1-69*01* germline gene sequence. (C) Each variant mAb was tested for binding to IsdB, and the half-maximal effective concentration (EC_{50}) for binding is shown. Biolayer interferometry was used to determine the on and off rate of each mAb for binding to NEAT2, and the calculated K_D is graphed.

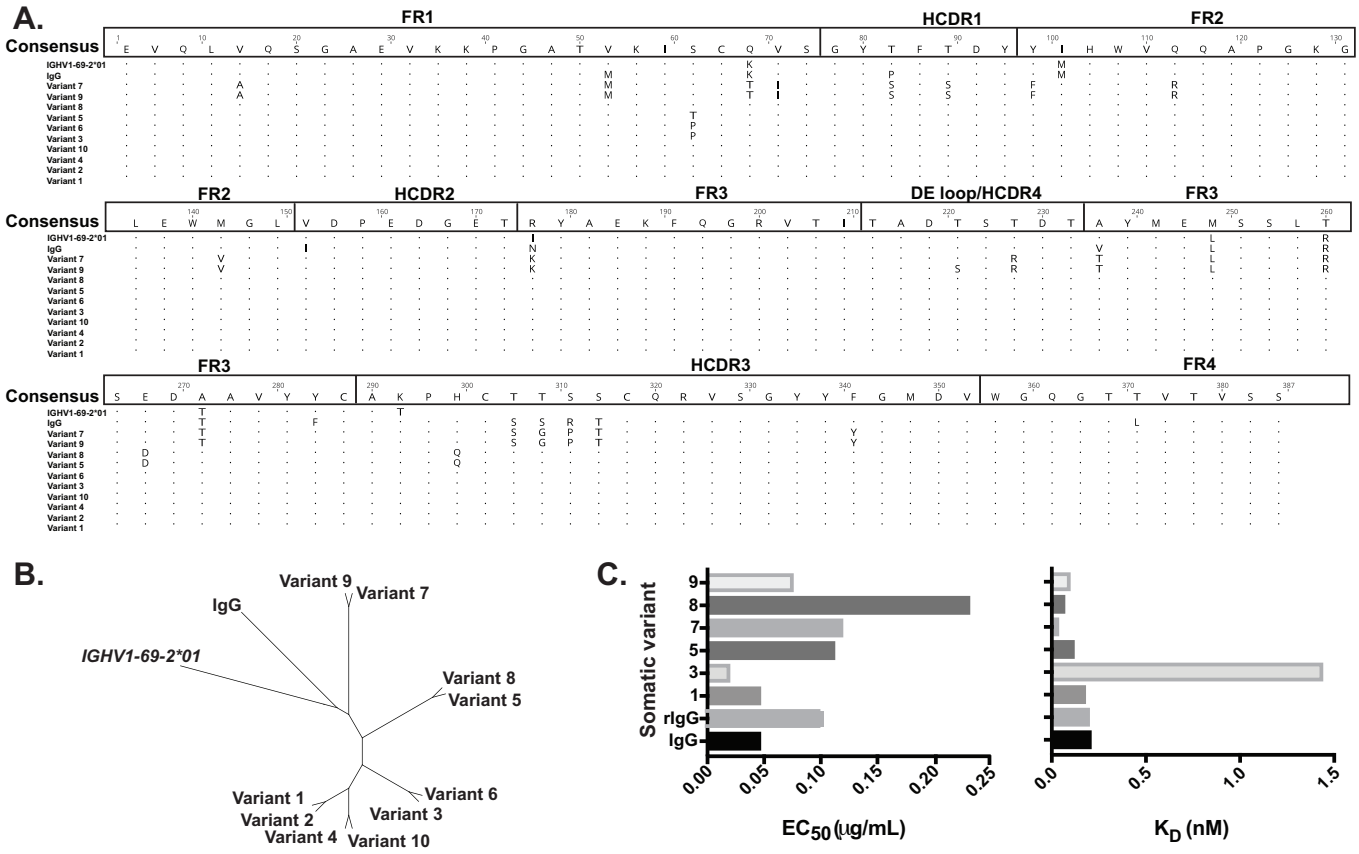

Figure 3-9. ***Sequence alignment of STAU-229 and clonal variants.***

A global alignment using Geneious was performed with the germline *IGHV1-69-2*01* sequence, hybridoma IgG, and all 229 clonal variants. Each HCDR and FR region is denoted with a consensus sequence shown. Point mutants that differ from the consensus are shown as individual amino acids whereas conserved residues are represented as dots. (B) Neighbor joining tree analysis of mAb clonal variants was performed and is rooted with the *IGHV1-69-2*01* germline gene sequence. (C) Each variant mAb was tested for binding to IsdB, and the half-maximal effective concentration (EC_{50}) for binding is shown. Biolayer interferometry was used to determine the on and off rate of each mAb for binding to NEAT2, and the calculated K_D is graphed.

Discussion

In this study, I present data that not only contribute to a broader understanding of a biologically important antigen, IsdB, but I also describe a panel of prophylactically protective *IGHV1-69*-encoded mAbs that exhibit therapeutic efficacy in *S. aureus* infection in mice. I report three antigenic sites on IsdB-NEAT2 and their biological importance *in vitro* and *in vivo*. I determine that these antibodies do not all function equally despite being encoded at the *IGHV1-69* locus and identify that those mAbs using a HCDR2 mode of binding to block the heme binding site were better at inhibiting *S. aureus*. I also look at the importance of somatic hypermutation in the development of *IGHV1-69*-encoded antibodies against *S. aureus* and determine that mutations hinder rather than fine-tune the immune response to IsdB.

The structural studies reveal that the *IGHV1-69*-encoded antibodies used multiple modes of binding to interact with IsdB-NEAT2. Although *IGHV1-69*-encoded antibodies typically are characterized by their hydrophobic HCDR2-mediated binding interactions and STAU-281 did use this method (Yeung et al. 2016), other identified mAbs to IsdB-NEAT2 did not. This is interesting, as key antibody-antigen interactions have been described for a number of pathogens using *IGHV1-69*-encoded antibodies, whether HCDR2 or HCDR3 mediated or both. For example, in influenza, the *IGHV1-69*-encoded mAb 27F3 broadly targets Influenza group 1 and 2 viruses at the HA stem using the IFY motif on the HCDR2 (Lang et al. 2017). In hepatitis C virus (HCV), the *IGHV1-69*-encoded antibodies, AR3A-D, broadly neutralize the E2 domain of HCV using a hydrophobic HCDR2 and long HCDR3 (Tzarum et al. 2019). Finally, for HIV, *IGHV1-69*-encoded antibodies that predominantly use both the HCDR2 as well as antibodies that

use both the HCDR2 and HCDR3 have been identified. HK20 uses the traditional hydrophobic IF motif on the HCDR2 to target gp41 of HIV (Sabin et al. 2010). In contrast, the *IGHV1-69*-encoded mAb VRC13 uses an HCDR3-mediated mechanism to broadly neutralize HIV by recognizing and blocking gp120 (Zhou et al. 2015). We can contrast these previously reported mAbs against viruses to the *IGHV1-69*-encoded antibodies isolated against *S. aureus* in this study. STAU-281 blocked the heme-binding pocket using the *PIF* residues on the tip of the HCDR2 while STAU-399 and STAU-229 did not directly block heme or hemoglobin and interacted with IsdB-NEAT2 using the HCDR3. Of the three antibodies tested, the canonical hydrophobic tip from STAU-281 of the HCDR2 was not only sufficient but also necessary to block the heme-binding site.

As mentioned previously, the *IGHV1-69* locus is highly polymorphic and the F/L polymorphism at position 54 (*PIF*) has been described to influence antibody function. Interestingly, all isolated antibodies and variants identified by next-gen sequencing in this study maintained a F54, however, this did not dictate function as the antibodies tested did not have equivalent blocking power and function against *S. aureus*. This implies that F54 is sufficient but not required for blocking *S. aureus* infection. Perhaps the F allele is overrepresented in individuals who mount a successful *S. aureus* infection, but it is unclear based on the studies done here. Regardless, these studies show the ability of genetic variability at the *IGHV1-69* locus to alter the humoral immune response and the potential value of harnessing that response for specific vaccine design.

The antibodies to alternate antigenic sites also diversify by somatic hypermutation, although the mutations reduced rather than enhanced binding. These data support the existence of a “somatic cloud” where mutations may accumulate within the B

cell repertoire but do not increase affinity for the antigen target. Instead, there is a cloud of somatic variants with similar affinity. Identification of high functioning *IGHV1-69*-encoded antibodies with relatively low numbers of somatic mutations is an important finding in rational vaccine development because achieving somatic hypermutation above 20% by vaccination alone can be difficult. Therefore, eliciting a protective response based on an immunodominant gene target that requires low levels of somatic hypermutation is an exciting and more feasible goal. Identification of common germline-encoded antibodies for a pathogen represents a unique opportunity to use vaccination to shape a targeted antibody response. By understanding aspects of *IGHV1-69*-encoded antibodies to *S. aureus* that contribute to a protective immune response, we can inform rational vaccine design and enable a better understanding of the correlates of protection against *S. aureus* infection.

Experimental Methods

Human subjects. Human blood was collected from patients at Vanderbilt University Medical Center after informed consent and subject assent. The studies were approved by the Institutional Review Board of Vanderbilt University Medical Center.

Generation of human monoclonal antibodies (mAbs). Peripheral blood mononuclear cells (PBMCs) were isolated by Ficoll density gradient centrifugation from de-identified blood samples. Human hybridomas were generated by transforming PBMCs with medium containing Epstein-Barr virus, CpG (Life Technologies), a Chk2 inhibitor

(Sigma), and cyclosporine A (Sigma). Cells were expanded from 384-well to 96-well plates containing a feeder layer of irradiated heterologous human PBMCs. After an additional five days, supernatants from expanded cells were screened in an enzyme-linked immunosorbent assay (ELISA) using recombinant *S. aureus* IsdB protein to identify wells containing B cells secreting antibodies reactive with IsdB. Transformed B cells in reactant cell culture wells were fused with HMMA2.5 myeloma cells by electrofusion. Monoclonal hybridoma lines were obtained using single-cell fluorescence-activated cell sorting on a sterile FACSAria III cell sorter.

Bacterial strains. The *S. aureus* strain Newman was grown at 37°C for 12-18 hours on tryptic soy agar (TSA) plates or in tryptic soy broth (TSB). Isogenic knockouts were made in a Newman background by using allelic replacement of the coding sequence with *ermC* (Bae and Schneewind 2006; Mazmanian et al. 2003; Torres et al. 2006). PCR fragments were assembled into the pCR2.1 DNA plasmid vector and then recombined into the pKOR1 plasmid to inactivate the gene.

Generation of recombinant IsdB and IsdB-NEAT2 protein. A cDNA of the sequence encoding IsdB, excluding the sorting signal and signal peptide, was cloned into the pET15b vector and expressed using BL21 (DE3) *E. coli* cells. For IsdB-NEAT2, only the NEAT2 encoding sequence was cloned into a pET15b vector. For both, bacteria were grown in Luria-Bertani (LB) broth for 36 hours total and induced after 6 hours at *30°C* with 1 mM isopropyl β-D-1-thiogalactopyranoside (IPTG). The culture was harvested by centrifugation and resuspended in 50 mM Na_2HPO_4 + 500 mM NaCl before disruption by

homogenization (Microfluidizer LM20). The protein was purified using a HiTrap TALON column, and the His-tag was cleaved with thrombin.

Growth curves in the presence of hemoglobin. *S. aureus* strain Newman or the *ΔisdB Δspa* strain were grown overnight in RPMI medium + 0.1 casamino acids + 0.5 mM EDDHA. The $O.D_{600}$ was normalized to 1 and subcultured into 200 µL of RPMI + EDDHA with 20 nM of human hemoglobin and 2 µg/mL mAb. Bacteria in 96-well plates were grown at 37°C and OD_{600} values were recorded at 3, 7, 24, and 36 hours in the Gen5 microtiter plate software (Bio-Tek). Human hemoglobin was purified from hemolysate by HPLC, as previously described (Pishchany et al. 2014).

Biolayer interferometry assays. K_D and blocking studies were performed on an Octet RED biosensor (Pall FortéBio). For K_D studies, individual antibodies were loaded onto anti-human Fc biosensors. Biosensor tips were washed first and then immersed into wells containing antibody (5 µg/mL). This was followed by an additional wash step before association with wells containing 2-fold dilutions of IsdB protein to create a concentration series ranging from 150 to 2.3 M. The k_{on} and k_{off} values for interaction were determined by a global fitting of the curves in the Octet software. Blocking studies were performed by first washing streptavidin biosensors and then associating them with biotinylated hemoglobin. The sensors then were associated with wells containing IsdB, IsdB + mAb, mAb alone, or kinetic buffer.

Mouse experiments. A murine septic model of *S. aureus* infection was used, as described previously (Bennett et al. 2018). 7-week-old female BALB/cJ mice were weighed and injected with 10 mg/kg mAb via the intraperitoneal route. Mice were anesthetized and injected retro-orbitally with 10^7 CFU *S. aureus* strain Newman in a 100 μL volume. After 96 hours, mice were euthanized by CO_2 inhalation and organs were collected and homogenized in PBS before serially diluting for colony enumeration. Mouse experiments were approved and performed according to the guidelines of the Vanderbilt University School of Medicine Institutional Animal Care and Use Committee (IACUC).

Hydrogen-deuterium exchange mass spectrometry. IsdB and Fab proteins were prepared at 10 pmol/μL. Labeling occurred in PBS pH 7.4 in D_2O at 20°C for 30 seconds or 4 hours. The reaction was quenched in PBS, 4 M guanidinium/HCl, 100 mM tris (2-carboxyethyl) phosphine to a pH of 2.3, 0°C. Samples were injected into a nano-ACQUITY UPLC system with HDX technology. Online digestion was performed at 15°C and a flow of 134 μL/min of 0.1% formic acid using an immobilized-pepsin column and simultaneously trapped at 0°C on a VanGuard™ BEH C18 1.7 μm column. Peptides were eluted using 5-35% acetonitrile, 0.1% formic acid in H_2O and separated on a ACQUITY UPLC BEH C18 1.7 μm, 1 mm × 100 mm column and analyzed using Xevo G2-XS in MS^E-mode. Peptide-identification was performed using Waters ProteinLynx Global Server 3.0.3 software and deuterium-uptake was calculated using DynamX 3.0 software. Results were averaged across replicate analyses, at a given time point and the standard deviation determined.

Crystallography. IsdB-NEAT2 protein was run on size exclusion chromatography (SEC) (HiLoad 16/600, Superdex 75 pg GE Healthcare Life sciences) in 20 mM Tris, 50 mM NaCl buffer. The antigen was concentrated to 10 mg/mL and incubated at room temperature with Fab at a 1:2 ratio. The incubated complex was run on SEC and concentrated to 10 mg/mL. All crystals were obtained using Hampton Research screens in various conditions. X-ray diffraction data were collected at the Advanced Photon Source LS-CAT beamline 21-ID-G or F. STAU-281 in complex with IsdB-NEAT2 crystalized in 0.1 M sodium citrate tribasic dehydrate pH 5.5 and 16% PEG 8K. STAU-399 Fab crystalized in 10% PEG 200, 18% PEG 8K, and 0.1 M BIS-TRIS propane pH 9.0. STAU-229 Fab crystalized in 0.1 M ammonium acetate, 0.1 M BIS-TRIS pH 5.5, and 17% PEG 10K. Images were indexed and scaled with X-ray Detector Software (Kabsch 2010) and molecular replacement was performed in Phaser (Adams et al. 2010) followed by manual refinement using subsequent rounds of COOT (Emsley et al. 2010) and Phenix (Adams et al. 2010).

Antibody variable gene sequence analysis. Total RNA was isolated from approximately 15 million PBMCs using the Qiagen RNeasy Mini Kit (Qiagen, CA). Purified total RNA samples were processed at AbHelix, LLC (www.abhelix.com, South Plainfield, NJ, USA). Briefly, RNA samples were reversed transcribed using the oligo $d(T)_{18}$ in 3-5 µg per 20 µL reaction (SuperScript IV Reverse Transcriptase, ThermoFisher, CA). Multiple reactions of reverse transcription were combined and purified using magnetic beads. The purified RT products were divided evenly for the first round of PCR amplification specific to human IgG, IgK, IgL, IgM and IgA. The 5′

multiplex PCR primers were designed within the leader sequences for each productive V-gene and the 3′ primers within the constant regions, but in close approximation to the J-C junctions. The resulting 1st round PCR products were purified with magnetic beads and subjected to a second round of PCR amplification to add Illumina index and adapter sequences. The resulting PCR products were purified with magnetic beads and pooled for sequencing with a PE250 protocol on an Illumina MiSeq sequencer. Phusion High-Fidelity DNA Polymerase (ThermoFisher, CA) was used in all PCR amplification reactions and care was taken to minimize the number of cycles to achieve adequate amplification. For IgG sequencing reads, subclass-specific sequences in the beginning of the constant regions were used to identify IgG1, IgG2, IgG3, or IgG4 subclasses.

Bioinformatics and processing of next-generation sequencing (NGS). The bioinformatics processing of all NGS data was done using our PyIR sequence processing pipeline (https://github.com/crowelab/PyIR) with sample and data management performed using our in-house proprietary laboratory information management system. We used BLAST (Altschul et al. 1990) and searched through the processed NGS data using the heavy chain V3J clonotypes belonging to monoclonal *IGVH1-69* hybridoma sequences. A BLAST database was constructed using all the unique V3J clonotypes derived from the NGS data (data from all isotypes were pooled together). We set the sequence identity threshold to 70% and the sequence alignment coverage to 95%. The BLAST parameters were set using the following values: word size=3, gap open and extension parameters were to 7 and 2 respectively.

Human mAb and Fab production. Fab fragments were expressed recombinantly by cloning the cDNA encoding the heavy and light chain variable gene regions into IgG expression vectors and transforming them into *E. coli*. MAb protein was produced by transient co-transfection of the Fab heavy chain and light chain DNA into either ExpiCHO or FreeStyle 293F cells (ThermoFisher Scientific) following the manufacturer's protocol. Recombinant Fab was purified from supernatant using an Anti-CH1 column (GE Healthcare).

Statistical analysis. All data were analysed in Prism v 7.0 (GraphPad Software Inc.).

CHAPTER IV

STAU-239 REVEALS A CROSS-REACTIVE EPITOPE

Introduction

Iron is a nutrient at the crux of nutritional immunity- bacteria require it for basic metabolic and enzymatic processes, while the human host sequesters up to 80% of free iron so it is not readily available (Skaar et al. 2004; Skaar 2010). Many Gram-positive bacteria overcome this issue by targeting the heme within hemoglobin by binding heme-iron using specialized NEAT (NEAr iron transporter) domains that are found specifically on cell wall anchored surface proteins (Honsa et al. 2014). Using NEAT domains, heme-iron is captured from hemoglobin, making this protein the most abundant iron source in the human body. Major Gram-positive pathogens including *B. anthracis*, *L. monocytogenes*, *C. perfrinogens*, *C. tetani*, *S. pyogenes*, and *S. aureus* all have NEAT-containing proteins (Andrade et al. 2002; Honsa et al. 2014; Marraffini et al. 2006). The conservation of this domain across species underscores its importance not only to heme function, but also points to its potential as a therapeutic target. As mentioned previously, *S. aure*us contains NEAT domains that bind both heme and hemoglobin. IsdB has IsdB-NEAT1 that binds hemoglobin and IsdB-NEAT2 that binds heme (Bowden et al. 2018; Fonner et al. 2014), while IsdA has only one NEAT domain that binds heme. In this chapter, I focus on a mAb that binds both IsdA and IsdB. Structural studies revealed that binding to the NEAT domain is responsible for the cross-reactivity of this mAb.

The broad reactivity of mAb STAU-239 also led to the hypothesis that it may bind other NEAT-containing Gram-positives, like *B. anthracis*, which show homology to the Isd proteins of *S. aureus*. *B. anthracis* has two hemophores, IsdX1 and IsdX2, which are extracellular proteins that are secreted and extract heme from hemoglobin and deliver it to IsdC within the cell wall (Fabian et al. 2009; Honsa et al. 2011; Maresso et al. 2008). Another protein identified for heme transport was BslK (*B. anthracis* S-layer protein K). Unlike the sortase-anchored proteins of the Isd system, BslK is non-covalently anchored to the cell wall. It binds heme and transports it to IsdC, serving as a redundant source of heme-acquisition along with IsdX1 and IsdX2 (Tarlovsky et al. 2010). Finally, *B. anthracis* also has a Hal heme uptake system with one NEAT domain that extracts heme from hemoglobin without the use of the canonical stabilizing tyrosine but instead has several leucine-rich repeats (Balderas et al. 2012). All of these proteins contain NEAT domains and are protein targets that STAU-239 may potentially bind.

In this chapter, I discuss STAU-239, which binds both IsdA and IsdB. Using X-ray crystallography, the specific residues important for STAU-239 binding to IsdA-NEAT1 are identified. The STAU-239-IsdB epitope is also described using HDX-MS, which detects peptides bound by the mAb. Interestingly, STAU-239 binds to IsdB-NEAT1, the hemoglobin-binding domain of IsdB but IsdA-NEAT1 is specific for heme binding. Perhaps this can be attributed to the conservation of this epitope, as performed genome conservation studies indicated that it contains very few mutations across more than 42,522 genomes queried. Finally, an experiment was performed to test whether STAU-239 binds another NEAT containing bacterial species, *B. anthracis*. STAU-239 was conjugated to a photoactivated dye, which can be visualized using super-resolution

microscopy. *B. anthracis* was grown under iron-limiting conditions to induce expression of NEAT domain proteins that bind heme-iron and mAb was added. Imaged slides showed that STAU-239 binds to *B. anthracis*, highlighting the therapeutic and diagnostic potential of targeting a cross-reactive epitope such as the NEAT domain.

I would like to acknowledge Wendy White and Dr. Kevin L. Schey for performing HDX-MS of STAU-239 in complex with IsdB. I would also like to acknowledge Dr. Timothy D. Read and Dr. Robert A. Petit III for doing *S. aureus* genome analysis. I would like to acknowledge Dr. Jinhui Dong for resolving the crystal structure of STAU-239-IsdA. I would finally like to acknowledge Dr. Mingfeng Bai and Meng Su for conjugating STAU-239 and Clare Laut for imaging slides.

STAU-239 binds IsdA and IsdB

STAU-239 was isolated using the traditional hybridoma process. PBMCs were transformed with EBV in the presence of CpG, Chk2, and cyclosporine A. After a week, I expanded the cells using irradiated feeder cells and screened for reactivity using an ELISA screen with recombinant protein. Supernatants that reacted by ELISA were fused with HMMA2.5 myeloma cells in HAT media. I continued to expand and screen the cells by ELISA before single cell sorting. STAU-239 was isolated from the PBMCs of subject 1, a 20-year-old female with MSSA of osteomyelitis and cellulitis (Table 2-1). I tested serial dilutions of STAU-239 for binding to purified recombinant IsdA and IsdB by ELISA. The mAb was able to bind both proteins, although it did bind better to IsdA than IsdB (Figure 4-1).

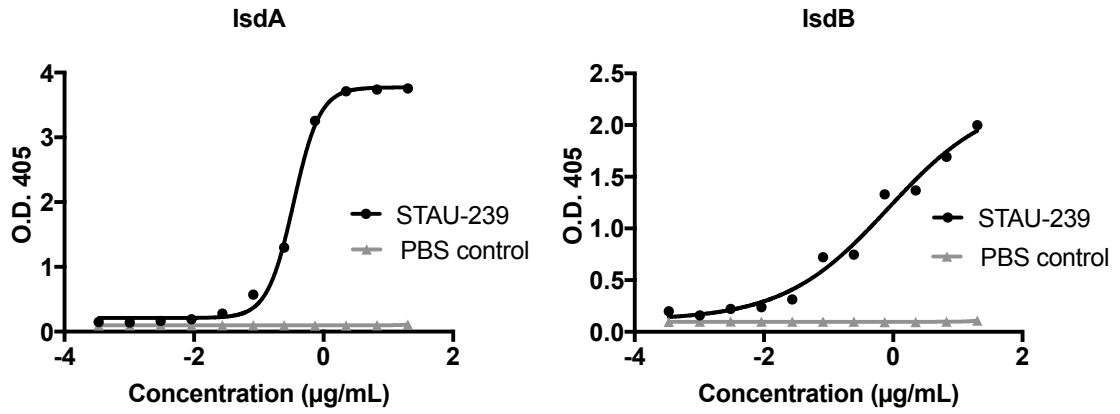

Figure 4-1. STAU-239 binding curves to IsdA and IsdB.

384 ELISA plates were coated with recombinant IsdA or IsdB before incubating with the serial dilutions of STAU-239 as the primary antibody. STAU-239 bound to IsdB at an (half-maximal effective concentration) value of 0.35 µg/ml and bound to IsdB at 0.84 µg/ml.

Structural characterization of STAU-239 in complex with IsdA and IsdB

A crystal structure of STAU-239 Fab was solved in complex with IsdA at 2.8-Å resolution with the help of Dr. Jinhui Dong. The structure identified STAU-239 binding to the heme-binding pocket of IsdA-NEAT1 with no heme found within the crystal structure. This indicates STAU-239 might have prevented heme from binding to the pocket directly, as other crystal structures of IsdA have had heme present (PDB IDs: 2ITF, 3QZL, 3QZM, 3QZN, 3QZO) (Grigg et al. 2007b; Grigg et al. 2011). The interaction of STAU-239 with IsdA relies heavily on the F55 in the HCDR2, which interjects directly into the heme pocket making polar contacts with Y166 and Y87 of IsdA (Figure 4-2). I overlaid a previously solved structure of IsdA (PDB ID: 2ITF (Grigg et al. 2007b) that contains heme to confirm the importance of the identified residues in preventing heme binding. The heme molecule would be in direct contact with F55 on

HCDR2 (Figure 4-2, bottom 2 ovals). This structure revealed that STAU-239 prevents heme from binding to the heme-binding site in the NEAT1 domain of IsdA. This structure independently supports previously obtained HDX-MS data (Figure 2-5), which also identified that STAU-239 bound the heme-binding site.

I worked with Wendy White in the mass-spec research center to determine the binding site of STAU-239 to IsdB using HDX-MS. HDX-MS can identify overlapping peptides involved in protein-protein interactions by comparing deuterium uptake. Purified recombinant STAU-239 Fab was tested for binding to IsdB and found to bind to IsdB-NEAT1, the hemoglobin-binding specific portion of IsdB. The binding site is modeled onto a previously crystallized structure of the NEAT domain (green), where the HDX-MS peptide residues are in blue (Figure 4-3 top). STAU-239 bound specifically to peptide residues 132-147, at the beginning of NEAT1. The structure was overlaid onto crystal structure containing hemoglobin to show the binding site's proximity to heme (Figure 4-3 bottom).

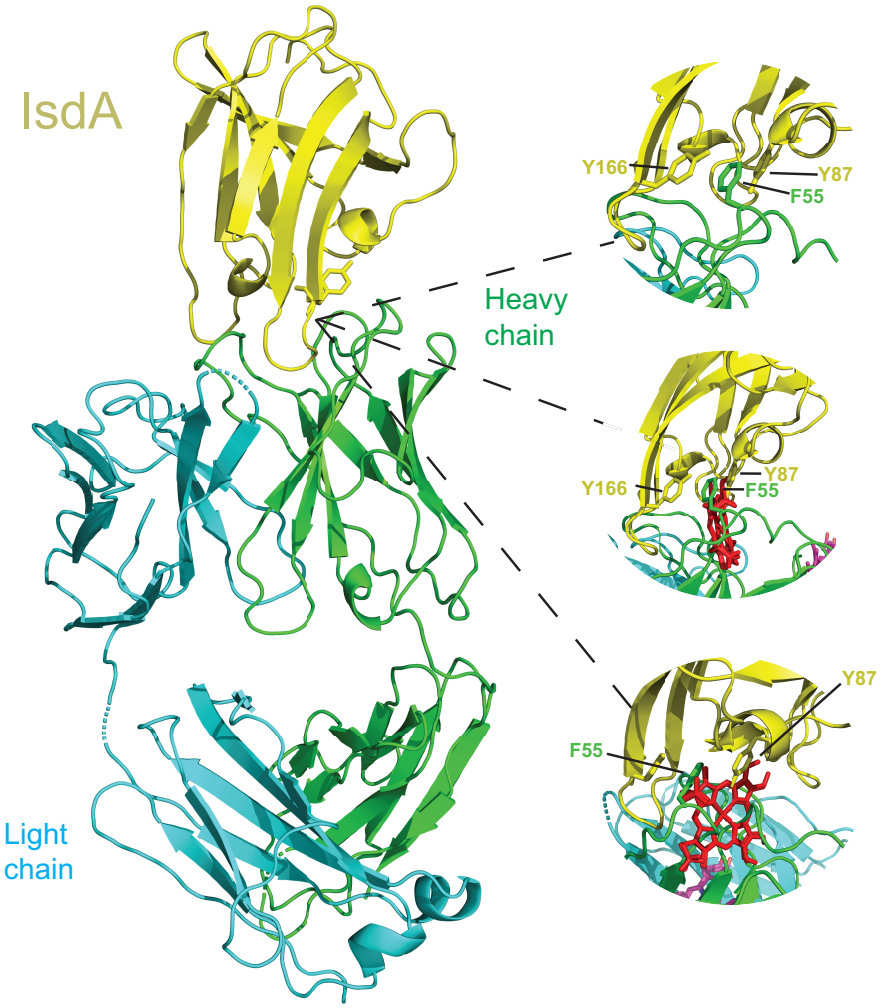

Figure 4-2. STAU-239 in complex with IsdA

A crystal structure of STAU-239 in complex with IsdA is shown at 2.8-Å resolution. STAU-239 was found to bind the heme-binding pocket of IsdA. Key residues on the HCDR2 were identified that prevent binding of heme within the pocket, including F55, which is shown in magnified view to the right. A previously solved structure of IsdA (PDB ID: 2ITF (Grigg et al. 2007b) that contains heme is overlaid (bottom 2 ovals).

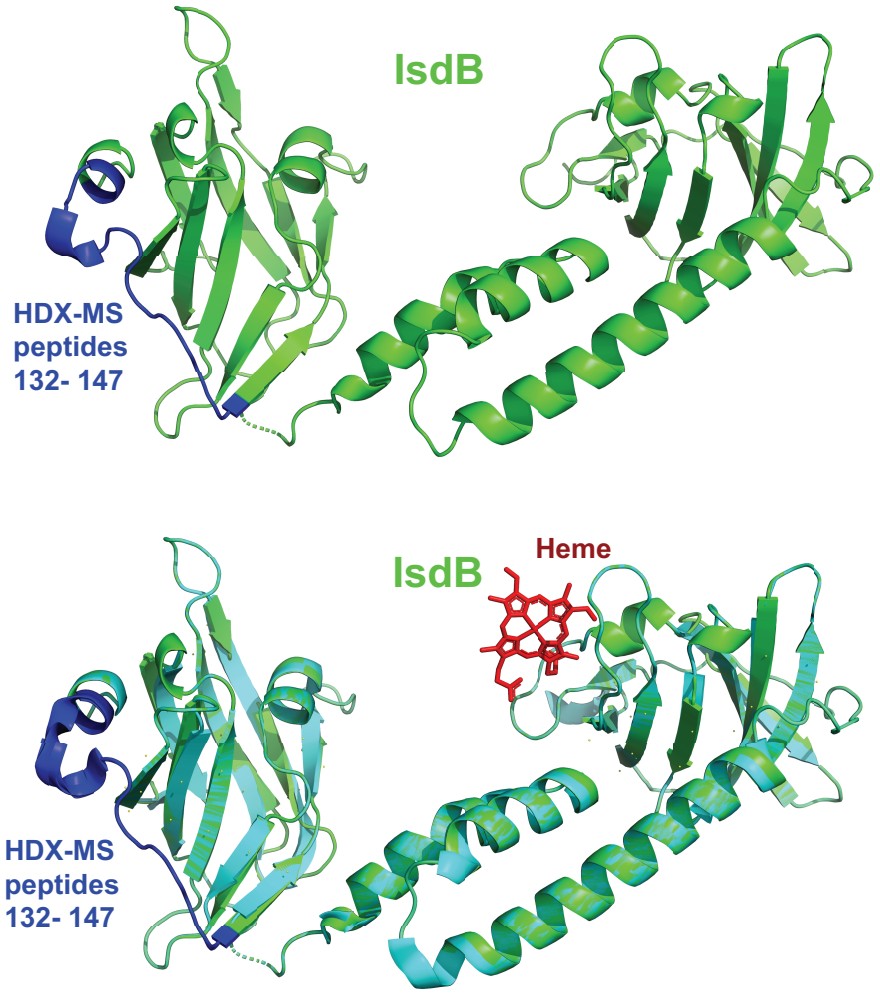

Figure 4-3. HDX-MS binding peptides of STAU-239 on IsdB.

The crystallized structure of IsdB (PDB ID: 5VMM (Bowden et al. 2018) is shown with the predicted binding sites of STAU-239 (blue) and heme (red). A previously solved structure of IsdB bound to hemoglobin and containing heme is overlaid (bottom) to show its relative position to the binding site of STAU-239.

Conservation of STAU-239 binding site on IsdA

The genetic variation of the STAU-239 binding site was also investigated in collaboration with Timothy Read's group as this mAb binds both IsdA and IsdB. The level of amino acid conservation was determined by comparing the *S. aureus* strain Newman IsdA protein sequence used here against protein sequences from 42,949 *S. aureus* genomes that are publicly available (Petit and Read 2018). The IsdA protein from the remaining genomes (42,522) was clustered based on 100% identity. The most common sequence had 16,416 strains (including Newman) and there were 29 strains (0.06%) that had predicted amino acid substitutions compared to the canonical Newman sequence at positions 159 and 167. 18 ST22 strains shared a glutamine to arginine mutation (Q163R) at position 163. Q163 is also a surface residue and the position farthest from heme in the binding site, which may be why amino acid variability is more tolerated at this position. All additional mutations were shared in less than 4 strains. Five of the amino acid sites were invariant in the 42,522 strains, underscoring the conservation of this epitope across *S. aureus*.

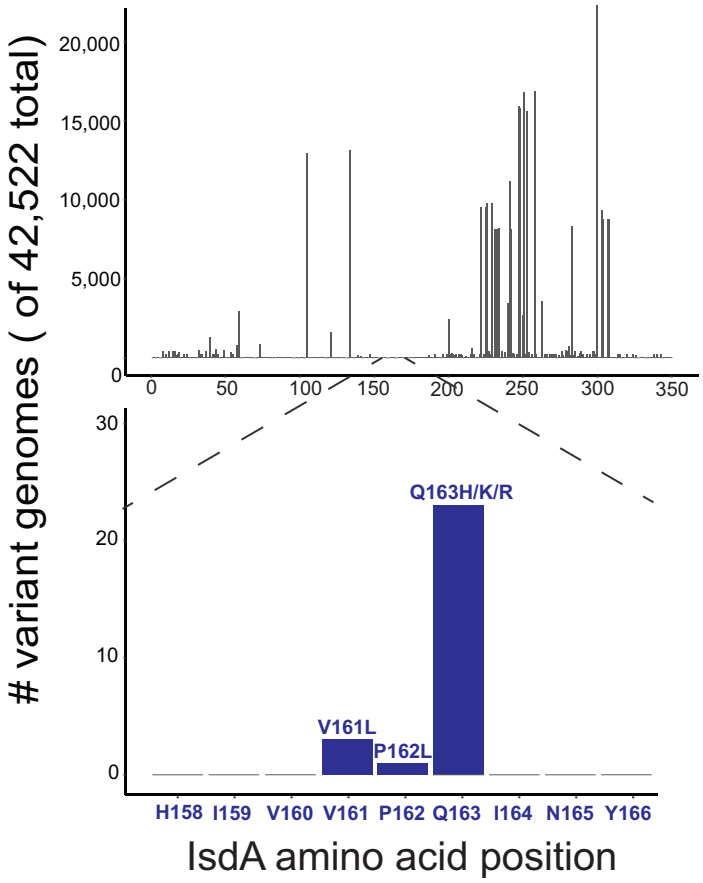

Figure 4-4. Conservation of STAU-239 binding site across *S. aureus* genomes

Amino acid changes in the *S. aureus* strain Newman IsdA protein were determined from publically available *S. aureus* genomes. The frequency distribution of these changes across all IsdA residues in *S. aureus* strains is shown (top). Amino acid changes in the mAb STAU-239 binding site (positions 158 to 166) are shown (bottom).

Cross-reactivity of STAU-239 with *B. anthracis*

STAU-239 is a broadly reactive mAb with specificity for IsdA and IsdB with a conserved epitope across thousands of *S. aureus* strains. This led to the hypothesis that this mAb may also bind another Gram-positive, *B. anthracis*, which contains a number of proteins with NEAT domains including IsdX1, IsdX2, IsdC, BslK, and Hal. (Fabian et al. 2009; Honsa et al. 2011; Maresso et al. 2008). A ClustalW alignment of the *B. anthracis* NEAT-containing proteins with the Isd surface proteins of *S. aureus* shows multiple shared residues (Figure 4-5). Notably, there is a serine (S) that is shared for every NEAT domain except IsdB-NEAT1. This difference is most likely because IsdB-NEAT1 binds hemoglobin instead of heme. There are also a number of tyrosines (Y) present in *B. anthracis* and *S. aureus*, which is not surprising as this residue has been described multiple times before as playing a critical role in stabilizing the binding interaction between heme and NEAT binding proteins (Grigg et al. 2007b; Grigg et al. 2011; Pluym et al. 2008). Once again, although IsdB-NEAT1 does not maintain the same terminal tyrosine as the heme-binding NEAT domains, it does have a similarly functioning YHY motif that is critical for hemoglobin binding. The Isd proteins of both species also maintain a glutamic acid (E) and methionine (M) (Figure 4-5).

To test the hypothesis that STAU-239 would bind proteins in *B. anthracis*, STAU-239 was conjugated to a photosensitizing dye, IR-700, with the help of Mingheng Bai's lab. This dye can be visualized using the far-red channel on a super-resolution microscope. *B. anthracis* strain Sterne was grown overnight in iron-chelating conditions to allow for the expression of NEAT domain containing proteins. *B. anthracis* was normalized by $O.D._{600}$ and subcultured with either conjugated STAU-239 or an isotype

control. After 30 minutes of shaking at 37° C, I prepared slides using a DNA dye called hoeschst (blue) and an Alexafluor-488 conjugated WGA cell wall dye (green). The slides were imaged with the help of Clare Laut on a Nikon SIM microscope. The isotype control mAb did not bind to *B. anthracis* (Figure 4-6 top), however, STAU-239 (pink) bound on the outside of the bacterial cells in multiple observed locations (Figure 4-6 bottom). These data show that STAU-239 does bind to *B. anthracis*, although it is unclear to which protein specifically.

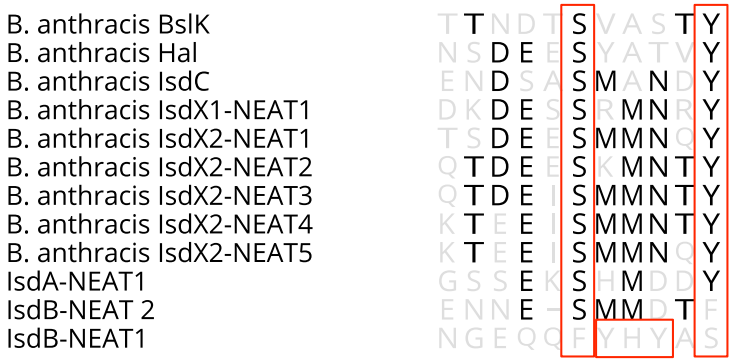

Figure 4-5. ClustalW alignment of NEAT domain containing proteins in *B. anthracis* and *S. aureus*

The NEAT domains of a number of *B. anthracis* proteins are shown along with the surface Isd proteins of *S. aureus*. These were aligned using a ClustalW sequence alignment tool. A conserved serine was present at the same location in 11/12 NEAT domains and a tyrosine was present in 10/12 NEAT domains.

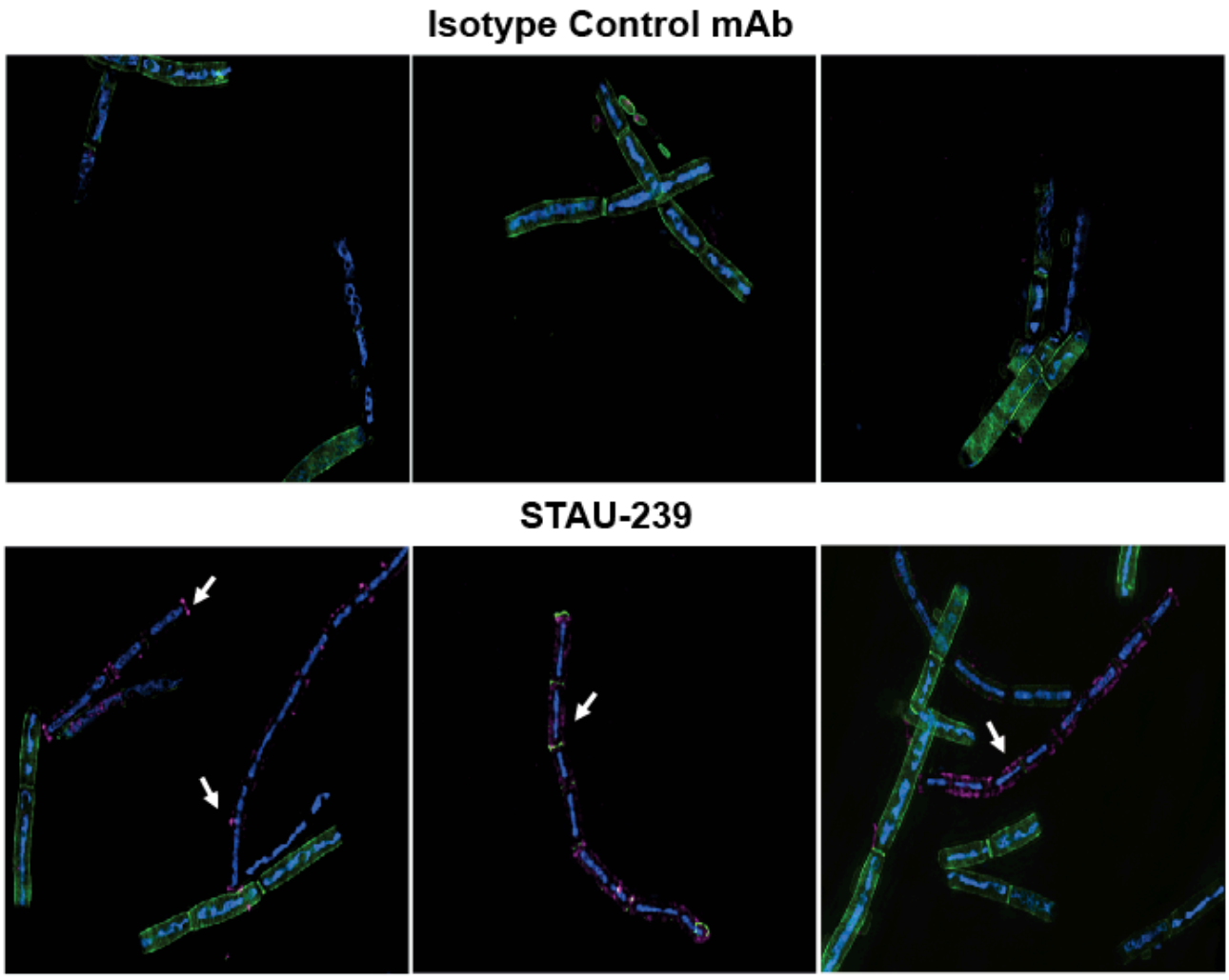

Figure 4-6 STAU-239 binds to *B. anthracis*

B. anthracis strain Sterne was grown overnight with 2,2-dipyridal to limit iron and then subcultured into fresh tubes with the addition of an irrelevant isotype control mAb or STAU-239. Slides were prepared with Hoeschst, a DNA dye (blue) and WGA, a cell wall dye (green). Antibody is shown in pink. The slides were imaged on a Nikon SIM microscope. Images are representative of multiple fields of view.

Discussion

In this chapter, I discuss a broadly reactive mAb, STAU-239, that binds to two separate *S. aureus* Isd proteins and cross-reacts with an iron-regulated protein in *B. anthracis*. STAU-239 binds to the heme-pocket of IsdA-NEAT1, where F55 of the HCDR2 makes polar contacts with Y87 and Y166 of IsdA within the pocket. Amino acid changes within the *S. aureus* strain Newman IsdA protein where STAU-239 bound was investigated from publicly available *S. aureus* genomes. The identified frequency of these mutations was minor, with the highest divergence from Newman being 0.06% of investigated strains that had predicted substitutions at positions 159 and 167. STAU-239 was also found to bind IsdB-NEAT1 at positions 132-147, a region of the protein involved in hemoglobin binding. Finally, this mAb displayed binding activity against *B. anthracis* when investigated by microscopy. Collectively, these results indicate this mAb may identify a more global epitope present in multiple NEAT containing proteins, not only within *S. aureus*.

The cross-specificity of STAU-239 is possible due to the conservation of heme-binding NEAT domains throughout *S. aureus* and *B. anthracis*. Interestingly, although NEAT domains themselves are conserved, the amino acids present within them change dramatically. Of 165 analyzed NEAT domains in one study, 48% maintain an YXXXY motif, where the first tyrosine binds iron and the second stabilizes the binding interaction by hydrogen-bonding the axial tyrosine (Fonner et al. 2014; Honsa et al. 2014). This 48% includes *B. anthracis* IsdX1, IsdX2 -NEAT1, -NEAT3, -NEAT4, and -NEAT5 and *S. aureus* IsdA and IsdB -NEAT2 but not IsdB-NEAT1 (Grigg et al. 2007b; Sharp et al. 2007). IsdB-NEAT1 lacks this heme-binding motif, but does maintain a tyrosine residue

at position 167 and a phenylalanine at position 164 that play a key role in interacting with hemoglobin (Fonner et al. 2014; Pishchany et al. 2014).

It is surprising that STAU-239 binds to both a heme (IsdA-NEAT1) and hemoglobin-binding (IsdB-NEAT1) domain, but it is difficult to do a complete comparison of the binding sites without a crystal structure of the IsdB binding site. I overlaid these two NEAT domains to give insight into similarities that may be responsible for the cross-reactivity (Figure 4-7). The alignment shows multiple strictly conserved residues between the two proteins with two sites of particular interest highlighted in red boxes. Polar amino acids such as serine and tyrosine are frequently found in heme and hemoglobin binding motifs and there is a serine present (S144) within the HDX-MS identified binding site of STAU-239 in IsdB-NEAT1 that is also conserved in IsdA. Conversely, Y166 was found to be a critical residue in the heme-binding pocket of IsdA and is also present at the same position in IsdB-NEAT1. The overlay also shows structural similarities between the two NEAT domains in the presence and absence of heme. Aromatic tyrosine is a key element of the binding interface for both IsdA and IsdB (Figure 4-7). These data indicate there may be a structural basis for STAU-239 binding to both a heme and hemoglobin-binding motif within *S. aureus* proteins.

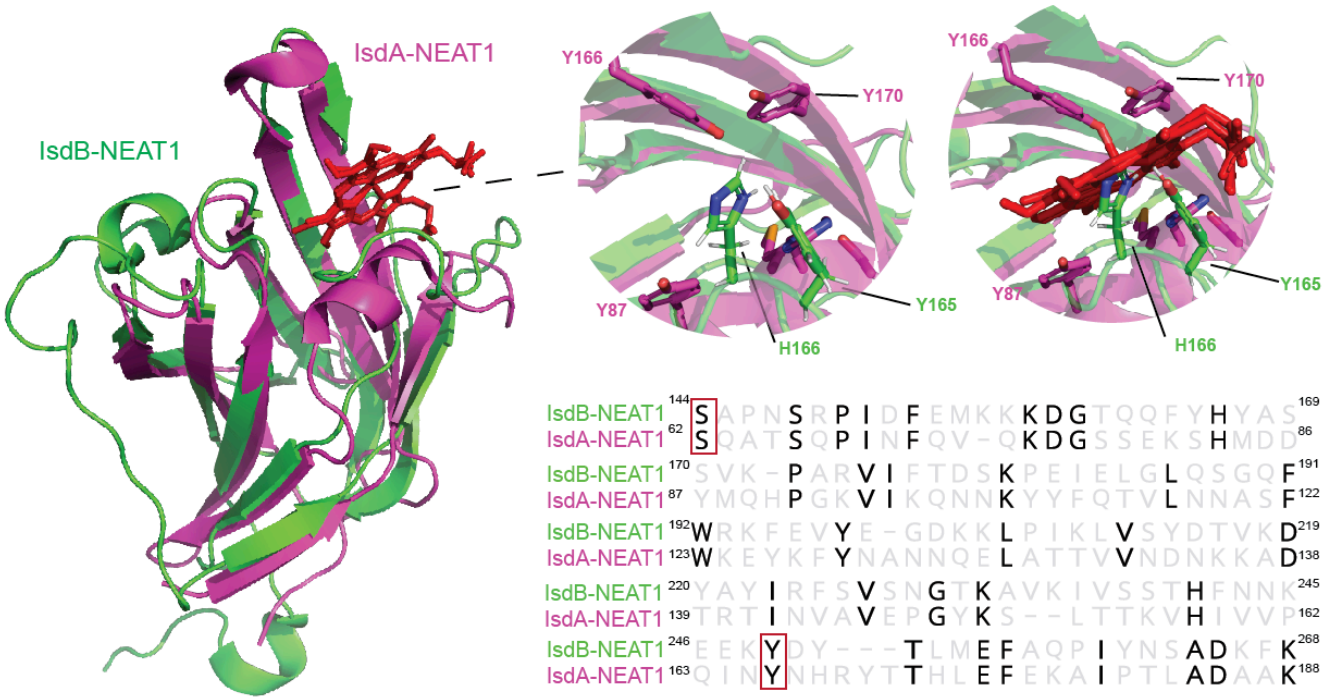

Figure 4-7. Structural and sequence comparison of IsdA-NEAT1 with IsdB-NEAT1.

An overlay of the NEAT domain of IsdA (PDB ID: 2ITF) and IsdB-NEAT2 (PDB ID: 2MOQ) was done in Pymol. IsdA is shown in pink and IsdB is in green. These sequences were also aligned using a ClustalW sequence alignment tool with agreements shown. Strictly conserved amino acids that correspond to obtained structural data are boxed in red.

Experimental Methods

Human subjects. Human blood was collected from patients at Vanderbilt University Medical Center after informed consent and this study was approved by the Institutional Review Board of Vanderbilt University Medical Center. The subjects were tested for previous history MSSA or MRSA.

Generation of human monoclonal antibodies (mAbs). PBMCs were isolated by Ficoll density gradient centrifugation from blood samples and then cryopreserved. PBMCs were

thawed and then transformed with medium containing Epstein-Barr virus, CpG (Life Technologies), a Chk2 inhibitor (Sigma), and cyclosporine A (Sigma) and plated on a 384-well plate. Cells were expanded then to 96-well plates containing a feeder layer of irradiated heterologous human PBMCs. Cell supernatants were screened by ELISA after an additional four to five days using recombinant *S. aureus* surface proteins to identify wells containing B cells secreting antibodies reactive with these antigens. Transformed B cells in reactant cell culture wells were fused with HMMA2.5 myeloma cells by electrofusion and plated in HAT media. Reactant supernatants were continually screened by ELISA and monoclonal hybridoma lines were obtained using single-cell fluorescence-activated cell sorting on a sterile FACSAria III cell sorter.

Bacterial strains. The *B. anthracis* strain Sterne was grown at 30°C overnight in LB broth with the addition of 0.25 mM dipyridyl.

Generation of recombinant Isd antigen. Soluble forms of the antigens of interest (excluding the sorting signal and signal peptide) were cloned into the pET15b plasmid vector and expressed recombinantly using the BL21 (DE3) *E. coli* expression system. Cultures were grown in Luria-Bertani (LB) broth and induced after 6 hours at 30°C with 1 mM IPTG. 36 hours later the cells were centrifuged and resuspended in 50mM Na_2HPO_4 + 500 mM NaCl before sonication. The soluble fraction was purified by affinity chromatography using a cobalt HiTrap TALON column. Purified IsdA or IsdB was used at a concentration of 2 μg/mL when screening PBMCs and supernatants for reactivity.

Human mAb and Fab production. Fab fragments were expressed recombinantly by cloning the cDNA encoding the heavy and light chain variable gene regions into IgG expression vectors and transforming them into *E. coli*. MAb protein was produced by transient co-transfection of the Fab heavy chain and light chain DNA into either ExpiCHO or FreeStyle 293F cells (ThermoFisher Scientific) following the manufacturer's protocol. Recombinant Fab was purified from supernatant using an Anti-CH1 column (GE Healthcare).

Hydrogen-deuterium exchange mass spectrometry. IsdB and Fab proteins were prepared at 10 pmol/μL. Labeling occurred in PBS pH 7.4 in D_2O at 20°C for 30 seconds or 4 hours. The reaction was quenched in PBS, 4 M guanidinium/HCl, 100 mM tris (2-carboxyethyl) phosphine to a pH of 2.3, 0°C. Samples were injected into a nano-ACQUITY UPLC system with HDX technology. Online digestion was performed at 15°C and a flow of 134 μL/min of 0.1% formic acid using an immobilized-pepsin column and simultaneously trapped at 0°C on a VanGuard™ BEH C18 1.7 μm column. Peptides were eluted using 5-35% acetonitrile, 0.1% formic acid in H_2O and separated on a ACQUITY UPLC BEH C18 1.7 μm, 1 mm × 100 mm column and analyzed using Xevo G2-XS in MS^E-mode. Peptide-identification was performed using Waters ProteinLynx Global Server 3.0.3 software and deuterium-uptake was calculated using DynamX 3.0 software. Results were averaged across replicate analyses, at a given time point and the standard deviation determined.

Crystallography. IsdA protein was run on size exclusion chromatography (SEC) (HiLoad 16/600, Superdex 75 pg GE Healthcare Life sciences) in 20 mM Tris, 50 mM NaCl buffer to further purify. The antigen was concentrated to 10 mg/mL and incubated at room temperature with Fab at a 1:2 ratio. The incubated complex was run on SEC and concentrated to 10 mg/mL. STAU-239 in complex with IsdA crystalized in 20% 2-Propanol, 0.1 M MES monohydrate pH 6.0, and 20% PEG 2K. X-ray diffraction data were collected at the Advanced Photon Source LS-CAT beamline 21-ID-G or F. Images were indexed and scaled with X-ray Detector Software (Kabsch 2010) and molecular replacement was performed in Phaser (Adams et al. 2010) followed by manual refinement using subsequent rounds of COOT (Emsley et al. 2010) and Phenix (Adams et al. 2010).

Mapping *isdA* genetic variation using *S. aureus* genomes. A BLAST+ (Camacho et al. 2009) database was created from 42,949 publically available *S. aureus* sequences (Petit and Read 2018). The *S. aureus* strain Newman IsdA protein sequence (NCBI Reference Sequence NZ_CP023391) was queried against the created BLAST + database (v2.7.1, blastp -db $BLASTDB -query $ISDA -outfmt 15). Proteins with 90% sequence coverage and 80% identity to the IsdA protein were extracted and clustered at 100% identity using CD-HIT (v4.6, cdhit -i $PROTEINS -o $OUTPUT -c 1.0) (Fu et al. 2012; Li and Godzik 2006). These cluster sequences were compared to Newman IsdA protein and changes were extracted from the BLAST alignment.

Microscopy of *B. anthracis*. *B. anthracis* was grown overnight in LB at 30°C with 0.25 mM dipyridyl. Overnight cultures were normalized to an $O.D._{600}$ of 0.5 and subcultured into fresh tubes with antibody treatment. Tubes were incubated at 37°C for 30 minutes. 500 ul of $O.D._{600}$ 0.5 tubes were spun down and washed in PBS. Tubes were resuspended with Alexaflour-488 conjugated to WGA for 5 minutes to stain the cell wall. After washing, tubes were stained for 5 minutes with Hoechst dye. Samples were washed and then fixed with PFA for 30 minutes. Coverslips were prepared and dried overnight. Slides were imaged using the super resolution microscope the Nikon SIM (structured illuminations microscope). The far-red channel was used to image the conjugated molecule label on STAU-239.

CHAPTER V

CONCLUSIONS AND FUTURE DIRECTIONS

Human antibody response to *S. aureus* Iron-regulated surface determinant system

S. aureus has proven to be a formidable pathogen for vaccine design. With multiple virulence strategies, redundant nutrient acquisition pathways, and a list of failed vaccines, it is critical to obtain a more thorough understanding of how to better target the relevant factors for treatment. A large body of work has shown that heme acquisition pathways are crucial for many living organisms to survive and that this molecule is necessary for full virulence in *S. aureus*. Moving forward, strategies to fully exploit this pathway may improve the efficiency and success of *S. aureus* vaccines.

My overarching project goal was to define the human B cell response to *S. aureus* iron-binding proteins by using human mAbs as tools. My hypothesis was that human mAbs to the *S. aureus* iron regulated surface determinant system would block iron acquisition and decrease pathogen growth and virulence. To begin, I isolated a panel of 29 antibodies to the three surface proteins of the Isd system, IsdA, IsdB, and IsdH using novel hybridoma technology. I was able to determine binding specificities and EC_{50} values for each mAb using purified recombinant protein and found that several antibodies were cross-reactive to all three surface proteins. Other antibodies were reactive to only two of the Isd proteins and some were specific to only one protein. I used biolayer interferometry to perform competition studies on this panel of antibodies and split them

into groups based on their inferred antigenic site. The antibodies against IsdA and IsdB fell into three distinct competition groups based on where they bind. I picked a representative mAb from each group and tested it *in vivo* to assess whether antibodies targeting this particular site would have a protective effect. For initial testing, I used a septic model of infection and combined two antibodies. These were injected into mice via the IP route before infecting mice with *S. aureus* retroorbitally. It was using this method that I was able to determine that two antibodies worked cooperatively to reduce bacterial burden over 100-fold. One of these mAbs worked by blocking heme acquisition whereas the other mAb used an Fc-mediated mechanism of action. By targeting two separate methods of inhibition, these antibodies were able to inhibit *S. aureus* burdens in mice to a greater degree than would normally be observed.

When analyzing the genes that encoded my antibody panel, I noticed a pattern emerge- nearly 40% of IsdB-specific mAbs are encoded by *IGHV1-69*. I thought this raised an interesting question about the importance of *IGHV1-69* antibodies in fighting *S. aureus* infections and whether these particular antibodies maintain a conserved mechanism for blocking IsdB. I hypothesized that functional *IGHV1-69*-encoded antibodies preserve hydrophobic residues in their HCDR2 loop in order to block hemoglobin from binding IsdB. To test this hypothesis, I obtained crystals of three antibodies, STAU-229, -399, or -281 as apo structures or in complex with IsdB-NEAT2. The solved crystal structure of STAU-281 in complex with IsdB-NEAT2 showed that STAU-281 blocked the heme-binding site of NEAT2 using the tip of its HCDR2. The hydrophobic resides *PIF* at the tip of the HCDR2 interact with multiple hydrophobic *Y* residues within the pocket, preventing binding of heme to NEAT2. While this supported

the initial hypothesis, the solved structure of STAU-229 and -399 showed a different mode of binding. Because these structures were apo Fabs, the binding interaction was determined by a combination of crystallography, HDX-MS and Rosetta modeling. Although both of these antibodies are *IGHV1-69*-encoded antibodies, neither bound directly to the heme pocket and used the HCDR3 as the primary contact loop. While it is more typical to see an antibody use a HCDR3 to bind to a specific antigen, it is less characteristic of *IGHV1-69*-encoded antibodies. The structural studies used three antibodies to identify three antigenic sites on IsdB-NEAT2 with both HCDR2 and HCDR3 dominated binding.

To determine the functional relevance of these structural findings, I tested whether these antibodies blocked the *in vitro* growth of *S. aureus*. Heme-dependent growth curves were performed in 96 well plates and not surprisingly given the binding site of these mAbs; STAU-281 was the only mAb that reduced *S. aureus* growth. I also wanted to test if there was an *in vivo* phenotype associated with these genetically encoded mAbs so I used them prophylactically in a systemic mouse model to determine if they reduced *S. aureus* burdens *in vivo*. Although STAU-281 was the most effective mAb at reducing burden, all three antibodies reduced bacterial burdens by at least 1-log in the kidneys. Because the structural studies revealed that STAU-229 and -399 did not block the heme-binding site, I hypothesized they may function *in vivo* by an alternative mechanism rather than direct antigen blocking. To test this, I infected mice using Fc variants and observed that these variants were no longer effective at reducing bacterial burden and showed similar CFU counts as the isotype control. This indicated that these

antibodies were able to use Fc-mediated mechanisms and binding of the full-length *IGHV1-69*-encoded IgG mAbs to FcγR contributes to the protection of these mAbs.

We next aimed to study the evolution of the *IGHV1-69*-encoded antibody repertoire to IsdB by performing deep sequencing analysis on the peripheral blood cells of a *S. aureus* infected patient. The hybridoma sequences were used to identify variant clones or siblings to STAU-229 and STAU-399, as well as an additional *IGHV1-69* mAb STAU-307. We defined variant as an antibody that uses the same variable (V) and joining (J) germline genes (ignoring allelic distinction) along with the CDR3 amino acid sequence (Soto et al. 2019). These siblings were tested for binding to IsdB as well as affinity (K_D) in comparison to each other and the original hybridoma. For STAU-399, some variants bound to IsdB as low as 27-fold less than the hybridoma due to somatic variants. For STAU-229, one variant was nearly 7 times less avid than the hybridoma due to one substitution. These changes supported the unexpected finding that acquisition of increased numbers of somatic mutations in clonal lineage variants does not always confer biological benefits. In fact, all of the somatic variants obtained for this lineage exhibited a similar reduction in binding and function.

Finally, I identified one mAb that showed considerable breadth, revealing a more global epitope found in both *S. aureus* and *B. anthracis* proteins. STAU-239 binds to the heme-pocket of IsdA-NEAT1 as well as IsdB-NEAT1. This mAb also bound *B. anthracis* when incubated under iron-starved conditions and then visualized via microscopy. While it is not completely clear which residues are responsible for this cross-reactivity, the motif most likely involves either tyrosine, serine or both as these residues were conserved throughout the individual binding sites.

FUTURE DIRECTIONS

Targeting multiple nutrient acquisition factors

The failure of multiple monovalent vaccines have taught us that *S. aureus* will not be successfully treated by targeting a single virulence factor, toxin, or adhesion. Similarly, when I started my thesis project, I hoped to completely knock out nutrient acquisition by targeting not just iron, but also zinc and manganese. We hypothesized there would be a decrease in the pathogenesis of *S. aureus* by crippling its ability to acquire the key nutrients needed for metabolic processes, enzyme kinetics, cellular respiration, and redox catalysis. To target this, I purified recombinant proteins not only from the Isd system, but also from MntABC, SirABC, and AdcABC. These are all ABC transporters and the substrate binding protein of the system was purified. For the MntABC system, MntC chelates manganese from the surrounding host environment and transfers it to the next protein in the system, MntB, which transports manganese through the membrane. Anti-MntC antibodies have been previously identified that can bind to both *S. aureus* and *S. epidermidis* cells and are also protective *in vivo* through the production of respiratory bursts (Anderson et al. 2012). MntC is one component of a 4-antigen vaccine that was in recent development by Pfizer (Begier et al. 2017).

S. aureus is known for its redundant nutrient acquisition pathways and iron is no exception. To address this, SirA, which stands for staphylococcal iron regulated, was also included in the original screen. SirA is an iron receptor that transfers the siderophore staphyloferrin B into the cell (Dale et al. 2004; Nobre and Saraiva 2014). Deletion of *sirA* in combination with another siderophore transporter, *hts*, leads to a reduction of bacterial

burden in a murine septic model of infection (Beasley et al. 2011). However, it is worth mentioning that it is the combination of blocking two iron sources, thus preventing redundant acquisition mechanisms that may lead to a greater *in viv*o phenotype than what is observed when knocking out either system individually. Finally, AdcA is a high affinity zinc-binding protein. Similarly to other transport systems, AdcABC has been shown to be redundant for the import of Zn. However, when *adcA* is knocked out alongside one other transporter, *cntA*, a significant reduction in staphylococcal burdens *in vivo* are observed (Grim et al. 2017).

When beginning the hybridoma pipeline to identify antibodies against nutrient acquisition transporters, B-cell secreting supernatants were screened for reactivity against IsdA, IsdB, IsdH, SirA, MntC, and AdcA recombinant proteins. EBV transformed PBMCs are referred to as LCLs or lymphoblastoid cell lines. I performed 383 hybridoma fusions based on ELISA data where reactive supernatants were screened for binding against recombinant protein. Of these LCLs, only 10 bound SirA (2.6% frequency), 13 bound AdcA (3.4% frequency), and 11 bound to MntC (2.9% frequency). For comparison, there were 79/383 reactive wells to IsdB pre-fusion (21% frequency). The majority of these did not survive the fusion portion of the hybridoma process. I did isolate one MntC mAb, but its specificity is unclear. I went on to characterize the binding of this MntC mAb as well as its activity *in vivo*, but it did not decrease bacterial burdens significantly (Figure 5-1). However, this one mAb is not necessarily representative of all antibodies to MntC and it would be worth trying to isolate more MntC specific antibodies in the future.

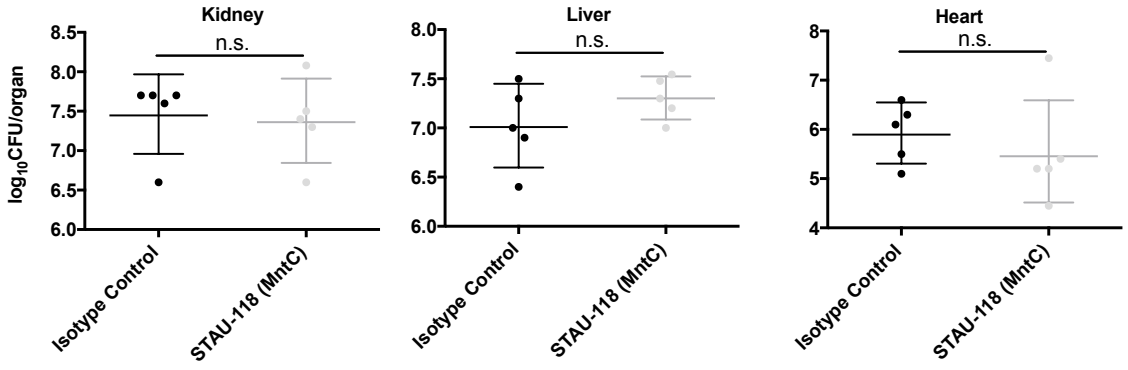

Figure 5-1. Anti-MntC mAb does not reduce bacterial burdens *in vivo*.

Mice were given 10 mg/kg of STAU-118, an anti-MntC mAb, via the IP route. Mice were then infected with *S. aureus* strain Newman retroorbitally and the infection continued for 96 hours before mice were sacrificed. The kidneys, liver, and heart were harvested and colony-forming units were determined.

Although the observed frequency of these additional antibody targets were low in the screened donors and I was unable to isolate antibodies to SirA or AdcA using the traditional hybridoma method, these are still valuable targets worth pursuing. There is now available technology within the Crowe lab that uses a combination of antigen specific B cell sorting with 10x sequencing instead of the hybridoma process to obtain human monoclonal antibodies. This would be an excellent alternative method to isolate a panel of antibodies to these other targets. Further, there are not human monoclonal antibodies to either SirA or AdcA, leaving the field open to define the human B cell response to these important proteins. Finally, by obtaining a panel of antibodies to the Isd system as well as SirA, AdcA, and MntC represents a unique opportunity to cripple *S. aureus* nutrient acquisition, which I hypothesize would result in a substantial decrease in pathogenesis that has not been shown previously.

Fc-effector functions of anti-staphylococcal antibodies

Fc receptors play an important role in the immune response by connecting the antibody response to cellular effector functions. Effector cells such as macrophages and natural killer cells have Fcγ receptors that engage the Fc portion of an antibody leading to downstream signaling. This can trigger antibody dependent cellular phagocytosis (ADCP), complement activation (CDC), and antibody-dependent cellular cytotoxicity (ADCC). For my studies, I tested variant forms of the antibodies that had mutations in the Fc region that prevented downstream effector functions. These variants were mutated at positions 234 and 235 of the CH2 domain from leucine to alanine (L234A/L235A or LALA). This specific mutation has been reported to knockout both ADCC and CDC by preventing binding of antibodies to both FcγR and C1q (Hezareh et al. 2001). While I did test LALA antibodies *in vivo*, this only establishes that the antibodies mediate Fc effector functions, but not which ones specifically. For STAU-239 and -245, I tested whether these antibodies engaged ADCP and I observed that STAU-245 showed an increased function. It would be beneficial, however, to also test whether these antibodies engage CDC and ADCC in order to get a clear picture of the importance of Fc function by anti-Isd antibodies. CDC and ADCC have also been shown to be very effective in fighting *S. aureus* infection previously (Cunnion et al. 2004; Gregory et al. 1996; Pancari et al. 2012; Verdrengh and Tarkowski 1997). To test complement deposition, one could use a flow-cytometry bead based assay similar to the ADCP experiment I performed. Fluorescent NeutrAvidin beads would be coupled to the antigen (IsdA or IsdB) overnight at 4° C. Beads would next be washed, incubated with the antibody of interest, and then incubated with a complement source. After a final wash, beads would be stained with

FITC anti-C3 and read by flow cytometry. The most common effector cells that mediates ADCC is natural killer cells, so a potential assay to test this function would be an NK-degranulation assay. ELISA plates would be coated with antigen (IsdA or IsdB) overnight at 4° C. Plates would be washed and blocked with BSA before adding the test antibody. After washing again, NK cells that have been isolated from the buffy coats of healthy donors would be added and the plates incubated at 37° C. Finally the cells would be washed, fixed, and permeabilized using Fix/Perm solutions. The assay would be read by flow cytometry using individual readouts such as intracellular cytokine staining IFNγ and CD107a, which is a marker for NK cell degranulation (Alter et al. 2004; Xia et al. 2012). Performing this triad of assays will help further evaluate the contribution of Fc mechanisms to Isd antibody function.

Reverse vaccinology and structure based vaccine design of Isd mAbs

The concept of reverse vaccinology (Rappuoli 2000) has already led to the production of effective vaccines against bacterial pathogens like *Neisseria meningitides* (Masignani et al. 2019) and could be useful in the race to find a vaccine to *S. aureus*. Reverse vaccinology and structure based vaccine design both focus on the antigen or epitope specific immunogens to induce a protective antibody response. If the target antigen has already been described as eliciting a protective antibody response, then using that antigen as an immunogen should also elicit an equally effective immune response. There is a great deal of structural information as well as described mAb epitopes for *S. aureus*. The studies here contribute this information as well as next-generation sequencing information regarding the evolution of antibody response to IsdB. While IsdB

may not be suitable in a monovalent vaccine against *S. aureus*, a myriad of failed vaccines support the idea that no antigen would be. Therefore, the body of information presented here would be useful in reverse engineering an IsdB immunogen to be used alongside other *S. aureus* antigens in a vaccine. An IsdB immunogen could be designed that specifically incorporates residues necessary for *IGHV1-69* antibody recognition. Not only that, but we provide information on three separate epitopes, enabling the design of an immunogen with multiple features. If *IGHV1-69* antibodies bind in different ways, then one needs to design a similarly complex multistate designed antigen, and this study illuminates how to do this. In the end, use of this immunogen would prime the immune system to produce other *IGHV1-69* anti-*S. aureus* mAbs.

Alternative functions for anti-Isd mAbs: diagnostics, conjugates, and molecular tools

One of the notable characteristics of the isolated antibody panel is its high affinity binding to the target proteins. This provides a number of opportunities to use these mAbs for alternative functions other than therapeutics or vaccine design, such as diagnostics. Currently, *S. aureus* can be diagnosed using a variety of different techniques starting with culture-based methods, which takes time or nucleic acid-based detection, which is expensive. Testing for the presence of *S. aureus* infection using immunological assays is cheaper than other approaches such as immuno-PCR or RT-PCR. Immunological assays are also faster and require less training to achieve reproducible results. The Isd proteins would be good target antigens for a diagnostic approach because they are widely conserved throughout *S. aureus* strains. Further, the isolated antibodies in this study are

naturally occurring human mAbs, which are more clinically relevant than the rabbit, mice, sheep or goat antibodies that are often used in these assays. Testing for Isd proteins via ELISA is a cheap and straightforward diagnostic approach that could be easily implemented. To determine if the isolated mAbs would be useful diagnostic tools, I recommend collaborating with the Vanderbilt Initiative for Personalized Microbial Discovery and Innovation to acquire *S. aureus* clinical isolates. This would enable you to test more representative *S. aureus* strains isolated from patients in the clinic at full virulence without lab-adapted mutations. I would then express recombinant IgG of the broadest anti-Isd mAbs to test for reactivity. These mAbs can then be used in an ELISA to check sensitivity against the clinical lab isolates. Other immunoassays could be tested as well including western blot or lateral flow.

Another alternative function for these mAbs is in the category of antibody conjugates, molecules that have gained traction recently for their effectiveness as a cancer therapy. Antibodies specific to the target of interest can be conjugated to a drug or small molecule using linkers. When the antibody binds to its target, the payload drug is released and is toxic. The antibody allows for specificity and the conjugated drug contributes the cytotoxicity. A similar application for antibody conjugates in the microbiology field is photodynamic therapy (PDT) using antibodies conjugated to a photoactivated drug. The photosensitizer can be used in combination with activating light at a specific wavelength to kill bacteria. This method is lethal because extreme photosensitization results in reactive oxygen species production, which damages cell walls, DNA, and ultimately targeted cell death of the bacterium. PDT has previously been shown in *E. coli*, *P. aeroginosa*, *S. pneumoniae*, as well as *S. aureus* (Park et al. 2010;

Usacheva et al. 2001). We decided to test whether Isd-conjugated mAbs would be effective tools to target *S. aureus* for PDT. The concept is that Isd-conjugated antibodies will bind to Isd surface proteins on *S. aureus*, coating the bacterium with the photosensitizer. When the bacteria are hit with light at a specific activating wavelength, reactive oxygen species are produced and *S. aureus* is killed, which is measurable by counting colony-forming units. The first step was to conjugate Isd mAbs to the photosensitizer, IR-700. This was done with the help of Dr. Mingfeng Bai's group. Next, the experiment is moved *in vitro* where *S. aureus* is grown overnight in the presence of the iron chelator, 2,2-dipyridyl. The bacteria is subcultured with the conjugated antibody and grown for 30 minutes. After washing, the culture is transferred to a plate and light treated with both blue (395 nm) and red (688 nm) light. Bacteria are then plated and colony-forming units are counted to determine amount of killing. These experiments are currently underway in the Skaar lab and represent an alternative novel use for the isolated Isd mAbs.

Similarly to the way conjugated STAU-239 was used to investigate antibody binding to *B. anthracis*, these mAbs can be used to visualize individual Isd proteins in *S. aureus* via microscopy. The intramolecular interactions of the Isd system could be investigated in order to unveil novel insights into how Gram-positive transport systems function. Previous experimental evidence suggests that the transfer of heme from surface receptors to the ABC transporter (IsdDEF) in the cytoplasmic membrane is unidirectional with strong sequence preservation controlling the heme transfer, however, the protein-protein interactions responsible for this conservation are unknown (Liu et al. 2008; Muryoi et al. 2008; Tiedemann and Stillman 2012). We hypothesize that there are

conserved structural interactions that contribute to the unidirectional transfer of heme through the cell wall. While there is a broad understanding of how the Isd system functions, there is little proof of where individual proteins lie in the cell, if these proteins form complexes, or whether the system functions independently or as a molecular machine. The conjugated Isd mAbs can be used as tools for targeted immunofluorescence of the Isd system. Visualization of these proteins could be accomplished via stochastic optical reconstruction microscopy or STORM microscopy and unveil the location of these proteins and how they interact. This understanding is not only relevant to iron transportation across the cell, but also in a broader context, as transportation across the Gram-positive cell wall is not well understood (Schneewind and Missiakas 2012; A. D. Smith and Wilks 2012).

STORM microscopy is an appropriate technique to achieve this goal as it uses specific labeling and photoswitching fluorophores to get 10-50 nm resolution (Rust et al. 2006). The *S. aureus* cell wall is between 20-40 nm thick, falling within the detection limit of superresolution microscopy (Giesbrecht et al. 1998). With the help of the Vanderbilt University CISR core, the STORM fluorescent microscope would be used to quantitatively image the spatial relationship between the individual Isd proteins. The Isd-conjugated antibodies will be used as molecular tools and are already in hand. Secondary antibody fragments would be labeled with a dye such as Alexa-647 (Olivier et al. 2013). The sample would be fixed before imaging using glutaraldehyde as it was shown to be the best fixative for structure preservation (Whelan and Bell 2015). The fluorophores on individual molecules blink at different intervals and a series of images can be captured. The ability to light-induce fluorophores to reversibly switch on and off based on temporal

fluctuations allows for a high-resolution image. The data from the microscope can be reconstructed in ImageJ using the plugin ThunderSTORM.

Once there is a more specific framework for the location of the Isd system, a more thorough understanding of how the individual proteins interact can be investigated. It would be beneficial to understand which molecular interactions are important for efficient translocation. By performing Co-IP studies, the intramolecular interactions within the Isd system would be elucidated. This will help determine if the Isd system functions as individual parts or as an interdependent molecular machine. In particular, it would be interesting to interrogate the protein-protein interactions between IsdA and IsdC as well as IsdC and IsdDEF. This would indicate if there is a structurally conserved mechanism for the unidirectional transportation of heme through the cell wall. This knowledge may also be applicable on a larger scale to how other pathogens manipulate translocation and secretion pathways for nutrient acquisition. The use of the specific Isd mAbs will increase specificity and decrease non-specific interactions that may often interfere with immunoprecipitation experiments. Western blot analysis may also ensure there is specificity of the antibody to its target. Bacterial cells would be harvested and the lysate incubated with the antibody and conjugated bead for two hours to ensure the formation of an immune complex with the particular Isd protein. The beads would then be washed to remove unbound material from the cell lysate. The Isd protein that was baited, as well as any interacting proteins, could be analyzed by SDS-PAGE and western blot to verify their identity and presence. Any interacting proteins that are not specific for an anti-Isd antibody can be identified by mass spectrometry. A positive control lysate with antibody and a negative group without antibody can serve as controls. There would

also be an isotype control sample run to ensure the specificity of the antibody. These experiments would help elucidate where IsdA, IsdB, and IsdH are in relation to IsdC in the membrane of *S. aureus* as well as inform on the general shape of these proteins.

In conclusion, anti-staphylococcal antibodies were used to investigate the humoral immune response to *S. aureus*. The variable gene *VH1-69* encodes a number of the isolated IsdB antibodies. Structural studies found that antibodies within this family use both HCDR2 and HCDR3 dominated binding interactions to interact with IsdB. These antibodies were found to decrease the burden of *S. aureus* both *in vivo* and *in vitro* using two distinct mechanisms: iron acquisition and Fc-mediated mechanisms. Additionally, two antibodies- STAU-239 and -245 used these two mechanisms to cooperatively reduce bacterial burden in a murine model to a greater degree when administered together than when either antibody was given alone. These studies underscore the importance of the Isd system to *S. aureus* pathogenesis and increase understanding of how anti-Isd antibodies contribute to a protective immune response, which informs rational vaccine design efforts and enables a better understanding of the correlates of protection against *S. aureus* infection.

BIBLIOGRAPHY

Adams, P. D., et al. (2010), 'PHENIX: a comprehensive Python-based system for macromolecular structure solution', *Acta Crystallogr D Biol Crystallogr,* 66 (Pt 2), 213-21.

Adhikari, R. P., et al. (2012), 'Lower antibody levels to *Staphylococcus aureus* exotoxins are associated with sepsis in hospitalized adults with invasive *S. aureus* infections', *J Infect Dis,* 206 (6), 915-23.

Alamyar, E., et al. (2012), 'IMGT((R)) tools for the nucleotide analysis of immunoglobulin (IG) and T cell receptor (TR) V-(D)-J repertoires, polymorphisms, and IG mutations: IMGT/V-QUEST and IMGT/HighV-QUEST for NGS', *Methods Mol Biol,* 882, 569-604.

Alter, G., Malenfant, J. M., and Altfeld, M. (2004), 'CD107a as a functional marker for the identification of natural killer cell activity', *J Immunol Methods,* 294 (1-2), 15-22.

Alter, G., Ottenhoff, T. H. M., and Joosten, S. A. (2018), 'Antibody glycosylation in inflammation, disease and vaccination', *Semin Immunol,* 39, 102-10.

Altschul, S. F., et al. (1990), 'Basic local alignment search tool', *J Mol Biol,* 215 (3), 403-10.

Anderson, A. S., et al. (2012), '*Staphylococcus aureus* manganese transport protein C is a highly conserved cell surface protein that elicits protective immunity against *S. aureus* and *Staphylococcus epidermidis*', *J Infect Dis,* 205 (11), 1688-96.

Andrade, M. A., et al. (2002), 'NEAT: a domain duplicated in genes near the components of a putative Fe3+ siderophore transporter from Gram-positive pathogenic bacteria', *Genome Biol,* 3 (9), RESEARCH0047.

Antony, S. J. (2006), 'Combination therapy with daptomycin, vancomycin, and rifampin for recurrent, severe bone and prosthetic joint infections involving methicillin-resistant *Staphylococcus aureus*', *Scand J Infect Dis,* 38 (4), 293-5.

Avnir, Y., et al. (2016), 'IGHV1-69 polymorphism modulates anti-influenza antibody repertoires, correlates with IGHV utilization shifts and varies by ethnicity', *Sci Rep,* 6, 20842.

Bae, T. and Schneewind, O. (2006), 'Allelic replacement in *Staphylococcus aureus* with inducible counter-selection', *Plasmid,* 55 (1), 58-63.

Bagnoli, F., Bertholet, S., and Grandi, G. (2012), 'Inferring reasons for the failure of *Staphylococcus aureus* vaccines in clinical trials', *Front Cell Infect Microbiol,* 2, 16.

Balderas, M. A., et al. (2012), 'Hal Is a *Bacillus anthracis* heme acquisition protein', *J Bacteriol,* 194 (20), 5513-21.

Bangaru, S., et al. (2018), 'A multifunctional human monoclonal neutralizing antibody that targets a unique conserved epitope on influenza HA', *Nat Commun,* 9 (1), 2669.

Beasley, F. C., et al. (2011), '*Staphylococcus aureus* transporters Hts, Sir, and Sst capture iron liberated from human transferrin by Staphyloferrin A, Staphyloferrin B, and catecholamine stress hormones, respectively, and contribute to virulence', *Infect Immun,* 79 (6), 2345-55.

Beasley, F. C., et al. (2009), 'Characterization of staphyloferrin A biosynthetic and transport mutants in *Staphylococcus aureus*', *Mol Microbiol,* 72 (4), 947-63.

Begier, E., et al. (2017), 'SA4Ag, a 4-antigen *Staphylococcus aureus* vaccine, rapidly induces high levels of bacteria-killing antibodies', *Vaccine,* 35 (8), 1132-39.

Bender, B. J., et al. (2016), 'Protocols for Molecular Modeling with Rosetta3 and RosettaScripts', *Biochemistry,* 55 (34), 4748-63.

Bennett, M. R., et al. (2018), 'Human mAbs to *Staphylococcus aureus* IsdA Provide Protection Through Both Heme-Blocking and Fc-Mediated Mechanisms', *J Infect Dis*.

Bowden, C. F. M., et al. (2018), 'Structure-function analyses reveal key features in *Staphylococcus aureus* IsdB-associated unfolding of the heme-binding pocket of human hemoglobin', *J Biol Chem,* 293 (1), 177-90.

Broker, B. M., Holtfreter, S., and Bekeredjian-Ding, I. (2014), 'Immune control of *Staphylococcus aureus* - regulation and counter-regulation of the adaptive immune response', *Int J Med Microbiol,* 304 (2), 204-14.

Brown, M., et al. (2009), 'Selection and characterization of murine monoclonal antibodies to *Staphylococcus aureus* iron-regulated surface determinant B with functional activity *in vitro* and *in vivo*', *Clin Vaccine Immunol,* 16 (8), 1095-104.

Buckley, R. H. (2004), 'Pulmonary complications of primary immunodeficiencies', *Paediatr Respir Rev,* 5 Suppl A, S225-33.

Camacho, C., et al. (2009), 'BLAST+: architecture and applications', *BMC Bioinformatics,* 10, 421.

Chaudhury, S., et al. (2011), 'Benchmarking and analysis of protein docking performance in Rosetta v3.2', *PLoS One,* 6 (8), e22477.

Chen, F., et al. (2019), '*VH1-69* antiviral broadly neutralizing antibodies: genetics, structures, and relevance to rational vaccine design', *Curr Opin Virol,* 34, 149-59.

Chen, H., et al. (2010), 'Allosteric inhibition of complement function by a staphylococcal immune evasion protein', *Proc Natl Acad Sci U S A,* 107 (41), 17621-6.

Choby, J. E. and Skaar, E. P. (2016), 'Heme Synthesis and Acquisition in Bacterial Pathogens', *J Mol Biol,* 428 (17), 3408-28.

Choo, J. M., et al. (2016), 'The NEAT Domain-Containing Proteins of *Clostridium perfringens* Bind Heme', *PLoS One,* 11 (9), e0162981.

Clarke, S. R., et al. (2006), 'Identification of *in vivo*-expressed antigens of *Staphylococcus aureus* and their use in vaccinations for protection against nasal carriage', *J Infect Dis,* 193 (8), 1098-108.

Colque-Navarro, P., et al. (2010), 'Levels of antibody against 11 *Staphylococcus aureus* antigens in a healthy population', *Clin Vaccine Immunol,* 17 (7), 1117-23.

Creech, C. B., et al. (2017), 'Safety, tolerability, and immunogenicity of a single dose 4-antigen or 3-antigen *Staphylococcus aureus* vaccine in healthy older adults: Results of a randomised trial', *Vaccine,* 35 (2), 385-94.

Cunnion, K. M., et al. (2004), 'Role of complement receptors 1 and 2 (CD35 and CD21), C3, C4, and C5 in survival by mice of *Staphylococcus aureus* bacteremia', *J Lab Clin Med,* 143 (6), 358-65.

Dale, S. E., Sebulsky, M. T., and Heinrichs, D. E. (2004), 'Involvement of SirABC in iron-siderophore import in *Staphylococcus aureus*', *J Bacteriol,* 186 (24), 8356-62.

Davis, J. S., Van Hal, S., and Tong, S. Y. (2015), 'Combination antibiotic treatment of serious methicillin-resistant *Staphylococcus aureus* infections', *Semin Respir Crit Care Med,* 36 (1), 3-16.

de Haas, C. J., et al. (2004), 'Chemotaxis inhibitory protein of *Staphylococcus aureus*, a bacterial antiinflammatory agent', *J Exp Med,* 199 (5), 687-95.

DeJonge, M., et al. (2007), 'Clinical trial of safety and efficacy of INH-A21 for the prevention of nosocomial staphylococcal bloodstream infection in premature infants', *J Pediatr,* 151 (3), 260-5, 65 e1.

den Reijer, P. M., et al. (2016), 'Detection of Alpha-Toxin and Other Virulence Factors in Biofilms of *Staphylococcus aureus* on Polystyrene and a Human Epidermal Model', *PLoS One,* 11 (1), e0145722.

Diep, B. A., et al. (2014), 'Identifying potential therapeutic targets of methicillin-resistant *Staphylococcus aureus* through *in vivo* proteomic analysis', *J Infect Dis,* 209 (10), 1533-41.

Dillen, C. A., et al. (2018), 'Clonally expanded gammadelta T cells protect against *Staphylococcus aureus* skin reinfection', *J Clin Invest,* 128 (3), 1026-42.

Dryla, A., et al. (2003), 'Identification of a novel iron regulated staphylococcal surface protein with haptoglobin-haemoglobin binding activity', *Mol Microbiol,* 49 (1), 37-53.

Ebert, T., et al. (2010), 'A fully human monoclonal antibody to *Staphylococcus aureus* iron regulated surface determinant B (IsdB) with functional activity *in vitro* and *in vivo*', *Hum Antibodies,* 19 (4), 113-28.

Ekworomadu, M. T., et al. (2012), 'Differential function of lip residues in the mechanism and biology of an anthrax hemophore', *PLoS Pathog,* 8 (3), e1002559.

Emsley, P., et al. (2010), 'Features and development of Coot', *Acta Crystallogr D Biol Crystallogr,* 66 (Pt 4), 486-501.

Fabian, M., et al. (2009), 'Heme transfer to the bacterial cell envelope occurs via a secreted hemophore in the Gram-positive pathogen *Bacillus anthracis*', *J Biol Chem,* 284 (46), 32138-46.

Foletti, D., et al. (2013), 'Mechanism of action and *in vivo* efficacy of a human-derived antibody against *Staphylococcus aureus* alpha-hemolysin', *J Mol Biol,* 425 (10), 1641-54.

Fonner, B. A., et al. (2014), 'Solution structure and molecular determinants of hemoglobin binding of the first NEAT domain of IsdB in *Staphylococcus aureus*', *Biochemistry,* 53 (24), 3922-33.

Foster, T. J., et al. (2014), 'Adhesion, invasion and evasion: the many functions of the surface proteins of *Staphylococcus aureus*', *Nat Rev Microbiol,* 12 (1), 49-62.

Fowler, V. G., Jr. and Proctor, R. A. (2014), 'Where does a *Staphylococcus aureus* vaccine stand?', *Clin Microbiol Infect,* 20 Suppl 5, 66-75.

Frenck, R. W., Jr., et al. (2017), 'Safety, tolerability, and immunogenicity of a 4-antigen *Staphylococcus aureus* vaccine (SA4Ag): Results from a first-in-human randomised, placebo-controlled phase 1/2 study', *Vaccine,* 35 (2), 375-84.

Fu, L., et al. (2012), 'CD-HIT: accelerated for clustering the next-generation sequencing data', *Bioinformatics,* 28 (23), 3150-2.

Giesbrecht, P., et al. (1998), 'Staphylococcal cell wall: morphogenesis and fatal variations in the presence of penicillin', *Microbiol Mol Biol Rev,* 62 (4), 1371-414.

Goldmann, O. and Medina, E. (2018), '*Staphylococcus aureus* strategies to evade the host acquired immune response', *Int J Med Microbiol,* 308 (6), 625-30.

Gregory, S. H., Sagnimeni, A. J., and Wing, E. J. (1996), 'Bacteria in the bloodstream are trapped in the liver and killed by immigrating neutrophils', *J Immunol,* 157 (6), 2514-20.

Grigg, J. C., Mao, C. X., and Murphy, M. E. (2011), 'Iron-coordinating tyrosine is a key determinant of NEAT domain heme transfer', *J Mol Biol,* 413 (3), 684-98.

Grigg, J. C., et al. (2007a), 'Heme coordination by *Staphylococcus aureus* IsdE', *J Biol Chem,* 282 (39), 28815-22.

--- (2007b), 'Haem recognition by a *Staphylococcus aureus* NEAT domain', *Mol Microbiol,* 63 (1), 139-49.

Grigg, J. C., et al. (2010), 'Structural biology of heme binding in the S*taphylococcus aureus* Isd system', *J Inorg Biochem,* 104 (3), 341-8.

Grim, K. P., et al. (2017), 'The Metallophore Staphylopine Enables *Staphylococcus aureus* To Compete with the Host for Zinc and Overcome Nutritional Immunity', *MBio,* 8 (5).

Guerra, F. E., et al. (2017), 'Epic Immune Battles of History: Neutrophils vs. *Staphylococcus aureus*', *Front Cell Infect Microbiol,* 7, 286.

Hammer, N. D. and Skaar, E. P. (2011), 'Molecular mechanisms of *Staphylococcus aureus* iron acquisition', *Annu Rev Microbiol,* 65, 129-47.

Harro, C., et al. (2010), 'Safety and immunogenicity of a novel *Staphylococcus aureus* vaccine: results from the first study of the vaccine dose range in humans', *Clin Vaccine Immunol,* 17 (12), 1868-74.

Hezareh, M., et al. (2001), 'Effector function activities of a panel of mutants of a broadly neutralizing antibody against human immunodeficiency virus type 1', *J Virol,* 75 (24), 12161-8.

Hogan, S., et al. (2015), 'Current and future approaches to the prevention and treatment of staphylococcal medical device-related infections', *Curr Pharm Des,* 21 (1), 100-13.

Honsa, E. S., Maresso, A. W., and Highlander, S. K. (2014), 'Molecular and evolutionary analysis of NEAr-iron Transporter (NEAT) domains', *PLoS One,* 9 (8), e104794.

Honsa, E. S., et al. (2011), 'The five near-iron transporter (NEAT) domain anthrax hemophore, IsdX2, scavenges heme from hemoglobin and transfers heme to the surface protein IsdC', *J Biol Chem,* 286 (38), 33652-60.

Hua, L., et al. (2014), 'Assessment of an anti-alpha-toxin monoclonal antibody for prevention and treatment of *Staphylococcus aureus*-induced pneumonia', *Antimicrob Agents Chemother,* 58 (2), 1108-17.

Jonsson, I. M., et al. (2002), 'On the role of *Staphylococcus aureus* sortase and sortase-catalyzed surface protein anchoring in murine septic arthritis', *J Infect Dis,* 185 (10), 1417-24.

Joshi, A., et al. (2012), 'Immunization with *Staphylococcus aureus* iron regulated surface determinant B (IsdB) confers protection via Th17/IL17 pathway in a murine sepsis model', *Hum Vaccin Immunother,* 8 (3), 336-46.

Kabsch, W. (2010), 'Xds', *Acta Crystallogr D Biol Crystallogr,* 66 (Pt 2), 125-32.

Kolata, J. B., et al. (2015), 'The Fall of a Dogma? Unexpected High T-Cell Memory Response to *Staphylococcus aureus* in Humans', *J Infect Dis,* 212 (5), 830-8.

Kuklin, N. A., et al. (2006), 'A novel *Staphylococcus aureus* vaccine: iron surface determinant B induces rapid antibody responses in rhesus macaques and specific increased survival in a murine *S. aureus* sepsis model', *Infect Immun,* 74 (4), 2215-23.

Laarman, A. J., et al. (2011), '*Staphylococcus aureus* metalloprotease aureolysin cleaves complement C3 to mediate immune evasion', *J Immunol,* 186 (11), 6445-53.

Laarman, A. J., et al. (2012), '*Staphylococcus aureus* Staphopain A inhibits CXCR2-dependent neutrophil activation and chemotaxis', *EMBO J,* 31 (17), 3607-19.

Lang, S., et al. (2017), 'Antibody 27F3 Broadly Targets Influenza A Group 1 and 2 Hemagglutinins through a Further Variation in VH1-69 Antibody Orientation on the HA Stem', *Cell Rep,* 20 (12), 2935-43.

Li, W. and Godzik, A. (2006), 'Cd-hit: a fast program for clustering and comparing large sets of protein or nucleotide sequences', *Bioinformatics,* 22 (13), 1658-9.

Liu, M., et al. (2008), 'Direct hemin transfer from IsdA to IsdC in the iron-regulated surface determinant (Isd) heme acquisition system of *Staphylococcus aureus*', *J Biol Chem,* 283 (11), 6668-76.

Lyman, L. R., Peng, E. D., and Schmitt, M. P. (2018), '*Corynebacterium diphtheriae* Iron-Regulated Surface Protein HbpA Is Involved in the Utilization of the Hemoglobin-Haptoglobin Complex as an Iron Source', *J Bacteriol,* 200 (7).

Maresso, A. W., Garufi, G., and Schneewind, O. (2008), '*Bacillus anthracis* secretes proteins that mediate heme acquisition from hemoglobin', *PLoS Pathog,* 4 (8), e1000132.

Marraffini, L. A., Dedent, A. C., and Schneewind, O. (2006), 'Sortases and the art of anchoring proteins to the envelopes of gram-positive bacteria', *Microbiol Mol Biol Rev,* 70 (1), 192-221.

Masignani, V., Pizza, M., and Moxon, E. R. (2019), 'The Development of a Vaccine Against Meningococcus B Using Reverse Vaccinology', *Front Immunol,* 10, 751.

Mazmanian, S. K., et al. (2002), 'An iron-regulated sortase anchors a class of surface protein during *Staphylococcus aureus* pathogenesis', *Proc Natl Acad Sci U S A,* 99 (4), 2293-8.

Mazmanian, S. K., et al. (2000), '*Staphylococcus aureus* sortase mutants defective in the display of surface proteins and in the pathogenesis of animal infections', *Proc Natl Acad Sci U S A,* 97 (10), 5510-5.

Mazmanian, S. K., et al. (2003), 'Passage of heme-iron across the envelope of *Staphylococcus aureus*', *Science,* 299 (5608), 906-9.

McGuinness, W. A., Malachowa, N., and DeLeo, F. R. (2017), 'Vancomycin Resistance in *Staphylococcus aureus*', *Yale J Biol Med,* 90 (2), 269-81.

Moriwaki, Y., et al. (2013), 'Heme binding mechanism of structurally similar iron-regulated surface determinant near transporter domains of *Staphylococcus aureus* exhibiting different affinities for heme', *Biochemistry,* 52 (49), 8866-77.

Muryoi, N., et al. (2008), 'Demonstration of the iron-regulated surface determinant (Isd) heme transfer pathway in *Staphylococcus aureus*', *J Biol Chem,* 283 (42), 28125-36.

Nobre, L. S. and Saraiva, L. M. (2014), 'Role of the siderophore transporter SirABC in the S*taphylococcus aureus* resistance to oxidative stress', *Curr Microbiol,* 69 (2), 164-8.

O'Riordan, K. and Lee, J. C. (2004), '*Staphylococcus aureus* Capsular Polysaccharides', *Clinical Microbiology Reviews,* 17 (1), 218-34.

Olivier, N., et al. (2013), 'Simple buffers for 3D STORM microscopy', *Biomed Opt Express,* 4 (6), 885-99.

Pancari, G., et al. (2012), 'Characterization of the mechanism of protection mediated by CS-D7, a monoclonal antibody to *Staphylococcus aureus* iron regulated surface determinant B (IsdB)', *Front Cell Infect Microbiol,* 2, 36.

Pappas, L., et al. (2014), 'Rapid development of broadly influenza neutralizing antibodies through redundant mutations', *Nature,* 516 (7531), 418-22.

Park, J. H., et al. (2010), 'Antimicrobial effect of photodynamic therapy using a highly pure chlorin e6', *Lasers Med Sci,* 25 (5), 705-10.

Petit, R. A., 3rd and Read, T. D. (2018), '*Staphylococcus aureus* viewed from the perspective of 40,000+ genomes', *PeerJ,* 6, e5261.

Pietrocola, G., et al. (2017), '*Staphylococcus aureus* Manipulates Innate Immunity through Own and Host-Expressed Proteases', *Front Cell Infect Microbiol,* 7, 166.

Pilpa, R. M., et al. (2006), 'Solution structure of the NEAT (NEAr Transporter) domain from IsdH/HarA: the human hemoglobin receptor in *Staphylococcus aureus*', *J Mol Biol,* 360 (2), 435-47.

Pilpa, R. M., et al. (2009), 'Functionally distinct NEAT (NEAr Transporter) domains within the *Staphylococcus aureus* IsdH/HarA protein extract heme from methemoglobin', *J Biol Chem,* 284 (2), 1166-76.

Pishchany, G., Dickey, S. E., and Skaar, E. P. (2009), 'Subcellular localization of the *Staphylococcus aureus* heme iron transport components IsdA and IsdB', *Infect Immun,* 77 (7), 2624-34.

Pishchany, G., et al. (2010), 'Specificity for human hemoglobin enhances *Staphylococcus aureus* infection', *Cell Host Microbe,* 8 (6), 544-50.

Pishchany, G., et al. (2014), 'IsdB-dependent hemoglobin binding is required for acquisition of heme by *Staphylococcus aureus*', *J Infect Dis,* 209 (11), 1764-72.

Pluym, M., et al. (2008), 'Heme binding in the NEAT domains of IsdA and IsdC of *Staphylococcus aureus*', *J Inorg Biochem,* 102 (3), 480-8.

Proctor, R. A. (2012), 'Challenges for a universal *Staphylococcus aureus* vaccine', *Clin Infect Dis,* 54 (8), 1179-86.

Rappuoli, R. (2000), 'Reverse vaccinology', *Curr Opin Microbiol,* 3 (5), 445-50.

Reniere, M. L. and Skaar, E. P. (2008), '*Staphylococcus aureus* haem oxygenases are differentially regulated by iron and haem', *Mol Microbiol,* 69 (5), 1304-15.

Rouha, H., et al. (2015), 'Five birds, one stone: neutralization of alpha-hemolysin and 4 bi-component leukocidins of *Staphylococcus aureus* with a single human monoclonal antibody', *MAbs,* 7 (1), 243-54.

Rupp, M. E., et al. (2007), 'Phase II, randomized, multicenter, double-blind, placebo-controlled trial of a polyclonal anti-*Staphylococcus aureus* capsular polysaccharide immune globulin in treatment of *Staphylococcus aureus* bacteremia', *Antimicrob Agents Chemother,* 51 (12), 4249-54.

Rust, M. J., Bates, M., and Zhuang, X. (2006), 'Sub-diffraction-limit imaging by stochastic optical reconstruction microscopy (STORM)', *Nat Methods,* 3 (10), 793-5.

Sabin, C., et al. (2010), 'Crystal structure and size-dependent neutralization properties of HK20, a human monoclonal antibody binding to the highly conserved heptad repeat 1 of gp41', *PLoS Pathog,* 6 (11), e1001195.

Schneewind, O. and Missiakas, D. M. (2012), 'Protein secretion and surface display in Gram-positive bacteria', *Philos Trans R Soc Lond B Biol Sci,* 367 (1592), 1123-39.

Sharp, K. H., et al. (2007), 'Crystal structure of the heme-IsdC complex, the central conduit of the Isd iron/heme uptake system in *Staphylococcus aureus*', *J Biol Chem,* 282 (14), 10625-31.

Sheldon, J. R. and Heinrichs, D. E. (2012), 'The iron-regulated staphylococcal lipoproteins', *Front Cell Infect Microbiol,* 2, 41.

Skaar, E. P. (2010), 'The battle for iron between bacterial pathogens and their vertebrate hosts', *PLoS Pathog,* 6 (8), e1000949.

Skaar, E. P., et al. (2004), 'Iron-source preference of *Staphylococcus aureu*s infections', *Science,* 305 (5690), 1626-8.

Smith, A. D. and Wilks, A. (2012), 'Extracellular heme uptake and the challenges of bacterial cell membranes', *Curr Top Membr,* 69, 359-92.

Smith, E. J., et al. (2011), 'The Sbi protein is a multifunctional immune evasion factor of *Staphylococcus aureus*', *Infect Immun,* 79 (9), 3801-9.

Soto, C., et al. (2019), 'High frequency of shared clonotypes in human B cell receptor repertoires', *Nature,* 566 (7744), 398-402.

Stapleton, M. R., et al. (2012), 'Identification of conserved antigens from staphylococcal and streptococcal pathogens', *J Med Microbiol,* 61 (Pt 6), 766-79.

Stemerding, A. M., et al. (2013), '*Staphylococcus aureus* formyl peptide receptor-like 1 inhibitor (FLIPr) and its homologue FLIPr-like are potent FcgammaR antagonists that inhibit IgG-mediated effector functions', *J Immunol,* 191 (1), 353-62.

Stranger-Jones, Y. K., Bae, T., and Schneewind, O. (2006), 'Vaccine assembly from surface proteins of *Staphylococcus aureus*', *Proc Natl Acad Sci U S A,* 103 (45), 16942-7.

Tarlovsky, Y., et al. (2010), 'A *Bacillus anthracis* S-layer homology protein that binds heme and mediates heme delivery to IsdC', *J Bacteriol,* 192 (13), 3503-11.

Thammavongsa, V., et al. (2015), 'Staphylococcal manipulation of host immune responses', *Nat Rev Microbiol,* 13 (9), 529-43.

Tiedemann, M. T. and Stillman, M. J. (2012), 'Heme binding to the IsdE(M78A; H229A) double mutant: challenging unidirectional heme transfer in the iron-regulated surface determinant protein heme transfer pathway of *Staphylococcus aureus*', *J Biol Inorg Chem,* 17 (7), 995-1007.

Tong, S. Y., et al. (2015), '*Staphylococcus aureus* infections: epidemiology, pathophysiology, clinical manifestations, and management', *Clin Microbiol Rev,* 28 (3), 603-61.

Torres, V. J., et al. (2006), '*Staphylococcus aureus* IsdB is a hemoglobin receptor required for heme iron utilization', *J Bacteriol,* 188 (24), 8421-9.

Tsuji, B. T. and Rybak, M. J. (2006), 'Etest synergy testing of clinical isolates of *Staphylococcus aureus* demonstrating heterogeneous resistance to vancomycin', *Diagn Microbiol Infect Dis,* 54 (1), 73-7.

Tzarum, N., et al. (2019), 'Genetic and structural insights into broad neutralization of hepatitis C virus by human *VH1-69* antibodies', *Sci Adv,* 5 (1), eaav1882.

Usacheva, M. N., Teichert, M. C., and Biel, M. A. (2001), 'Comparison of the methylene blue and toluidine blue photobactericidal efficacy against gram-positive and gram-negative microorganisms', *Lasers Surg Med,* 29 (2), 165-73.

Verdrengh, M. and Tarkowski, A. (1997), 'Role of neutrophils in experimental septicemia and septic arthritis induced by *Staphylococcus aureus*', *Infect Immun,* 65 (7), 2517-21.

Verkaik, N. J., et al. (2010), 'Heterogeneity of the humoral immune response following *Staphylococcus aureus* bacteremia', *Eur J Clin Microbiol Infect Dis,* 29 (5), 509-18.

Vu, C. H., et al. (2016), 'Adaptive immune response to lipoproteins of *Staphylococcus aureus* in healthy subjects', *Proteomics,* 16 (20), 2667-77.

Walters, M. S., et al. (2015), 'Vancomycin-Resistant *Staphylococcus aureus* - Delaware, 2015', *MMWR Morb Mortal Wkly Rep,* 64 (37), 1056.

Weisman, L. E., et al. (2009), 'Safety and pharmacokinetics of a chimerized anti-lipoteichoic acid monoclonal antibody in healthy adults', *Int Immunopharmacol,* 9 (5), 639-44.

Wertheim, H. F., et al. (2005), 'The role of nasal carriage in *Staphylococcus aureus* infections', *Lancet Infect Dis,* 5 (12), 751-62.

Whelan, D. R. and Bell, T. D. (2015), 'Image artifacts in single molecule localization microscopy: why optimization of sample preparation protocols matters', *Sci Rep,* 5, 7924.

Wines, B. D., et al. (2000), 'The IgG Fc contains distinct Fc receptor (FcR) binding sites: the leukocyte receptors Fc gamma RI and Fc gamma RIIa bind to a region in the Fc distinct from that recognized by neonatal FcR and protein A', *J Immunol,* 164 (10), 5313-8.

Wu, X., et al. (2011), 'Focused evolution of HIV-1 neutralizing antibodies revealed by structures and deep sequencing', *Science,* 333 (6049), 1593-602.

Xia, Z., et al. (2012), 'A 17q12 allele is associated with altered NK cell subsets and function', *J Immunol,* 188 (7), 3315-22.

Yeung, Y. A., et al. (2016), 'Germline-encoded neutralization of a *Staphylococcus aureus* virulence factor by the human antibody repertoire', *Nat Commun,* 7, 13376.

Yousfi Monod, M., et al. (2004), 'IMGT/JunctionAnalysis: the first tool for the analysis of the immunoglobulin and T cell receptor complex V-J and V-D-J JUNCTIONs', *Bioinformatics,* 20 Suppl 1, i379-85.

Yu, X. Q., et al. (2017), 'Safety, Tolerability, and Pharmacokinetics of MEDI4893, an Investigational, Extended-Half-Life, Anti-*Staphylococcus aureus* Alpha-Toxin Human Monoclonal Antibody, in Healthy Adults', *Antimicrob Agents Chemother,* 61 (1).

Zapotoczna, M., et al. (2013), 'Iron-regulated surface determinant B (IsdB) promotes *Staphylococcus aureus* adherence to and internalization by non-phagocytic human cells', *Cell Microbiol,* 15 (6), 1026-41.

Zhang, L., et al. (1998), 'A second IgG-binding protein in *Staphylococcus aureus*', *Microbiology,* 144 (Pt 4), 985-91.

Zhang, L., et al. (1999), '*Staphylococcus aureus* expresses a cell surface protein that binds both IgG and beta2-glycoprotein I', *Microbiology,* 145 (Pt 1), 177-83.

Zhou, T., et al. (2015), 'Structural Repertoire of HIV-1-Neutralizing Antibodies Targeting the CD4 Supersite in 14 Donors', *Cell,* 161 (6), 1280-92.